

Release Probability
of the
Readily Releasable Vesicles
during Short Term Plasticity

Cover: *Picture of coins falling from a slot machine. This type of slot machine was very common on fairs in my home village. Upon dropping money in the machine your coin would be pushed against the other coins already in the machine. One would hope that more than one coin would fall off at the other side and would be returned to the player. The coins falling from the machine reminded me of the synaptic vesicles in the nerve terminal. There were always a couple of coins at the verge of falling, reminiscent of the vesicles in the readily releasable pool, while the “release probability” would not always be as one would expect from the laws of gravity.*

Print: Proefschriftmaken.nl

ISBN: 978-90-8891-095-1

**Release Probability of the Readily Releasable Vesicles
during Short Term Plasticity.**

De afgiftewaarschijnlijkheid van de direct beschikbare neurotransmitter
blaasjes gedurende korte termijn plasticiteit.

PROEFSCHRIFT

ter verkrijging van de graad van doctor aan de
Erasmus Universiteit Rotterdam
op gezag van de
rector magnificus

Prof.dr. S. W. J. Lamberts

en volgens besluit van het College voor Promoties.

De openbare verdediging zal plaatsvinden op

woensdag 4 maart 2009 om 15.45 uur

door

Ronald Leonardus Philomina Habets

geboren te Heerlen



Promotiecommissie

Promotor: Prof.dr. J. G. G. Borst

Overige leden: Prof.dr. W. J. Wadman
Prof.dr. M. A. Frens
Dr. Y. Elgersma

The research described in this thesis was conducted at the Department of Neuroscience of the Erasmus MC in Rotterdam. Initial experiments were started at the Swammerdam Institute of Life Sciences at the University of Amsterdam.

Financial support was given by the Nederlandse Organisatie voor Wetenschappelijk Onderzoek (NWO; Pionier subsidy), Neuro-Bsik grant and a Human Frontier Science Program collaborative grant.

CONTENTS

<i>Preface</i>	9
<i>Chapter 1:</i> Introduction	11
<i>Chapter 2:</i> Dynamic development of the calyx of Held synapse	25
<i>Chapter 3:</i> Post-Tetanic Potentiation in the Rat Calyx of Held Synapse	43
<i>Chapter 4:</i> An Increase in Calcium Influx Contributes to Post-Tetanic Potentiation at the Rat Calyx of Held Synapse	77
<i>Chapter 5:</i> Kinetics of the Readily-Releasable Pool during Post-Tetanic Potentiation in the Rat Calyx of Held Synapse	101
<i>Chapter 6:</i> General discussion	127
<i>Nederlandse samenvatting</i>	143
<i>Dankwoord</i>	146
<i>Curriculum Vitae</i>	148
<i>Publications</i>	149
<i>List of abbreviations</i>	150
<i>References</i>	151

Preface

Neurons are excitable cells in the brain. Billions of neurons are interconnected and organized into neuronal networks, making behaviour like locomotion, language, thought, learning and social interaction possible. A brief change in the membrane potential of a neuron, called the action potential, is used to signal to other neurons. The timing and frequency of occurrence of these action potentials contains essential information. To communicate this information to other cells in the network, nerve cells in the brain are connected through specialized structures, called synapses. The majority of synapses are chemical synapses, meaning that they use neurotransmitters to signal to the neighbouring cell. This signal can be inhibitory or excitatory depending on the type of chemical used. These neurotransmitters are stored in lipid vesicles in the transmitting end (the presynaptic terminal) of the synapse and are so small that they can only be visualized with electron microscopy (Figure 1C).

The action potential travels along a specialized compartment of the nerve cell called the axon and when it reaches the presynaptic terminal it opens voltage gated calcium channels. The calcium flowing into the cell through these channels is the final trigger for neurotransmitter containing vesicles to fuse with the membrane. Through this fusion the content of the vesicles is released outside the cell where it diffuses in the extracellular space to the receiving (postsynaptic) cell. Glutamate is the main excitatory neurotransmitter used by the brain and upon binding to its receptors, it opens cation channels, leading to a depolarization of the membrane. This depolarization can, but does not necessarily need to, result in an action potential in the postsynaptic cell.

This uncertainty of inducing an action potential in the postsynaptic cell contributes to the computational properties of a neuronal network. In some systems it is necessary that multiple cells release simultaneously onto the postsynaptic cell in order for it to fire an action potential. In other systems the postsynaptic cell can only fire an action potential when it is relieved from inhibition. Another way of increasing the chances of postsynaptic action potential firing is when two or more action potentials arrive at the presynaptic terminal in short succession. Such bursts of action potential, next to summing up the postsynaptic potentials, often lead to changes in the properties of the synapse. This change, called synaptic plasticity, can in itself be a requisite for postsynaptic action potential firing. The mechanisms of synaptic plasticity can be subdivided in mechanisms that change the postsynaptic response to a vesicle, such as incorporation of more receptors in the postsynaptic membrane, and mechanisms that increase the number of vesicles released. The latter was the topic of my research and is described in this thesis.

Chapter 1

Introduction

Short term plasticity

Changing the strength of a synapse can be used to store information; it enables an organism to adapt to its environment or to learn and remember cues in that environment. There are different forms of memory and one way of differentiating memory is based on the duration of the learned cue. Short term plasticity has been proposed to be the molecular substrate for short term memory (Silva *et al.*, 1996; Fisher *et al.*, 1997) and at the NMJ, short term plasticity has been implicated in muscle control. Interestingly, forms of short term plasticity that increase the response to single stimuli, like facilitation and potentiation were reduced at the NMJs of *Drosophila* memory mutants (Zhong & Wu, 1991). Short term potentiation has also been proposed to add filtering properties to neuronal networks. Depression of responses during trains of activity could act as a low-pass filter, i.e. only the onset of an action potential train is passed on to the next neuron, while potentiation and facilitation could act as high-pass filters, only activating postsynaptic cells when action potentials are grouped in bursts. In sensory systems synaptic plasticity is most likely a mechanism to adapt to prolonged stimulation, making the system more or less sensitive to change. For example, in the snail *Aplysia californica*, short term plasticity is responsible for the habituation of the gill withdrawal reflex (Fisher *et al.*, 1997). In conclusion: short term plasticity has been implicated in short term memory, filtering properties of neuronal networks and adaptation to sensory stimulation, thus making the understanding of the mechanisms involved in short term plasticity important for deciphering how the brain works.

Synaptic plasticity is often subdivided based on the duration of the change in excitability of the cells. Short term plasticity is defined as changes that last up to an hour after stimulation and both an increase and a decrease in excitability have been described. Short term plasticity is again subdivided in several forms of plasticity, presumed to have different mechanisms of action (Fisher *et al.*, 1997; Zucker & Regehr, 2002). The forms of synaptic plasticity with the briefest duration are known as paired pulse facilitation (PPF) and paired pulse depression (PPD) and occur after a single action potential. If vesicle release is reduced when a second action potential arrives at a nerve terminal in short succession after the first, this is called paired pulse depression. A sustained depression during a train of action potentials is also known as short term depression (STD). Short term depression has been observed at many synapses, including the calyx of Held synapse (Barnes-Davies & Forsythe, 1995; Borst *et al.*, 1995). The opposite phenomenon, paired pulse facilitation or simply facilitation, is an increase in vesicular release after a conditioning action potential and is found for example in many hippocampal boutons or in the parallel fiber to Purkinje cell synapse. Cortical layer 2/3 pyramidal cells can even express both PPD and PPF depending on the

type of cell they synapse on (Rozov *et al.*, 2001). Facilitation can accumulate during a train of action potentials and has been subdivided in fast- (F₁) and slow (F₂) decaying components. Short term plasticity is manifested as an increase or decrease in the number of neurotransmitter filled vesicles being released per action potential. This change in the number of synaptic vesicles can result from altered availability of the vesicles or from changes in the usage of the available vesicles.

Release probability and the size of the readily releasable pool of synaptic vesicles

Neurotransmitters are stored in lipid vesicles that fuse with the plasma membrane upon arrival of the action potential. In electron microscopic images (Figure 1C) it can be clearly seen that nerve terminals are packed with synaptic vesicles. This provides the synapse with a supply of vesicles to sustain vesicle release during high frequency stimulation. This supply of vesicles can be categorized into several populations or pools. These pools are functionally distinct in that the vesicles from a certain pool release under different circumstances. During prolonged stimulation only a subset (15-30%) of vesicles can be labelled with the vesicle markers like FM1-43 (de Lange *et al.*, 2003; Rizzoli & Betz, 2005). This subset of vesicles is called the recycling pool and is composed of the readily releasable pool (RRP) and the reserve pool (Heuser & Reese, 1973; de Lange *et al.*, 2003; Rizzoli & Betz, 2005). The readily releasable pool is the pool the terminal draws upon when stimulated with a single action potential. This pool of vesicles is associated with the vesicles “docked” to the active zones in electron microscopic images of nerve terminals (Schikorski & Stevens, 2001). After release of vesicles, the RRP is supplied with vesicles from the reserve pool in a process called replenishment. In summary; the RRP is a supply of vesicles that is physiologically and morphologically defined as being immediately available for fusion with the plasma membrane.

The release probability (P_r) describes the chance that a vesicle fuses with the presynaptic membrane. This P_r can be defined as the chance a vesicle is released from an active zone or as the chance that a vesicle is released from the RRP (Zucker & Regehr, 2002). Since more than one vesicle can be ready for release at an active zone there is a difference and from this point onward the latter definition of P_r will be used. The average P_r can then be calculated by dividing the number of vesicles released due to an action potential by those in the RRP.

Release of vesicles leads to current flowing through activated glutamate receptors in the postsynaptic cell, which can be measured as an excitatory postsynaptic current (EPSC)

with an electrophysiological technique (voltage clamp). In the absence of stimulation, the postsynaptic recording exhibits small miniature EPSCs, which result from spontaneously fusing vesicles. By carefully examining the amplitude of these spontaneously fusing vesicles, the average amplitude of the postsynaptic response to the release of a single vesicle, the so-called quantal size (q), can be determined. The number of vesicles released by an action potential is called the quantal content and can be calculated by comparing the response evoked by an action potential to the quantal size. An increase in vesicular release during synaptic plasticity can therefore be the result of an increase in the average P_r or because the RRP has become larger.

Post-Tetanic Potentiation

Longer lasting forms of short term plasticity can be induced with prolonged stimulation. Such repetitive stimulation is called a tetanus, hence the name (post-) tetanic potentiation (PTP). Nearly seventy years ago, Feng (Feng, 1941) was the first to report PTP. Feng studied the synaptic responses in the synapse between motoneurons and muscles, which is called the neuromuscular junction (NMJ). At this synapse the synaptic potentials are called endplate potentials. He was the first to describe an increase in the end-plate potentials after high frequency stimulation:

“The end-plate responses to the brief low-frequency stimuli during the few min. after the termination of the C.S. (continuous stimulus) are much larger than the control response to the same stimulus before the C.S.”

He already noticed that the time course of this form of plasticity was temperature dependent and that the amplitude was dependent on the duration and frequency of the tetanus. Subsequent research discovered that PTP was accompanied by a long lasting rise of the presynaptic calcium concentration (henceforth called residual calcium) and that this residual calcium was both necessary and sufficient to induce PTP (Kamiya & Zucker, 1994). Residual calcium is taken up by the mitochondria during tetanic stimulation and is slowly released into the cytosol afterwards (Tang & Zucker, 1997).

Presynaptic calcium dynamics

Neurotransmitter release is highly dependent on calcium. The calcium necessary for evoked release flows into the terminal through voltage gated calcium channels, during the action potential. Vesicles are released at specialized structures called active zones

(Figure 1C). The calcium channels of the presynaptic terminals are presumed to cluster at these active zones and opening of the channels leads to a local increase in the calcium concentration. Circumventing channel-vesicle topology, it has been shown that uniformly raising the intracellular calcium concentration with photolytic calcium chelators is sufficient to trigger the release of vesicles (Delaney & Zucker, 1990; Heidelberger *et al.*, 1994; Bollmann *et al.*, 2000; Schneggenburger & Neher, 2000) for review see (Augustine, 2001). These studies also showed that vesicle release has a fourth or fifth order dependence on calcium, meaning that if you double the intraterminal calcium concentration, release is increased more than 16-fold. It is thought that this high order (supralinear) dependence on calcium reflects the binding of multiple calcium ions to a putative calcium sensor for release. Synaptotagmin is proposed to act as this calcium sensor for release, because it has two calcium binding domains, binding two calcium ions each and because evoked release is severely decreased in animals lacking the gene for synaptotagmin (Geppert *et al.*, 1994; Marek & Davis, 2002; Sun *et al.*, 2007). The calcium concentration needed to release about half the vesicles in the RRP per ms, differs between different preparations (Neher & Sakaba, 2008), but is always in the micromolar range. In contrast the average increase in calcium concentration during an action potential is in the nanomolar range (Jackson *et al.*, 1991; Regehr *et al.*, 1994; Helmchen *et al.*, 1997). This prompted scientists to hypothesize that release sites are localized close to the calcium channels, where the calcium concentration can be much higher. The localized increases in calcium concentration have been termed calcium microdomains and have also been found experimentally (Llinas *et al.*, 1992; DiGregorio *et al.*, 1999; Zenisek *et al.*, 2003) for review see Oheim *et al.* (2006). The influence of microdomain calcium on vesicle release is determined by the location of the release sites relative to the calcium channels, the amount of calcium influx and the concentration and affinity of calcium buffers present in the terminal. Due to the steep dependence of release for calcium, changing calcium influx, calcium buffering or the calcium channel-vesicle topology has a huge influence on the release of neurotransmitter (Dodge & Rahamimoff, 1967; Adler *et al.*, 1991; Borst & Sakmann, 1999b; Schneggenburger *et al.*, 1999; Wadel *et al.*, 2007). This makes calcium buffers and calcium channels good candidates to induce synaptic plasticity (Borst & Sakmann, 1998b; Cuttle *et al.*, 1998; Felmy *et al.*, 2003).

Proteins involved in PTP

The original hypothesis, postulated by Bernard Katz (Katz & Miledi, 1968), to explain facilitation of end-plate potentials states that calcium ions remaining from a previous stimulation add up to the calcium ions flowing into the terminal during an action

potential. This model therefore suggests that the calcium-binding protein which is responsible for triggering release is also responsible for inducing PTP. When the calcium sensitivity for release turned out to be in the high micromolar range in the retinal bipolar cell terminals (Heidelberger *et al.*, 1994), while the concentration of residual calcium is typically $< 1 \mu\text{M}$ (Wojtowicz & Atwood, 1985; Delaney & Tank, 1994; Zhong *et al.*, 2001), the existence of a separate high-affinity calcium sensor for synaptic plasticity was postulated.

Several molecules have been put forward as candidates for the calcium sensor involved in plasticity mentioned above. These molecules can be grouped into calcium binding proteins, containing C2 domains like protein kinase C (PKC), synaptotagmin, Munc-13, RIM, Piccolo, Rabphilin and Doc2 (Barclay *et al.*, 2005) and proteins that are activated by calcium dependent kinases like calcium/calmodulin-dependent protein kinase II (CaMKII). An example of the latter are synapsins, which are vesicle binding proteins, thought to be involved in vesicle recruitment to the active zone. In synapsin-1 knock-out animals PTP was found to be normal (Rosahl *et al.*, 1993) and PTP was reduced in mice lacking both synapsin-1 and 2 (Rosahl *et al.*, 1995). CaMKII was shown to be involved in PTP at the squid giant synapse (Augustine *et al.*, 1994). Interestingly, PTP was increased in mice lacking one or both copies of the gene for α -CamkII (Chapman *et al.*, 1995; Silva *et al.*, 1996), but see also (Stevens *et al.*, 1994). The canonical function of this kinase is to phosphorylate AMPA receptors in the postsynaptic compartment during long term potentiation, but it has also been found to act presynaptically by phosphorylating synapsins (De Camilli *et al.*, 1990). Members of the cAMP second messenger pathway have been implicated in facilitation and potentiation at the *Drosophila* NMJ, the central nervous system of *Aplysia californica* and the hippocampal mossy fibre terminals (Kandel & Schwartz, 1982; Zhong & Wu, 1991; Alle *et al.*, 2001). PTP was also shown to be sensitive to manipulation with phorbol esters, activators of protein kinase C and Munc-13 and these molecules have therefore been put forward as regulators of PTP at mammalian central synapses (Alle *et al.*, 2001; Brager *et al.*, 2003; Junge *et al.*, 2004). The results of the studies mentioned here indicate that there might be not a single calcium sensor for PTP, but that in different organisms and tissues, different mechanisms are used for changing the synaptic output.

The calyx of Held

Many forms of short term plasticity have a presynaptic origin. Studying presynaptic mechanisms in the CNS, however, is hampered by the small size of the synaptic terminals, which are typically $< 1 \mu\text{m}$. We therefore used a giant terminal, called the

calyx of Held (Figure 1), as a model system. Because of its large size, it is possible to make patch-clamp recordings from this terminal. The calyces of Held form at the end of axons originating from the globular bushy cells in the cochlear nucleus. They are part of the superior olivary complex, which is involved in the localization of sound in space. The calyx of Held terminals are glutamatergic and synapse onto the glycinergic principal cells in the medial nucleus of the trapezoid body (MNTB) (Figure 1A, B). The proposed function of the calyx of Held-principal cell synapse is that it inverts the excitatory signal from the contra-lateral cochlear nucleus to an inhibitory input on the cells of the lateral superior olivary nucleus (LSO) (Schneeggenburger & Forsythe, 2006).

The postsynaptic cell expresses alpha-amino-3-hydroxy-5-methyl-4-isoxazole propionic acid (AMPA-) and (at neonatal age) N-methyl-D-aspartic acid (NMDA-) receptors. Because the calyx of Held (Figure 1D and E) synapses on the soma of the principal cells, the latter contain few dendrites and their AMPA receptors are located close to the postsynaptic recording site. These traits are very favourable for obtaining high quality whole cell voltage clamp measurements (Borst *et al.*, 1995). Thus, in the absence of receptor desensitization, AMPA mediated EPSCs are a very good measure for vesicle release at this synapse (Wong *et al.*, 2003).

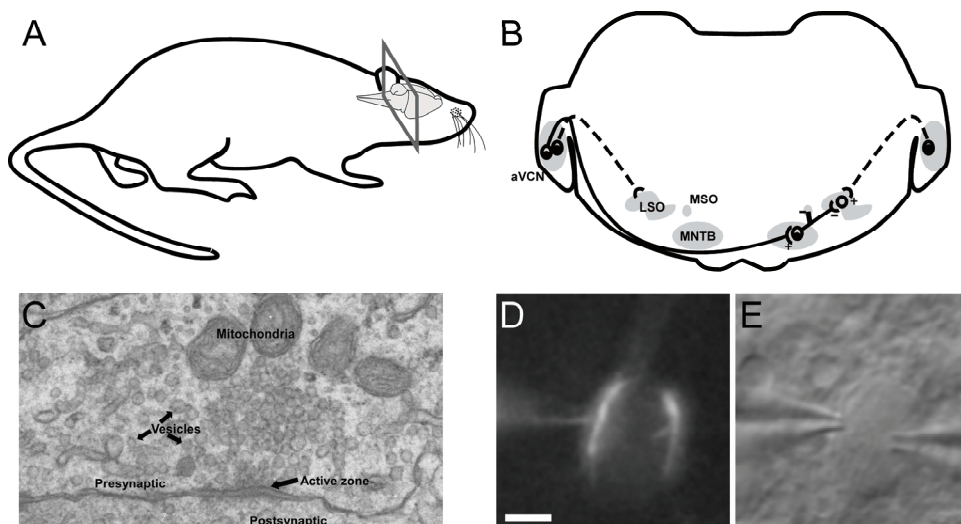


Figure 1: Location and morphology of the calyx of Held. A: schematic drawing of the rat and the location of the coronal section through the brain depicted in B, where the superior olivary complex is indicated. B: Schematic view of the superior olivary complex and its nuclei; anteroventral cochlear nucleus (aVCN), lateral superior olive (LSO), medial superior olive

(MSO) and medial nucleus of the trapezoid body (MNTB). Indicated are the excitatory connections from the cochlear nucleus to the ipsilateral LSO and the contralateral MNTB. The latter are the axons that end as calyces of Held and synapse on the glycinergic principal cells, which invert the signal and send it to the MSO and LSO. C: Electron microscopic picture of a part of the calyx of Held containing an active zone, synaptic vesicles and mitochondria, as indicated. D: Fluorescent image of a calyx of Held filled with a calcium-sensitive dye, via the patch pipette. Calibration bar represents 7.5 μm . E: Differential interference contrast image corresponding to the image shown in D. The postsynaptic principal cell was also patched with the pipette on the right hand side.

Calyx of Held formation

Most experiments at the calyx of Held are performed in neonatal animals because ongoing myelination of the brainstem, where these nerve terminals are located, make electrophysiological manipulation of the cells and terminals progressively more challenging. However, a detailed understanding of how the calyx of Held develops during the first days is lacking. Calyx-type nerve terminals form between one and four days after birth, going through a protocalyx intermediate stage. During calyx development the nerve terminals contain filopodia-like structures, known as calycine collaterals (Morest, 1968b), but the function of these collaterals is at present unknown. As the calyx matures, it loses these collaterals and in addition transforms from a cup-shaped structure into a fenestrated finger-like innervation of the principal cell (Kandler & Friauf, 1993; Rodriguez-Contreras *et al.*, 2006).

Early in development muscle fibres are innervated by multiple endplates originating from different motoneurons. During development endplates are pruned until muscle fibres are contacted by a single endplate in a process called synapse elimination, which has also been proposed for innervation of the purkinje cell by climbing fibres (Lichtman & Colman, 2000). The vast majority of principal cells however receive only one calyx during development, meaning that calyces are not pruned after overinnervation of the MNTB (Bergsman *et al.*, 2004; Hoffpauir *et al.*, 2006; Rodriguez-Contreras *et al.*, 2006), unlike the mammalian NMJ and the cerebellar climbing fibre synapse. The onset of hearing starts around eleven days after birth in rats, with a progressive gain of hearing in the first few days. The calyx of Held-principal cell connection is thus made long before the MNTB starts receiving sensory input. It is conceivable that spontaneous activity in the auditory system is sufficient for proper one-on-one formation of the calyx-principal cell pair, but in mice lacking evoked release from the inner hair cells the exocytic machinery of the calyx of Held is unaffected

(Erazo-Fischer *et al.*, 2007), indicating that calyx formation is not affected by a severe reduction in spontaneous activity. How the brain manages to get each principal cell connected to only one calyx is therefore to this date unresolved.

Short term plasticity at the calyx of Held

Several forms of short term plasticity have been observed at the calyx of Held synapse, which I will discuss here in detail.

Short term depression

EPSCs in the principal cells generally depress upon repetitive stimulation of the calyceal terminal (Barnes-Davies & Forsythe, 1995; Borst *et al.*, 1995). This depression has several causes (Schneppenburger *et al.*, 2002; von Gersdorff & Borst, 2002), of which postsynaptic receptor desensitization (Wong *et al.*, 2003), calcium current inactivation (Xu & Wu, 2005) and depletion of the RRP (Wu & Borst, 1999) are the most prominent. The severe contribution of postsynaptic receptor desensitization to short term depression becomes evident when desensitization is prevented by cyclothiazide or high concentrations of a competitive glutamate antagonist (gamma-D-glutamylglycine (γ DGG) or kynurenic acid). Instead of depressing, the second response to a paired stimulus is now facilitated at stimulus intervals shorter than ten milliseconds (Wong *et al.*, 2003)(see also Figure 3A, chapter 3). In the absence of postsynaptic receptor desensitization, EPSCs still depress during a prolonged train of action potentials at the calyx of Held. At lower frequencies ($<100\text{Hz}$), this depression has been attributed to inactivation of the P/Q type calcium channels. This inactivation is calcium-dependent and depends on calmodulin (Xu & Wu, 2005; Nakamura *et al.*, 2008) and metabotropic glutamate receptors (Takahashi *et al.*, 1996). At higher ($\geq 100\text{Hz}$) frequencies, depletion of the RRP is proposed as the dominant mechanism for depression at the calyx of Held (Wu & Borst, 1999). As the rats mature, the RRP and the number of release sites of the calyx increase (Taschenberger & von Gersdorff, 2000; Taschenberger *et al.*, 2002) and depression becomes less pronounced, enabling the synapse to transmit information at higher frequencies. At other synapses, depression has been shown to be caused by depletion of vesicles (Foster & Regehr, 2004) for review see (Zucker & Regehr, 2002). Other mechanisms that might contribute to short term depression are: 1) Feedback from metabotropic glutamate receptors (von Gersdorff *et al.*, 1997; Billups *et al.*, 2005), 2) depletion of Ca^{2+} from the synaptic cleft (Borst & Sakmann, 1999a) and 3) manipulation by various other transmitters (von Gersdorff & Borst, 2002). In conclusion, short term depression has

been well characterized at the calyx of Held and it was found that multiple mechanisms, i.e. RRP depletion, calcium current inactivation and postsynaptic receptor desensitisation all contribute, depending on the frequency and duration of the stimulus.

Facilitation

Paired pulse facilitation is observed at the calyx of Held at short inter-stimulus intervals, when the release probability has been lowered by reducing extracellular calcium (Barnes-Davies & Forsythe, 1995; Borst *et al.*, 1995) or, as mentioned above, when postsynaptic glutamate receptors are protected against desensitization. Several mechanisms, such as summation of residual and microdomain calcium and buffer saturation (Felmy *et al.*, 2003), action potential broadening, facilitation of the calcium channels and facilitation of the release process itself, have been proposed to account for paired pulse facilitation (Neher & Sakaba, 2008). Felmy *et al.* (2003) showed that summation of residual calcium and microdomain calcium was responsible for only 30% of facilitation (Felmy *et al.*, 2003). This study measured the calcium sensitivity of release with release of calcium by the photolysable calcium buffer DM-nitrophen. Elevation of the calcium concentration did not increase the sensitivity for calcium of the release process. This result prompted these investigators to propose that microdomain calcium was elevated due to saturation of the calcium buffers by the residual calcium from the first action potential. Calcium binding proteins, such as calbindin, parvalbumin and calretinin could act as buffers and are widely expressed in the brain (Burnashev & Rozov, 2005; Muller *et al.*, 2005). During an action potential, these buffers compete for the microdomain Ca^{2+} with the Ca^{2+} sensor for release. The relatively high affinity for Ca^{2+} of for instance calbindin (Nagerl *et al.*, 2000) has the effect that Ca^{2+} is still bound to the buffer when a second action potential invades the terminal. This means that there is less buffer available to capture calcium ions entering with the second action potential and, consequently, the Ca^{2+} concentration in the vicinity of the release sites will be higher during this second stimulus. This calcium buffer saturation hypothesis was first put forward by Neher (Klingauf & Neher, 1997; Zucker & Regehr, 2002) to explain why vesicle release depended supralinearly on the concentration of residual calcium. Furthermore, a computer model of buffer saturation could explain the amplitude and most of the temporal characteristics of facilitation, at the crayfish neuromuscular junction (Matveev *et al.*, 2004). Experimental evidence for this hypothesis was obtained by loading the fast calcium buffer BAPTA into nerve terminals, which shifted synaptic release from depressing to facilitating (Rozov *et al.*, 2001). In neurons from calbindin-D28K knock-out mice that exhibit a defect in

facilitation, infusion of exogenous calbindin through the patch pipette rescues facilitation (Blatow *et al.*, 2003). Before the onset of hearing, when most experiments in the calyx of Held are performed, the calcium buffering capacity is rather low (Helmchen *et al.*, 1997), but as the rats mature, calcium buffering proteins like parvalbumin and calretinin become more abundant (Felmy & Schneggenburger, 2004).

Modulation of the Calcium Influx

Increasing microdomain Ca^{2+} can also be accomplished by increasing the influx of Ca^{2+} . When the action potential arrives at the terminal, Ca^{2+} flows into the calyx mostly through P/Q type voltage-gated calcium channels (Iwasaki & Takahashi, 1998; Wu *et al.*, 1999). An increase in the calcium influx has been reported due to facilitation of the voltage gated calcium channels (Borst & Sakmann, 1998a; Cuttle *et al.*, 1998) in these terminals. In knock-out mice lacking the gene for the α_1A -subunit, the P/Q-type calcium current is absent and facilitation of the EPSCs is greatly reduced (Inchauspe *et al.*, 2004; Ishikawa *et al.*, 2005; Muller *et al.*, 2008). Calcium current facilitation is calcium dependent and was found to be enhanced when neuronal calcium sensor-1 peptides were infused in terminal (Tsujiimoto *et al.*, 2002). Another efficient way of increasing calcium influx into nerve terminals is broadening of the action potential (Zucker & Lara-Estrella, 1979; Eliot *et al.*, 1993; Geiger & Jonas, 2000), which was also observed at the calyx of Held (Borst *et al.*, 1995; Borst & Sakmann, 1999b).

In summary, we find that multiple mechanisms contribute to short term plasticity at the calyx of Held. While people agree to a certain extent that postsynaptic receptor desensitization, calcium current inactivation and depletion of the RRP contribute to short term depression, the mechanism of facilitation is still fiercely debated (Inchauspe *et al.*, 2004; Inchauspe *et al.*, 2007; Muller *et al.*, 2008). Calcium buffer saturation and calcium current facilitation are among the most favoured hypotheses at the calyx of Held. In this thesis I investigated whether these mechanisms can also account for PTP.

Spontaneous release

In the absence of action potentials, terminals release vesicles at low rates. Cummings (Cummings *et al.*, 1996) and others (Propst & Ko, 1987) show that there can be large discrepancies between evoked and spontaneous release with respect to synaptic plasticity. Differential changes between these two modes of release can arise due to

several mechanisms. Vesicle depletion might mask facilitation (Otsu *et al.*, 2004). An increase or decrease in calcium current specifically affects evoked release while spontaneous release is unaffected. The nonlinear dependence of transmitter release on calcium concentration might result in different effects of residual calcium on spontaneous and evoked release (Zucker & Lara Estrella, 1983; Zucker & Regehr, 2002). In addition, the release sites for spontaneous release and evoked release might be morphologically (Ceccarelli *et al.*, 1979; Ko, 1981), biochemically (Deitcher *et al.*, 1998) or physiologically different. We therefore looked very closely at spontaneous release during PTP, to see whether it could give us a clue to how potentiation of vesicle release occurs.

Scope of this thesis

In this thesis, we first examined how the calyx of Held forms during the first postnatal days and what the function of calyceal filopodia is (Chapter 2). Furthermore, we investigated whether forms of synaptic plasticity longer than facilitation, could be induced at the calyx of Held synapse. In contrast to a study that showed post-tetanic depression (Forsythe *et al.*, 1998), we found that EPSCs were much larger after prolonged stimulation (Chapter 3). We set out to examine what made this synapse double its output after a period of high activity. We used several experimental approaches to try and answer this question. In particular we started by looking at spontaneous release, trains of action potentials and levels of residual calcium. We combined pre- and postsynaptic recordings of electrical activity and investigated calcium influx and calcium buffering during a single action potential (Chapter 4). Lastly, we compared changes in P_r and RRP more closely during the decay of PTP and extended our analysis to PTP at physiological temperature (Chapter 5).

Chapter 2

Dynamic development of the calyx of Held synapse

Adrián Rodríguez-Contreras, John Silvio Soria van Hove, Ron L. P. Habets, Heiko Locher, and J. Gerard G. Borst

Proc. Natl. Acad. Sci. USA. 2008 Apr 8;105(14):5603-8

ABSTRACT

The calyx of Held is probably the largest synaptic terminal in the brain, forming a unique one-to-one connection in the auditory ventral brainstem. During early development, calyces have many collaterals, whose function is unknown. Using electrophysiological recordings and fast-calcium imaging in brain slices, we demonstrate that these collaterals are involved in synaptic transmission. We show evidence that the collaterals are pruned and that the pruning already begins 1 week before the onset of hearing. Using two-photon microscopy to image the calyx of Held in neonate rats, we report evidence that both axons and nascent calyces are structurally dynamic, showing the formation, elimination, extension, or retraction of up to 65% of their collaterals within 1 hour. The observed dynamic behavior of axons may add flexibility in the choice of postsynaptic partners and thereby contribute to ensuring that each principal cell eventually is contacted by a single calyx of Held.

INTRODUCTION

Studying the formation of individual, identified synapses in the CNS presents a formidable challenge because of their small size, their incredibly high density, and their protracted formation period (McAllister, 2007). Imaging studies in living animals have provided insights into the structural changes that presynaptic axons undergo during development, which complements our understanding of how specific brain connections form (Cohen-Cory & Lom, 2004). An emerging view from these studies is that axonal dynamics are age- and cell type-dependent (Portera-Cailliau *et al.*, 2005) and strongly correlated with the formation of synaptic contacts, which may ultimately guide the growth of the axonal arbour (Cohen-Cory & Lom, 2004; Javaherian & Cline, 2005; Meyer & Smith, 2006; Ruthazer *et al.*, 2006).

Here, we study the development of a CNS synapse that can be identified relatively easily because it is probably the largest synaptic contact in the mammalian brain (Schneggenburger & Forsythe, 2006). The calyx of Held connects the globular bushy cells of the anteroventral cochlear nucleus and the principal cells of the medial nucleus of the trapezoid body (MNTB) in the brainstem. Studies in rodents have shown that shortly before birth, the principal cells of the MNTB are innervated by small glutamatergic boutons (Kil *et al.*, 1995). Morphological and functional identification of nascent calyces is possible between postnatal days 3 and 5 (Kandler & Friauf, 1993; Kil *et al.*, 1995; Hoffpauir *et al.*, 2006), which suggests that the characteristic one-to-one innervation observed in mature animals is achieved very rapidly (Hoffpauir *et al.*,

2006). However, previous studies have not been able to study the dynamic aspects of the calyx of Held development.

As a first step toward elucidating the cellular mechanisms that ensure that each MNTB principal cell is always innervated by only a single calyx of Held, we sought an imaging approach. Because it has not been possible to study this unique synapse in culture, we carried out studies *in vivo*. We developed a surgical procedure to label brainstem axons in anesthetized rat pups and imaged them with a two-photon microscope. Using this approach, we provide evidence of structural dynamics related to the development of the calyx of Held synapse. In combination with electrophysiological and optical recordings in brain slices, neuronal tracing, and immunohistochemistry we show that single axons in the MNTB can innervate multiple postsynaptic cells through the collaterals of the calyx of Held.

MATERIALS & METHODS

Rats.

Wistar rats were purchased from Harlan and housed at the Erasmus MC facilities. The litters used in this work were born from timed pregnancies, taking the day of birth as P0. Experiments complied with institutional and international guidelines for the use of laboratory animals.

Immunohistochemistry.

VGLUT immunohistochemistry was performed as described (Rodriguez-Contreras *et al.*, 2006) and SI Materials and Methods.

Multispectral Laser-Scanning Microscopy.

Confocal imaging was performed as described (Dickinson, 2005) and SI Materials and Methods).

Surgery and Tracer Injections.

Neonate (P0–3) rat pups were anesthetized with isoflurane (2%, 1 liter of O₂ per min⁻¹), supine-positioned on top of a homeothermic blanket heated to 36–37°C (FHC, Inc.) and secured to a custom-made head holder. After skin retraction, fat and muscle layers overlying the trachea were bluntly removed. Animals were tracheotomized, intubated, and mechanically ventilated using a MiniVent type 845 mouse ventilator (80 breaths per min⁻¹, 60 µl; Hugo-Sachs Elektronik). At this point, anesthesia was reduced to 1.5% and carefully monitored on the basis of pedal reflexes or signs of distress. A small craniotomy (3 × 2 mm) was drilled above the basilar artery where the anterior inferior cerebellar artery branches, and the dura was opened and retracted. Broken borosilicate glass micropipettes (tip 10–20 µm) were filled with a 10% solution of Alexa Fluor 568–dextran amine tracer (Invitrogen) initially diluted in 0.4 M KCl, but in later experiments in 0.5 M NaCl. Tracer-filled electrodes were positioned next to the basilar artery $\approx 300 \pm 50$ µm rostral to the anterior inferior cerebellar artery by using a micromanipulator under visual control. Iontophoretic injections of tracer were delivered at a depth of 100–200 µm with continuous 0.25-s pulses of positive current (0.5 µA) applied through a customized pipette holder at ≈ 2 Hz for 15 s. After tracer injection, the craniotomy was irrigated every 15 min for 1–2 h with 0.9% saline solution until the start of the imaging session. Subsequent histological analysis confirmed that these injections were correctly targeted to the caudal pole of the MNTB (Fig. S2).

Two-Photon Imaging and Analysis.

In vivo imaging was performed with a custom-built two-photon laser-scanning microscope. Excitation at 800 nm was done with a Ti:sapphire MIRA 900 laser pumped by a 5-W Verdi laser (Coherent, Inc.) coupled into a BX50WI Olympus microscope. Fluorescence was bandpass-filtered (580–680 nm; Semrock) and detected in epifluorescence mode by a cooled PMT (Hamamatsu photosensor module H7422-40). Maximum laser power was ≈ 150 mW, measured after the objective. Image stacks were acquired with a water-immersion objective (Olympus LUMPlanFl, 40 \times /0.8 IR) and consisted of 100–150 optical sections (1,024 × 1,024 pixels; ≈ 0.25 -µm per pixel; interval 1–3 µm). Image stacks were imported into Volocity (Improvision), and collaterals were drawn digitally using built-in functions. Axon collaterals <2 µm were excluded from the analysis. For each collateral, the length at 1 h was subtracted from its initial length, and these numbers were used to further categorize collaterals in five groups. Criteria for categorizing axon and calyx of Held collaterals are provided in SI Materials and Methods.

Slice Electrophysiology and Calcium Imaging.

Brain slices were prepared as described in chapter 3, except that rat pups were between P0 and P4 of age. Some experiments also included the application of an anterograde tracer to label afferent axons (Rodriguez-Contreras *et al.*, 2006). Whole-cell recordings were performed as described in ref. 30. Details of intracellular solutions and drugs are given in SI Materials and Methods. Calyces of Held in brainstem slices containing the MNTB were loaded with the calcium indicator Oregon green BAPTA-1 (OGB-1, 100 μ M) via the patch pipette and imaged with two-photon excitation at 800 nm. Four presynaptic action potentials at 10-ms intervals were elicited with depolarizing current injections of 100–300 pA. Line scans along a curved line drawn on the image, passing through one or more collaterals and part of the calyx, were made continuously at 0.125–0.25- μ m per pixel at a pixel dwell time of 2 μ s. In addition, to correlate morphology and calcium transients, a z-stack was collected.

RESULTS

Relation Between Large Axosomatic Contacts and Synaptic Clusters.

Brainstem sections containing the MNTB at different postnatal ages were stained immunohistochemically for VGLUT, a presynaptic marker of excitatory synapses, and analyzed by using fluorescence microscopy (Fig. 1). At postnatal day 2 (P2) and younger ages, punctate labeling was observed both in the neuropil and around cell bodies in the MNTB. At P3 and beyond, large perisomatic presynaptic clusters (LPCs) of VGLUT staining were present (Fig. 1 A and B). The fraction of cells surrounded by LPCs increased with age. In the medial part of the MNTB, the increase was more rapid than in the lateral part (t test, $P < 0.001$; two animals per age and at least two images per animal; Fig. 1 C). We examined the relationship between the synaptic marker staining and axonal morphology by prelabeling the axons with a fluorescent tracer. At P3, large axosomatic contacts were observed, which stained positive for VGLUT, but only 30% of these contacts showed an LPC (Fig. 1 B, compare Left and Center, and D). In control P8 sections, the majority of large terminals could be associated with an LPC (Fig. 1 B, Right, and D). Therefore, it is unlikely that the fluorescent tracer interfered with the immunohistochemical marking of the presynaptic clusters at P3. Next, we used image segmentation and colocalization procedures to estimate the density and size of VGLUT clusters within labeled axons [see supporting information (SI) Materials and Methods]. This analysis showed only modest differences between axons at ages P1 and P3 (Fig. 1 E and F). In contrast, the relative volume of VGLUT clusters associated with large axosomatic contacts at P3 was clearly larger (Fig. 1 F). Overall, these results suggest that

most large axosomatic contacts take at most 1 day to form but that the packing of these early calyces with synaptic glutamatergic vesicles generally takes several days.

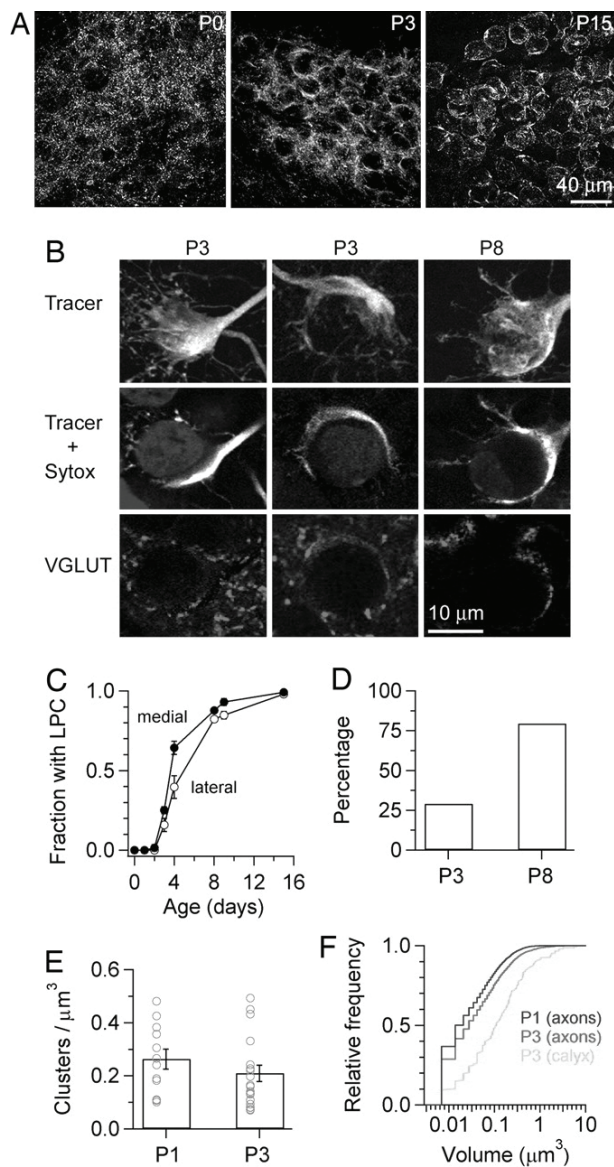


Figure 1. Presynaptic clusters during postnatal development.

(A) Confocal z-stack projections show the distribution of VGLUT label in the medial half of the MNTB at P0, P3, and P15. Lateral is right, dorsal is up. (B) Perisomatic labeling of VGLUT-positive clusters is revealed in triple-stained tissue. (Top) Z-stack projection of calyces

that were labeled with a fluorescent dextran (grey scale). (Middle and Bottom) Single confocal sections from the same focal plane demonstrating the location of the postsynaptic cell (counterstained with SYTOX) and the presynaptic clusters, respectively. (C) The fraction of perisomatic LPCs in medial and lateral regions of the MNTB increased during postnatal development. (D) Percentage of large axosomatic contacts that were colabeled with an LPC at P3 (31 contacts from three animals) and in control sections at P8 (29 contacts from one animal). (E) Density of presynaptic clusters in labeled axons at P1 and P3. (F) Cumulative histogram of presynaptic cluster volume for axons at P1 and P3 (dark grey and grey, respectively) and for calyces of Held at P3 (light grey; 31 labeled axons). Confocal images were contrasted with Adobe Photoshop.

Measurement of Synaptic Responses in Principal Cells During the Period of Calyx Formation.

Examination of labeled tissue at P3 showed the presence of relatively small presynaptic clusters outside the large axosomatic contact area (Fig. 1 B, Center), suggesting that synaptic terminals from nonlabeled axons were also contacting these postsynaptic cells. Therefore, we examined the possibility that principal cells receive synaptic inputs from multiple axons at ages P2–3. We made whole-cell recordings of principal cells in slices in which trapezoidal axons were prelabeled with a fluorescent tracer (see Fig. S1). In these experiments, excitatory postsynaptic currents (EPSCs) were evoked by electrical stimulation at the midline. Despite the prominent presence of delayed release (Chuhma & Ohmori, 1998), it was clear that the average amplitude increased with increasing stimulus intensity ($n = 10$ of a total of 10 cells; Fig. 2). Together with our histological analysis (see Fig. S1), the data are consistent with the recruitment of multiple axons with distinct activation thresholds. We conclude that during early postnatal development, MNTB cells receive small-amplitude glutamatergic contacts from multiple axons.

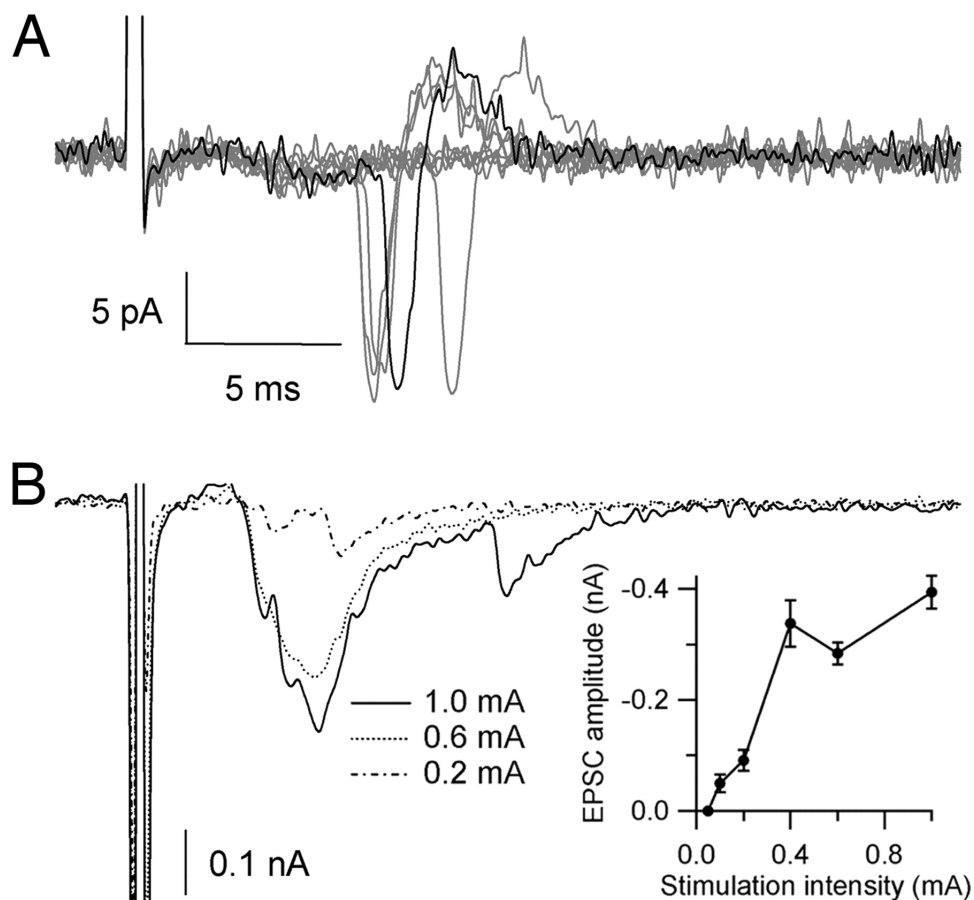


Figure 2. Multiple glutamatergic inputs to MNTB cells in neonate rats.

(A) Cell-attached recordings show action potential currents at 1-mA stimulation. (B) Whole-cell voltage-clamp recordings show the responses of the MNTB cell to different stimulation intensities (dashed-punctate, punctate, or continuous lines). (Inset) Input–output curve shows a graded increase in the amplitude of the EPSC with increasing stimulation intensity (mean \pm SEM, 10 traces per stimulus intensity). Note that EPSC amplitude is displayed as a vertical increase, and the negative sign indicates the inward current.

***In Vivo* Imaging of Axons and Synaptic Terminals in the MNTB of Neonate Rats.**

We used two-photon microscopy to image axons that had been prelabeled by injecting a fluorescent tracer in anesthetized rat pups (Fig. 3). In these acute experiments, we were able to visualize several individual axons, confirming the presence of calyx-like

structures at P3 (Fig. 3 A and B). Retrospective analysis confirmed that these structures were large axosomatic contacts located in the MNTB (see Fig. S2). Next, we reconstructed the trajectory of >100 axons in two-photon image stacks and measured the length and density of all visible extensions per axon (total measured axon length, 30 mm; average axon segment, $200 \pm 10 \mu\text{m}$, $n = 12$ rats). Cumulative histogram analysis of the length and number of axonal extensions suggested that during the 1st days of postnatal life, axons grow both by adding and by extending collaterals (Fig. 3 C and D).

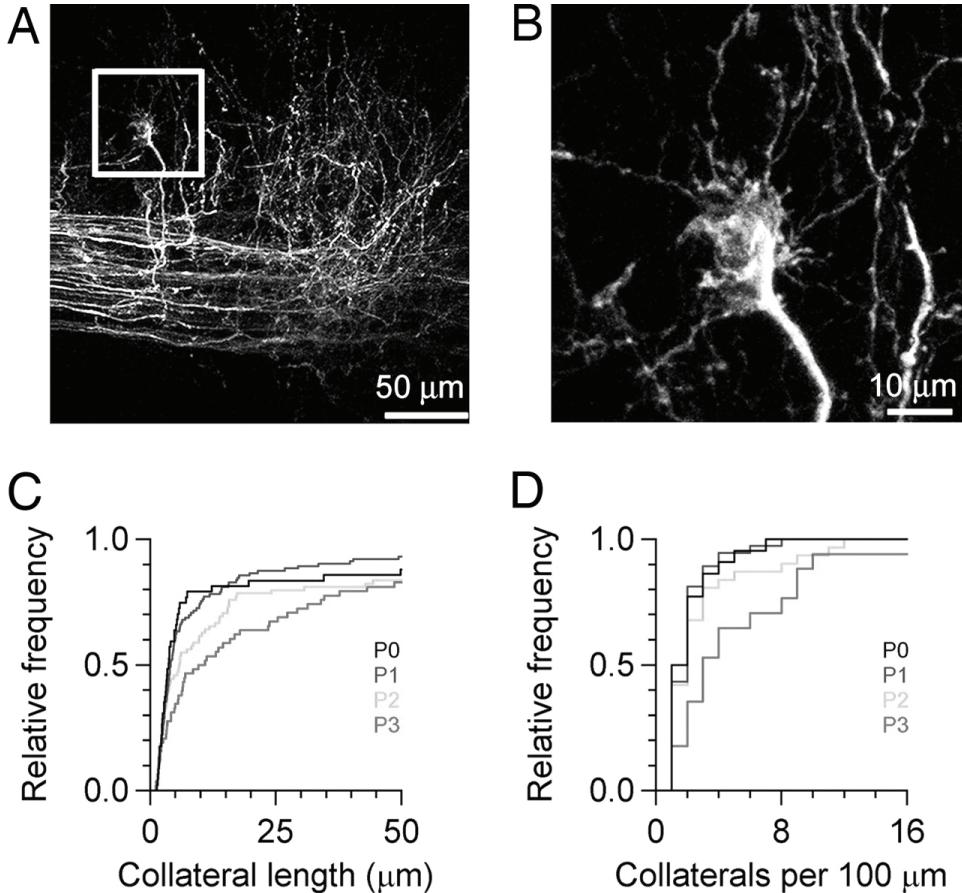


Figure 3. In vivo two-photon imaging in the MNTB of neonate rats.

(A) Exemplar image of labeled axons at P3. (Inset) Location of a calyx of Held terminal. (B) Close-up view of the labeled calyx in A. (C) Axon collateral length was traced in at least three z-stacks from different animals and plotted as a cumulative histogram. (D) Cumulative

histogram of the number of collaterals per 100 μm of axon. Two-photon images are collapsed z-stacks of >50 optical slices acquired at 1- μm intervals.

To study the dynamics of axon collateral growth, we carried out time lapse experiments in different animals between ages P1 and P3. A striking feature of the data was the dynamics of the axons. Whereas the average increase in the length of the collaterals between P0 and P3 was <10 μm per day, only approximately one-third of the axons were stable within the observation period of 1 h. Some collaterals formed from axonal shafts by interstitial growth (Portera-Cailliau *et al.*, 2005), whereas others extended, retracted or disappeared, within a time frame of minutes (Fig. 4 A–C). To quantify and compare the structural changes in a larger sample of imaged axons across different ages, we plotted the initial length of a total of 301 individual axon collaterals against their corresponding length 1 h later (Fig. 4 G). Using conservative criteria to score for changes in collateral length (see SI Materials and Methods), we identified five categories of axon collaterals: stable, added, lost, extended, and retracted (Javaherian & Cline, 2005).

The dynamics of the axons were age-dependent. P1 appears to be a period of expansion, with 21% of axons added and 24% extended, and only 3% lost and 14% retracted (see Table S1). At P2 and P3, close before and during the formation of calyx-type synapses, a large fraction of collaterals were either added or lost (P2: 24% added, 32% lost; P3: 25% added, 15% lost), with fewer collaterals changing their length (P2: 7% extended, 8% retracted; P3: 10% extended, 20% retracted). The calyx of Held collaterals were also dynamic at P3 (Fig. 4 D–F). Although the percentage of calyx collaterals that were added or lost within the 1-h observation period was smaller than of axon collaterals at the same age (14% added, 11% lost), the fraction of collaterals changing their length was similar to the situation at P1 (26% extended, 15% retracted).

The average length of the collaterals that formed or disappeared was typically much smaller than the collaterals that were in the stable, extended, or retracted category, except for P2, where relatively short collaterals were observed (see Table S2). In summary, these data show that axon and calyx of Held collaterals form interstitially and that a majority of the collaterals exhibit different levels of turnover (addition and loss) and motility (extension and retraction) across ages. Based on the observed structural dynamics in the calyx of Held terminal, we wondered whether the collaterals of the calyx of Held could have an involvement in synaptic function during postnatal development.

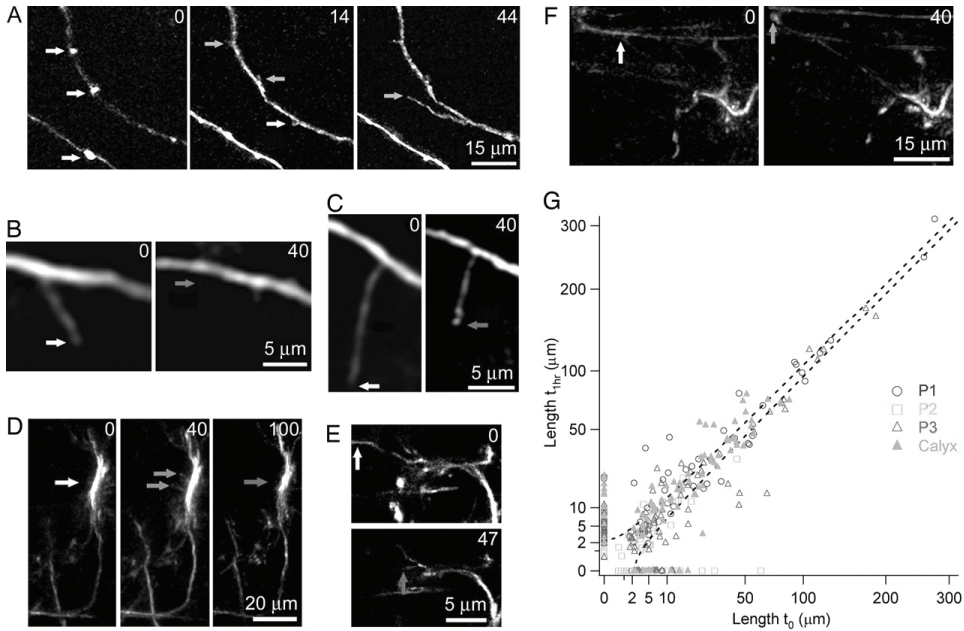


Figure 4. Turnover and motility of axon and calyx of Held collaterals.

Time lapse images were acquired at ages P1–3. (A) Sequence of images obtained at different time points shows three swellings on two labeled axons at P1 (Left, white arrows). One axon formed three short protrusions (Center, two formed near swellings, grey arrows, and one formed from the shaft of the axon, white arrow). Two of the small protrusions did not change, whereas the third one increased in length (Right, grey arrow). The second axon did not add branches within this time period, but some changes in the identified swelling were noticed. (B) Short axon collateral at P2 (Left, white arrow). In this case, the collateral could not be located anymore after 40 min, indicating that it was lost (Right, grey arrow). (C) Image sequence of an axon collateral at P2 (Left, white arrow) shows the retraction of the collateral tip (Right, grey arrow). (D) Time lapse imaging revealed the formation (Center, grey arrows) and loss (Right, grey arrow) of calyx of Held collaterals. (E) Retraction of a calyx of Held collateral (Lower, grey arrow). (F) Calyx of Held collateral (Left, white arrow) extended after 40 min (Right, grey arrow). (G) Plot of the initial collateral length vs. the corresponding length 1 h later. Data are compared between collaterals of the calyx of Held at P3 vs. axons at ages P1–3 as indicated by different shades of grey and symbols. Images are collapsed stacks of at least three optical slices acquired at $1\mu\text{m}$ intervals. Dashed black lines in G indicate the confidence interval for assigning a change in length (see SI Materials and Methods). (A–F) Numbers on the Top Right or Left corners indicate the time in minutes.

Functional Analysis of Calyx of Held Collaterals.

To test whether calyx of Held collaterals make functional synaptic contacts, we carried out paired patch clamp recordings in brain slices between a presynaptic terminal and an off-target MNTB cell. Presynaptic action potentials triggered small, short-latency EPSCs (Fig. 5 A and B). In these experiments, we were able to confirm a morphological apposition between the calyx of Held collateral and the dendrite of the postsynaptic cell ($n = 3$ connected pairs of 11 paired recordings at P4; Fig. 5 B, Inset). In two experiments, the slice was fixed, resectioned, and processed for VGLUT immunohistochemistry. Doing so confirmed the presence of an LPC in the recorded terminal and demonstrated that smaller, punctate presynaptic clusters can originate from calyx of Held collaterals (see Fig. S3). Interestingly, the MNTB cells did not generally show an LPC in connected pairs, although examples of cells with an LPC were observed in nonconnected pairs.

To determine whether MNTB cells with a calyceal input also received smaller inputs, possibly from collaterals of another calyx of Held, we tested the response of principal cells to afferent stimulation in slices at P4. These experiments indicated that MNTB cells with a large input also received short-latency, smaller-amplitude inputs (see Fig. S4).

Finally, we carried out experiments in which we loaded calyx terminals with the calcium dye Oregon green BAPTA-1. We then triggered a sequence of four action potentials at 100 Hz by current injection via the patch pipette while measuring fluorescence by rapidly scanning along a line through both calyx and its collaterals. Action potential-evoked calcium transients were observed in 31 of a total of 41 collaterals from 14 calyces (seven animals, ranging from P5 to P8). Calcium transient amplitudes in collaterals ranged from 15 to 100% $\Delta F/F_0$ and were generally somewhat smaller than the calcium transient evoked simultaneously in the calyx, where the average response ranged from 25 to 125% $\Delta F/F_0$. In some cases, collateral transients were localized to thickenings (Fig. 5 C and D). Interestingly, although their time course generally matched the time course of the calcium transients evoked simultaneously in the calyx, both the time course and the amplitudes of the calcium transients varied considerably, not only within a single collateral (Fig. 5 D) but also within one calyx (data not shown). We conclude that many calyx of Held collaterals can make functional contacts with off-target principal cells and that voltage-dependent local increases in calcium are available to support chemical transmission in these structures.

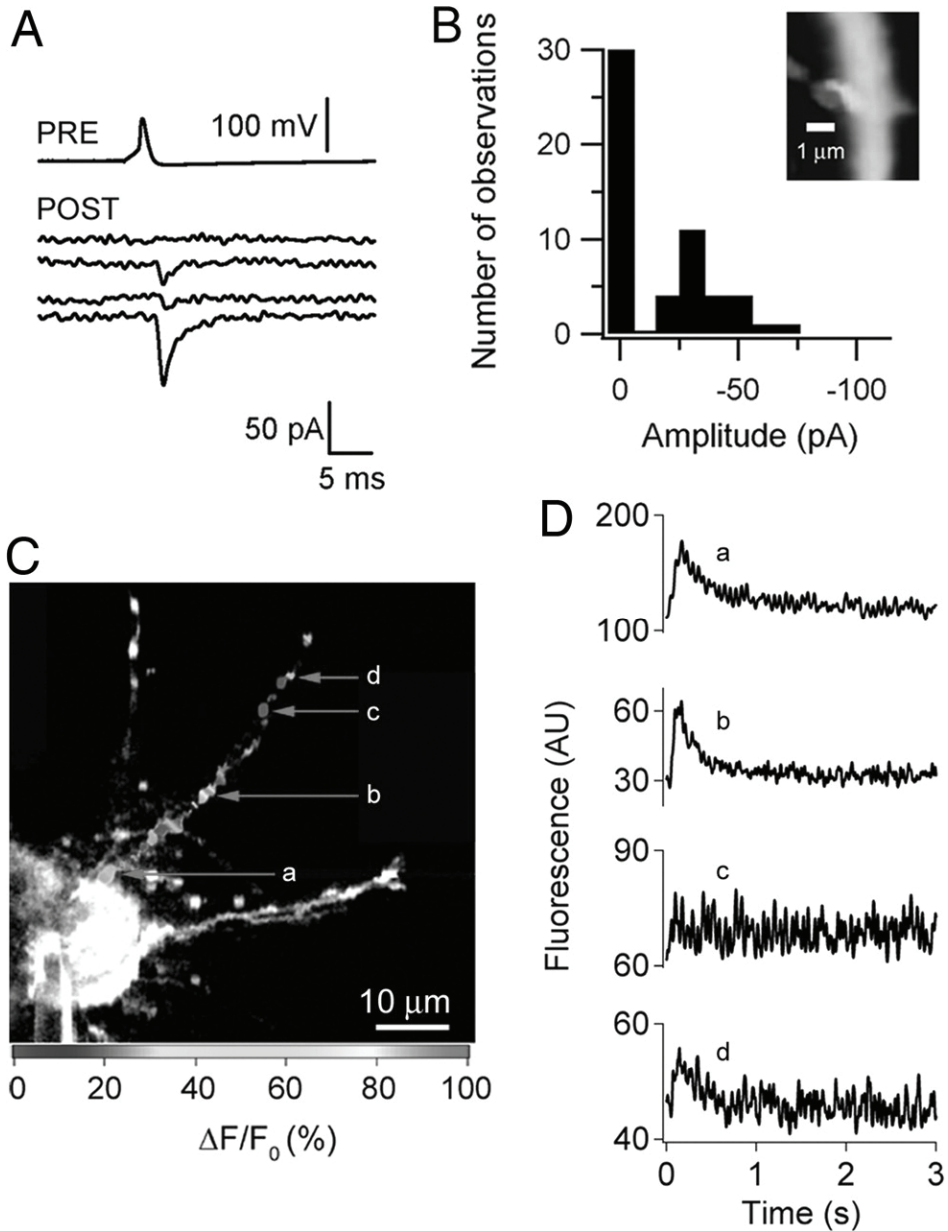


Figure 5. Calyx of Held collaterals can form functional synapses on adjacent principal cells. Paired recordings between a calyx of Held and a nearby principal cell were performed in acute slices at P4. (A) Presynaptic action potentials were triggered in current clamp mode in the calyx (PRE) by injecting 0.3 nA for 2 ms at 0.2 Hz, whereas EPSCs were measured in voltage clamp in the postsynaptic cell (POST). After presynaptic action potentials, a failure, two

small responses, and a larger response were observed in the postsynaptic recording. Postsynaptic traces have been vertically offset for display purposes. (B) Amplitude distribution of EPSCs. Note the presence of failures after >50% of the stimulations. Bin size is 10 pA. (Inset) Contact region between the calyx of Held collateral (dark grey) and a spine-like structure on the dendrite of the postsynaptic MNTB cell (light grey). Note the inverted horizontal axis, with larger EPSCs being more negative. (C) Localized AP-evoked calcium transients in a calyx of Held collateral filled with OGB-1 using a patch pipette. The color code for the spatial distribution of the peak $\Delta F/F_0$ fluorescence is shown on the Bottom. (D) Representative calcium transients recorded during rapid line scanning at locations a–d indicated in C.

Time Course of Pruning of the Calyx of Held Collaterals.

The calyx of Held undergoes a dramatic functional and structural transformation between the 2nd and 3rd postnatal weeks (Kandler & Friauf, 1993; Taschenberger *et al.*, 2002; Wimmer *et al.*, 2006). To evaluate the stereotypical pruning of the calyx of Held collaterals, we injected fluorescent tracers in brain slices to label axons in the MNTB between postnatal ages P3 and P16. We then imaged labeled calyces and traced the collaterals to determine the age-dependent changes in length and number of collaterals. Both collateral length and number decreased with age (Fig. 6). Collateral length showed a gradual decrease, whereas collateral number showed more abrupt changes between P12 and 13 and between P13 and 16. These data show that a decrease in collateral length already begins at P4, 1 week before the onset of hearing, which in the rat takes place \approx P10–12 (Uziel *et al.*, 1981) but continues afterward. Based on the electrophysiological, optical, and morphological data, we conclude that pruning of the calyx of Held collaterals results in the elimination of synapses in the MNTB.

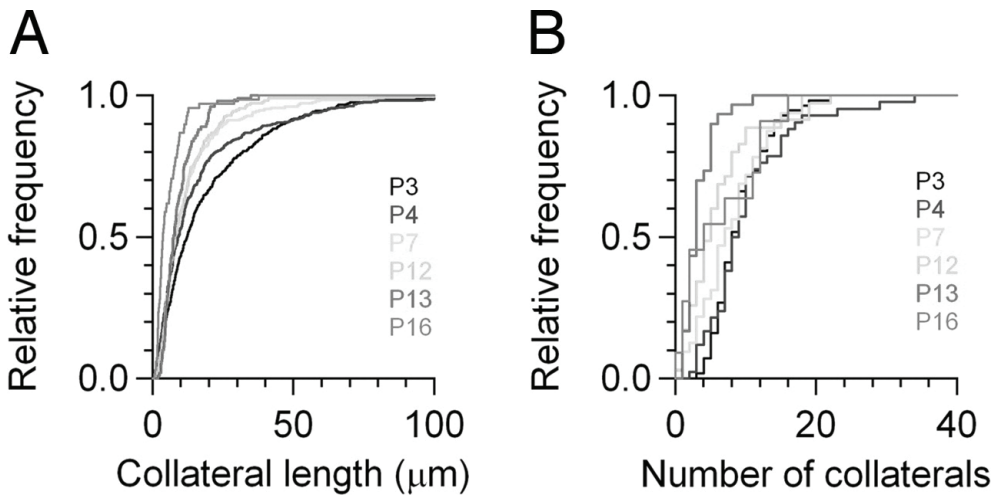


Figure 6. Calyx of Held collaterals are pruned during postnatal development.

Axons were labeled in brain slices, fixed, and imaged with a confocal microscope. The length and number of collaterals were traced at different ages. (A) Cumulative histogram of collateral length shows a gradual decrease in collateral length between P3 and P16. (B) Cumulative histogram of the number of branches per calyx shows abrupt changes between P13 and P16.

DISCUSSION

In this work, we show that it is possible to perform *in vivo* two-photon imaging of developing axons in the mammalian brainstem. In combination with immunohistochemistry and cell physiology, we show evidence that the development of the calyx of Held synapse consists of two stages. In the first 3 postnatal days, a surprisingly high level of collateral dynamics in both axons and nascent synaptic terminals was observed, and principal cells received synaptic inputs from multiple axons. During this period, formation of a calyx synapse took place on the majority of principal cells at P3. In the second phase, which continued at least until the onset of hearing, large presynaptic clusters of VGLUT-positive vesicles appeared, and the calyx of Held collaterals gradually disappeared, although we showed that during this period collaterals of nascent calyces were able to sustain synaptic transmission with other MNTB cells.

Comparison with Previous Studies.

We find that the calyx of Held largely forms around P₃ but that there is a much slower phase of refinement during which the calyceal collaterals gradually disappear. To the extent that a comparison is possible, this time course matches earlier experiments performed in rat, cat, mouse, or gerbil (Morest, 1968b; Kandler & Friauf, 1993; Kil *et al.*, 1995; Hoffpauir *et al.*, 2006), suggesting that the development of this synapse is highly conserved across species. The essential steps are happening largely before the onset of hearing, supporting the view that sensory activity does not play a major role in the formation of this synapse (Hoffpauir *et al.*, 2006; Erazo-Fischer *et al.*, 2007; Youssoufian *et al.*, 2008). The formation of the large presynaptic clusters of glutamatergic vesicles was also surprisingly slow. Although we did not directly correlate these stainings with synaptic transmission, our data suggest that one should be cautious in using the amplitude of postsynaptic currents to identify calyceal inputs (Futai *et al.*, 2001; Bergsman *et al.*, 2004; Hoffpauir *et al.*, 2006), without additional criteria such as immunohistochemistry or the presence of a prespike.

Origin and Functional Properties of the Calyceal Collaterals.

The calyceal collaterals were already identified in the first Golgi studies (Morest, 1968a), but it was unknown what their functional significance was and whether they formed before or after the calyx. We present evidence from immunohistochemistry, calcium imaging, and electrophysiology that the calyceal collaterals can innervate adjacent principal cells. Using *in vivo* two-photon imaging, we could directly observe the addition of new calyceal collaterals. The emergence of collaterals from the calyx of Held is in agreement with what has been observed at the frog neuromuscular junction, where differentiated presynaptic sites are hot spots for the emergence of new branches (Javaherian & Cline, 2005). Interestingly, the turnover of calyx of Held collaterals showed a balance between additions and losses that was not present in axon collaterals at the same age. Studies in cultured neurons (Ahmari *et al.*, 2000) and in living animals (Alsina *et al.*, 2001; Hu *et al.*, 2005; Meyer & Smith, 2006; Ruthazer *et al.*, 2006) have shown a link between branch dynamics and the presence and strength of synaptic terminals. Therefore, it is tempting to speculate that the calyx of Held could stabilize the axonal arbor. We obtained indirect evidence that some calyceal collaterals formed already before the calyx. We showed that MNTB principal cells receive multiple inputs at P_{2–3} and that principal cells receive small- and large-amplitude inputs at P₄. The small inputs differed from the noncalyceal inputs described (Banks & Smith, 1992; Hamann *et al.*, 2003; Hoffpauir *et al.*, 2006) because their threshold differed only

slightly from the larger inputs and they typically had short latency and fast rise times. A parsimonious interpretation of these findings is that some calyx of Held collaterals are remnants of the initially divergent innervation of principal cells by afferent axons.

How Does Each Principal Cell End Up with a Single Calyx of Held?

We observed that the postnatal axons that ultimately form the calyx of Held are very dynamic, suggesting that they are actively exploring the local environment. With the 1-h sampling period, we may have even underestimated the dynamics (Witte *et al.*, 1996). It is tempting to speculate that the dynamic behavior of these axons and synaptic terminals increases the number of principal cells that are contacted by each axon and thereby increases the flexibility and reliability of the mechanism that ensures the one-to-one innervation of this auditory pathway. The mechanisms that favor the formation of a calyx of Held from its axonal precursors are independent of sensory function. They deserve further study, and we expect that the *in vivo* imaging approach that we present here will help toward the further elucidation of the different steps involved in the formation of this synapse.

Chapter 3

Post-Tetanic Potentiation in the rat calyx of Held synapse

Ron L. P. Habets and J. Gerard G. Borst

J Physiol. 2005 Apr 1;564(Pt 1):173-87

ABSTRACT

We studied synaptic plasticity in the calyx of Held synapse, an axosomatic synapse in the auditory brainstem, by making whole-cell patch-clamp recordings of the principal cells innervated by the calyces in a slice preparation of 7-10 day old rats. A five minute 20 Hz stimulus train increased the amplitude of excitatory postsynaptic currents (EPSCs) on average more than twofold. The amplitude of the synaptic currents took several minutes to return to control values. The post-tetanic potentiation (PTP) was accompanied by a clear increase in the frequency, but not the amplitude of spontaneous EPSCs, which returned back to baseline more rapidly than the potentiation of evoked release. The size of the readily releasable pool of vesicles was increased by about 30%. In experiments in which presynaptic measurements of the intracellular calcium concentration were combined with postsynaptic voltage clamp recordings, PTP was accompanied by an increase in the presynaptic calcium concentration to about 210 nM. The decay of the PTP matched the decay of this increase. When the decay of the calcium transient was shortened by dialyzing the terminal with EGTA, the PTP decay sped up in parallel.

Our experiments suggest that PTP at the calyx of Held synapse is due to a long-lasting increase in the presynaptic calcium concentration following a tetanus, which results in an increase in the release probability of the vesicles of the readily releasable pool. Although part of the PTP can be explained by a direct activation of the calcium sensor for phasic release, other mechanisms are likely to contribute as well.

INTRODUCTION

The calyx of Held is a large glutamatergic nerve terminal that synapses onto glycinergic principal cells in the medial nucleus of the trapezoid body (MNTB). The MNTB acts as a sign-inverting relay in the process of localizing sound (Grothe, 2003). The view of a synapse that faithfully transmits the presynaptic action potentials is at odds with the multitude of different forms of synaptic plasticity that have been observed in a slice preparation of the MNTB (von Gersdorff & Borst, 2002). During brief stimulus trains, the responses generally depress. If the release probability is lowered, a short-term facilitation of responses is uncovered (Borst *et al.*, 1995). It is not yet known whether this synapse displays post-tetanic potentiation (PTP) following longer stimulus trains.

PTP is a form of synaptic enhancement with a duration in the order of minutes (Fisher *et al.*, 1997; Zucker & Regehr, 2002). In several preparations PTP is accompanied by a long-lasting increase in the presynaptic calcium concentration, which decays with a similar time course as the PTP. We will refer to this long-lasting increase in calcium concentration as “residual calcium”, a term coined for the calcium ions that linger in the terminal after an action potential, which are essential for short-term facilitation (Katz & Miledi, 1968). However, in contrast to the increase in presynaptic calcium concentration involved in facilitation, part of the sustained calcium transient following a tetanus may be due to exchange of sodium ions that accumulate in the presynaptic cytoplasm during the tetanus for calcium ions (Lev-Tov & Rahamimoff, 1980). The sustained calcium increase is thought to be insufficient to directly activate the calcium sensor for phasic release, both in the case of short-term facilitation and of PTP (Zucker & Regehr, 2002). However, a direct test of the involvement of the phasic calcium sensor in short-term facilitation in the calyx of Held synapse showed that it is responsible for up to 30% of the increase in transmitter release (Felmy *et al.*, 2003). In the case of PTP, several alternative mechanisms have been proposed to contribute to the increase in transmitter release, including an increase in calcium influx during an action potential, saturation of an endogenous calcium buffer, the presence of a separate, high-affinity calcium sensor, an increase in the number of releasable vesicles, or the modification of their release probability through an effect of second messengers such as protein kinase C (PKC) or protein kinase A (PKA).

The calyx of Held synapse has distinct advantages for studying the mechanisms of short-term plasticity (von Gersdorff & Borst, 2002). Presynaptic calcium dynamics have been well characterized (Meinrenken *et al.*, 2003). It is possible to discriminate between changes in release probability and changes in the readily-releasable pool (Schneggenburger *et al.*, 2002). In this paper, we show that PTP can be induced at the calyx of Held synapse. We explore different possible mechanisms, including changes in

action potential waveform, a direct activation of the presynaptic calcium sensor, changes in the releasable pool and postsynaptic changes.

A preliminary account of the data has been published in Abstract form (Habets *et al.*, 2003).

MATERIALS & METHODS

Preparation of slices

Preparation of slices and electrophysiological measurements were done as described previously (de Lange *et al.*, 2003). Animal procedures were in accordance with guidelines provided by the animal committee of the Erasmus MC.

In brief, seven to ten day old Wistar rats were decapitated without prior anaesthesia. The brainstem was dissected and immersed in ice-cold saline containing (in mM): 125 NaCl, 2.5 KCl, 3 MgSO₄, 0.1 CaCl₂, 1.25 NaH₂PO₄, 0.4 ascorbic acid, 3 myo-inositol, 2 pyruvic acid, 25 D-glucose, 25 NaHCO₃ (Merck); pH 7.4 when bubbled with carbogen (95% O₂, 5% CO₂); osmolarity 320 mOsmol. Transverse slices of 200 µm thickness were cut with a vibratome (Vibratome, St. Louis, MO). Slices were transferred to a holding chamber containing normal Ringer solution, which had the same composition as the solution that was used for slicing, except that the concentration of CaCl₂ and MgSO₄ were 2 and 1 mM, respectively. Slices were incubated for 30 minutes at 37 °C. Thereafter, they were kept at room temperature until they were used.

Electrophysiological recordings

Slices were transferred to a recording chamber, which was continuously (2 ml min⁻¹) perfused with normal Ringer solution. In some experiments kynurenic acid (2 mM; Tocris, Bristol, UK) was added, to reduce postsynaptic receptor saturation and desensitization. Neurons were visualized with an upright microscope (BX-50; Olympus, Tokyo, Japan), equipped with infrared differential interference contrast optics. Axons originating from the cochlear nucleus were stimulated (0.1 ms, 0.03-0.5 mA) in the midline by a bipolar electrode (Frederic Hear & Co, Bowdoinham, ME). Cells were selected when extracellular recordings indicated postsynaptic action potential firing (Borst *et al.*, 1995). Electrophysiological recordings were made at room temperature with an Axopatch 200B amplifier (Axon Instruments, Union City, CA). Pipette solutions contained (in mM): 125 K-gluconate, 20 KCl, 10 Na₂-phosphocreatine, 4 MgATP, 0.3 Na₂GTP, 10 HEPES (Sigma) and 0.05 fura-2 (Molecular Probes, Eugene, OR) or 0.5 EGTA for pre- or postsynaptic recordings, respectively. Holding potential in voltage clamp experiments was -80 mV. Potentials were corrected for a -11 mV junction potential. Postsynaptic series resistance (<15 MΩ) was electronically compensated by 80-98% with a lag of 5 µs. Signals were low-pass (2 kHz) filtered with a 4-pole Bessel filter. Only cells with a membrane resistance higher than 100 MΩ were accepted for analysis. Signals were sampled at 20-50 kHz with a Digidata 1320A (Axon

Instruments). Data acquisition and analysis was done with pClamp 8 (Axon Instruments) or Igor (Wavemetrics, Lake Oswego, OR).

Imaging

Terminals were pre-filled with fura-2 for 10 min via the patch pipette. Only cells in which a GΩ outside-out patch formed after retraction were selected for analysis. The tissue was illuminated through a 40X objective (NA 0.8, Olympus, Tokyo, Japan) by a monochromator (Polychrome IV; 8 nm bandwidth, TILL Photonics, Martinsried, Germany). Emission light was filtered through a 525/80 bandpass filter and detected with a cooled CCD camera (Sensicam, PCO, Kelheim, Germany). Every 30 seconds, a set of two images was taken at 360 nm (isosbestic) and at 380 nm (calcium-sensitive wavelength). Images were integrated for 100 ms and binned 4x4 on the CCD chip. Calcium concentrations were calculated using a standard equation for ratiometric dyes (Grynkiewicz *et al.*, 1985):

$$[Ca^{2+}] = K_{eff} \frac{(R - R_{min})}{(R_{max} - R)} \quad (1),$$

where R is the background-corrected fluorescence ratio F_{360}/F_{380} ; R_{max} (4.64 ± 0.98 , $n = 3$) and R_{min} (0.74 ± 0.02 , $n = 3$) were the fluorescence ratio in terminals filled with pipette solution plus 1 mM $CaCl_2$ or 10 mM EGTA, respectively and $K_{eff} = K_d \cdot (R_{max}/R_{min})$. For the dissociation constant (K_d) of fura-2, a value of 273 nM was assumed (Helmchen *et al.*, 1997).

Data analysis

The average EPSC amplitude at a stimulation frequency of 0.1 Hz was taken as baseline. The amount of PTP was calculated as the percentage increase of the average amplitude of the first three EPSCs after tetanic stimulation relative to the average amplitude of the last three EPSCs before the tetanus. The readily-releasable pool (RRP) size was estimated by summing the EPSC amplitudes evoked by a 100 or 200 Hz train of action potentials, after subtraction of the steady state component (Elmqvist & Quastel, 1965; Schneggenburger *et al.*, 1999). An estimate of the release probability (P_r) was obtained by dividing the EPSC amplitude by the RRP size. The decay $A(t)$ of the increases in release or calcium was fitted with a single exponential function with time constant τ :

$$A(t) = A_0 e^{(-t/\tau)} + B \quad (2),$$

where A_0 is the increase in amplitude directly after the tetanus ($t=0$) and B is the average amplitude during the baseline period.

Spontaneous release events were identified using Clampfit 9.0 (Axon Instruments) by a template made of averaged, manually selected, spontaneous EPSCs.

Data are given as mean \pm standard error of the mean (SEM). Statistical comparisons were done using Student's t -test.

THEORY

Relation between the time course of residual calcium and PTP

In this section we will explore theoretically whether changes in the intracellular calcium concentration, the affinity of the calcium sensor for calcium or the power relation between calcium and transmitter release may differentially affect the time course of the decay of the potentiation of spontaneous and of action-potential evoked release.

Phasic transmitter release depends strongly on the local calcium transient experienced by the releasable vesicles during an action potential. For low release probabilities, it has been observed at many synapses that release is proportional to the intracellular calcium concentration raised to a power m of about 4 (Augustine, 2001). However, for increasing calcium concentration, this release probability will eventually reach a maximum, at which point an action potential releases all vesicles of the readily-releasable pool. As a simple approximation, we therefore assume that the release probability of the vesicles in the readily-releasable pool during an action potential (P_r) is described by a Hill equation (Reid *et al.*, 1998):

$$P_r = 1/(1 + F^m) \quad (3),$$

and $F = K_d/[Ca]$. K_d is the $[Ca]$ at which half-maximal activation of the calcium sensor occurs.

Although there are more realistic schemes available for the binding of Ca^{2+} to the calcium sensor, this equation does provide an excellent fit of Fig. 2D in (Meinrenken *et al.*, 2003); results not shown). From this equation it is apparent that a potentiation of evoked release can be due to a change in m , K_d and/or in $[Ca]$.

We define β as the fractional change in F after a tetanus:

$$F = F_c - \beta F_c \quad (4)$$

where F_c is the value of F before the tetanus.

The release probability will then be:

$$P_r = 1/(1 + (F_c(1 - \beta))^m) \quad (5),$$

As long as $\beta \ll 1$, the first Taylor polynomial, $f(1 - \beta) = f(1) - \beta f'(1)$:

$$P_r \approx 1/(1 + (F_c)^m) + \beta m (F_c)^m / (1 + (F_c)^m)^2 \quad (6)$$

represents a good approximation of this function. Therefore, for constant m , as long as changes in F are small, they can be well approximated by a linear function of the relative changes in F . If these changes are linearly dependent on residual calcium, the change in release probability of action-potential-driven release after the tetanus can also be approximated by a linear function of residual calcium. For most terminals, m is around 4 and P_r ranges between 0.05 and 0.5 (Augustine, 2001; Zucker & Regehr, 2002). This means that F ranges between 1 and 2. Therefore, a 5% increase or decrease in F (due to a change in K_d or $[Ca]$) will lead to a 10-20% change in P_r . The linear approach is accurate within 10% for F between 1 and 2, as long as the changes in F are less than 10%.

Analogously, one can define γ as the fractional change in m after the tetanus. In that case:

$$P_r = 1/(1 + F^{m_c(1-\gamma)}) \quad (7)$$

where m_c is the value of m before the tetanus. For $\gamma < 1$, the first Taylor polynomial

$$P_r \approx 1/(1 + F^{m_c}) + \gamma m F^{m_c} \ln(F) / (1 + (F)^{m_c})^2 \quad (8)$$

again proves to be a good approximation, with small changes in m leading to $\ln(F)$ times larger changes in P_r than the same fractional changes in F . This means that for spontaneous release, the relative increase will be clearly larger than for evoked release, since F is much smaller in the latter case. The linear approach is accurate to within 10% for values of F between 1 and 2, as long as changes in m are less than 15%.

Consequences for decay time course

From Equations 6 and 8 we conclude that as long as the fractional changes in F or in m after the tetanus are small, the potentiation is well approximated by a linear function of β or γ , respectively. What does this mean for the time course of PTP? As an example, we assume that the change in F (or in m) returns back to its original value with the same time course as the residual calcium. Then, if the decay of residual calcium is well approximated by a single exponential function with time constant τ_{Ca} , the decay of PTP will also show an exponential decay, with time constant τ_{PTP} equalling τ_{Ca} .

A comparison of the effect of changes in K_d and $[Ca]$ after the tetanus on spontaneous and evoked release yields some interesting differences. Assuming that the same sensor is responsible for evoked and for spontaneous release, it can be seen that small fractional changes in F will lead to approximately m times larger changes in release. Therefore, an (isolated) change in K_d that leads to a 10% change in evoked release, will lead to a change in the spontaneous frequency that is also only about 10%. The same is obviously not true for changes in $[Ca]$. An increase in the calcium transient that is experienced by a vesicle of the readily-releasable pool during an action potential can be due to residual calcium, depletion of calcium buffers that compete with the phasic calcium sensor, or an increased calcium influx. The latter two will not affect spontaneous release. In contrast, changes in evoked release due to a direct effect of residual calcium will lead to a much larger effect on the spontaneous release, since the relative change of the calcium concentration will be much larger for the spontaneous release. What does this mean for the decay of the potentiation of spontaneous release? As long as the residual calcium concentration is much smaller than the K_d of the calcium sensor, F^m in equation (3) is much larger than 1 and eq. 3 can be approximated by:

$$P_{r, \text{spont}} \approx ([Ca]/K_d)^m \quad (9)$$

As long as residual calcium is much larger than basal calcium, the contribution of basal calcium to release and the contribution of calcium-independent spontaneous release can both be neglected. In the absence of changes in K_d , if spontaneous release after the tetanus is proportional to residual calcium raised to the power m , it follows that the decay of the spontaneous release rate to basal values after the tetanus will be proportional to the decay of residual calcium raised to a power m :

$$P_{r, \text{spont}}(t) \propto (e^{-t/\tau_{Ca}})^m = e^{-mt/\tau_{Ca}} \quad (10)$$

Therefore, as long as $m > 1$, spontaneous release is expected to decay more rapidly than evoked release under these conditions.

In conclusion, synaptic potentiation that is caused by a direct effect of residual calcium on the phasic calcium sensor is predicted to result in differential decay of the potentiation of spontaneous and of evoked release. Additional, indirect effects may also differentially affect spontaneous and evoked release. A decrease of competing endogenous calcium buffer due to saturation (Neher, 1998), or an increase in calcium influx due to calcium current facilitation will specifically promote evoked release. A change in K_d of the phasic calcium sensor will also affect spontaneous release, however, the effects are predicted to be relatively small.

RESULTS

Post-tetanic potentiation at the calyx of Held

To study plasticity at the calyx of Held synapse, the axons leading to the calyces were stimulated with a 20 Hz tetanus for five minutes. During the tetanus, the EPSCs showed prominent synaptic depression (Fig. 1). However, after the train, the amplitude of the EPSCs was increased by $123 \pm 22\%$ (mean \pm SEM; range 25-452%; $n = 23$). In the example shown in Fig. 1B, the EPSC amplitude at a holding potential of -80 mV increased from -1.6 nA before the 20 Hz stimulation to -4.7 nA after the tetanus. The increase in EPSC size decayed back to baseline over a time course of minutes, as shown in detail below, and was therefore classified as post-tetanic potentiation (Fisher *et al.*, 1997; Zucker & Regehr, 2002).

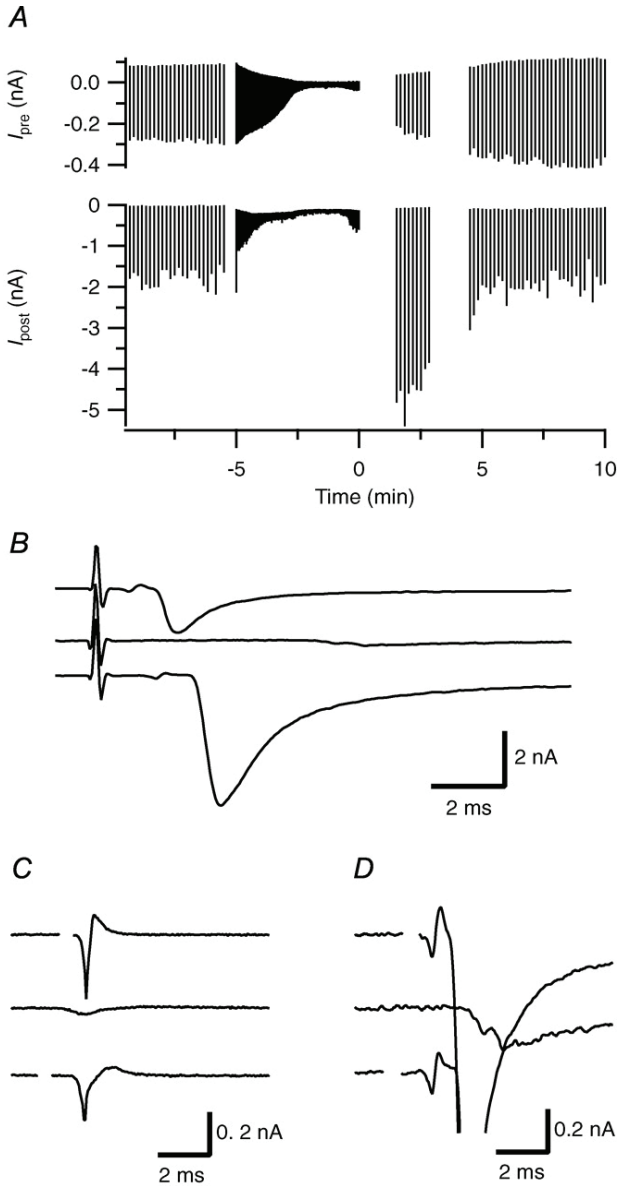


Figure 1. Post-tetanic potentiation at the calyx of Held synapse.

Cells were stimulated by an electrode placed in the ventral midline of the slice. A baseline period of 0.1 Hz stimulation preceded a 20 Hz tetanus of five minutes. One to two minutes after the tetanus, EPSCs were again evoked at 0.1 Hz. Before and after the tetanus, stimulation was interrupted to measure spontaneous release. A, Top traces: presynaptic recording in cell-attached configuration. Bottom traces: EPSCs simultaneously recorded in

postsynaptic whole-cell configuration. B, Postsynaptic recording. Top trace: last EPSC of the baseline period. Middle: response to last stimulus of the 5 min, 20 Hz tetanus. Bottom: first EPSC, evoked 1 min after the tetanus. C, Presynaptic traces at the same time points as the signals shown in B, shown at high magnification to illustrate the changes in the cell-attached presynaptic action potential. D, enlargement of the prespikes preceding the EPSCs shown in B. Signals in C and D were aligned on the negative peak of the recorded presynaptic action potential. In A, C and D, stimulation artifacts were removed. In the postsynaptic recordings shown in A, prespikes were removed as well.

The presynaptic action potential

A change in the shape of the presynaptic action potential will result in a change in calcium influx. During high frequency trains, an increase of the action potential width will broaden calcium influx at this synapse (Borst & Sakmann, 1999b). Since EPSC size critically depends on calcium influx, we measured the action potential during and after tetanic stimulation. However, during presynaptic whole-cell current clamp recordings, the EPSCs suffered from use-dependent rundown (data not shown). The presynaptic action potential was therefore monitored either in cell-attached recordings (Fig. 1A,C) or as a prespike (Forsythe, 1994) in postsynaptic recordings (Fig. 1B,D). During the tetanus the prespike amplitude (Fig. 1B,D, middle) was reduced, often disappearing into the noise. Only half of the cells fired action potentials throughout the 5 min, 20 Hz tetanus. In the other half, presynaptic action potential failures were apparent. Action potential failures were more pronounced in seven and eight day old rats than in nine or ten day old rats. However, there was no clear correlation between the ability of the terminal to follow the stimulus and the amount of PTP. One minute after the tetanus, the difference between the negative and the positive peak of the prespike was significantly decreased to $76 \pm 5\%$ of control ($p < 0.01$; $n = 19$). At the same time, the time between the negative and the positive peak of the prespike increased by $25 \pm 11 \mu\text{s}$ ($p < 0.05$). In whole cell recordings, changes in AP shape were small (results not shown).

We conclude that the PTP was accompanied by a change in the presynaptic action potential shape, which is expected to result in a change in calcium influx. The relative change in prespike amplitude was not correlated with differences in the amount of PTP between experiments. After the tetanus, the interval between the stimulation artifact and the prespike increased by at least 0.1 ms in 15 of 19 experiments (Fig. 1B). Following the tetanus, the average increase was 0.44 ± 0.09 ms ($p < 0.01$; $n = 19$). The interval between the peak of the presynaptic cell-attached recording and the peak of the EPSC also increased significantly.

Spontaneous release

To discriminate between pre- and postsynaptic mechanisms for the generation of PTP, we measured the amplitude and frequency of spontaneous release in principal cells before and in the first minute after the tetanus (Fig. 2*A,B*). Although changes in amplitude of the spontaneous EPSCs comparable to the results shown in Fig. 2*C* could be found in four out of eight experiments, on average the amplitude of the spontaneous EPSCs was 35.5 ± 1.6 pA before and 37.2 ± 2.5 pA after the tetanus, which was not significantly different (Fig. 2*D*; $p = 0.25$).

In contrast to the lack of changes in the average amplitude of the spontaneous EPSCs, their frequency clearly increased (Fig. 2*B*). On average the frequency increased from 0.91 ± 0.45 Hz before the tetanus to 8.65 ± 1.6 Hz after the tetanus (Fig. 2*E*; $n = 8$).

The increase in frequency of spontaneous events following a tetanus, without a significant effect on their size indicates that PTP at the calyx of Held synapse -similar to the situation at most other synapses that have been studied (Zucker & Regehr, 2002) - is a presynaptic form of synaptic plasticity.

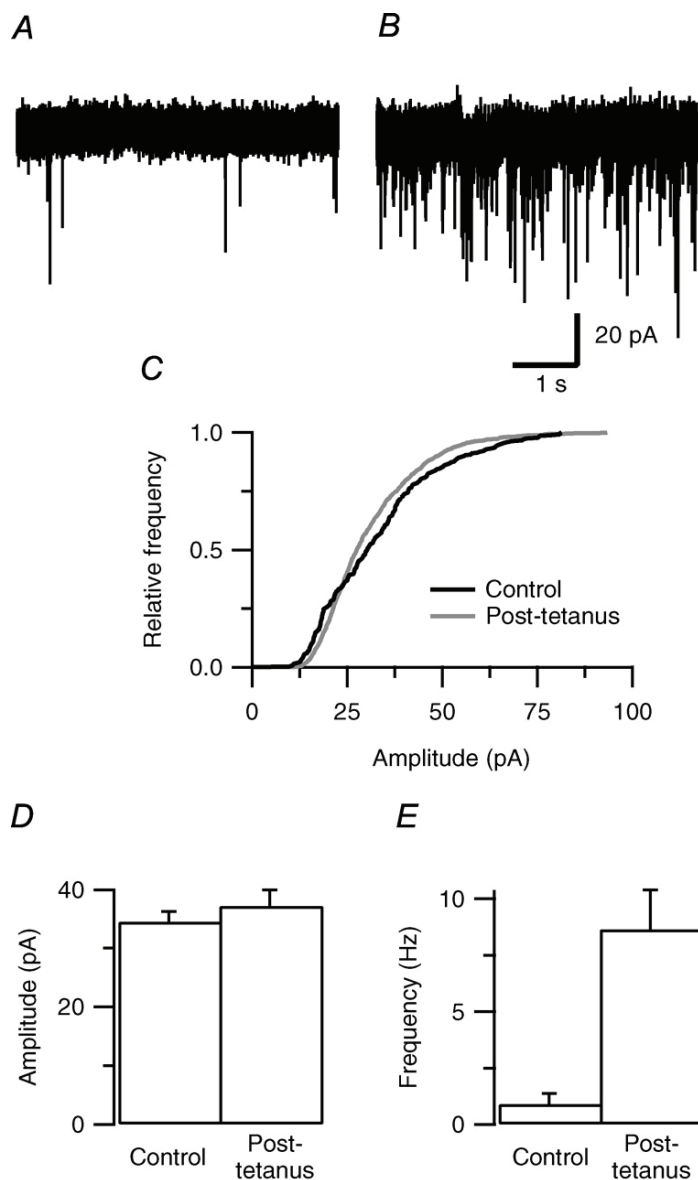


Figure 2. Increase of spontaneous release after a 5 min, 20 Hz tetanus.

A, Postsynaptic voltage-clamp recording before the tetanus. *B*, Increase in frequency of spontaneous EPSCs directly following the tetanus. *C*, Cumulative amplitude distribution of the spontaneous EPSCs of the experiment illustrated in *A* and *B*. *D*, Average amplitude of the spontaneous EPSCs (8 cells). *E*, Mean of the average frequency of spontaneous EPSCs ($n = 8$).

Pool size and release probability

After establishing that the mechanism underlying PTP had a presynaptic origin we considered two mechanisms: an increase in the number of vesicles immediately available for release (the “readily-releasable pool”, RRP) or an increase in the probability of release of the available vesicles (P_r). To distinguish between these two mechanisms, we estimated the RRP and P_r from the amplitudes of EPSCs elicited by a high frequency train before and after tetanization (Schneggenburger *et al.*, 1999; Wu & Borst, 1999); Fig. 3A). We waited one minute after the tetanus to ensure that replenishment of the RRP was complete (Wu & Borst, 1999). After the tetanus, a small ($22 \pm 6\%$, $n = 9$) but significant ($p < 0.01$) increase in the RRP estimate was seen (Fig. 3B). To minimize possible confounding effects of postsynaptic receptor saturation and desensitization, we repeated these experiments in the presence of the competitive glutamate receptor antagonist kynurenic acid (Wu & Borst, 1999; Neher & Sakaba, 2001; Wong *et al.*, 2003). Kynurenic acid (2 mM) reduced the amplitude of the EPSCs to $5.1 \pm 0.8\%$ ($n = 6$) of control. In agreement with earlier results (Wong *et al.*, 2003), the pre-tetanus estimate of the RRP size increased and the estimate of P_r decreased in the presence of the drug. Under these conditions, tetanization increased the RRP estimate by $31 \pm 22\%$, which was similar to the increase in the absence of kynurenic acid. However, the largest contribution to PTP was an increase in release probability (Fig. 3B,C). The relative increase in release probability was even larger in kynurenic acid ($153 \pm 31\%$, $n = 6$) than in Ringer solution ($51 \pm 12\%$, $n = 9$, $p < 0.01$). Probably, the release probabilities in normal Ringer solution were overestimated (Neher & Sakaba, 2001; Wong *et al.*, 2003). The larger increase in release probability in kynurenic acid therefore can probably be attributed to a better estimation of the pool size, due to reduction of desensitization of postsynaptic glutamate receptors, rather than a direct effect of kynurenic acid on PTP induction.

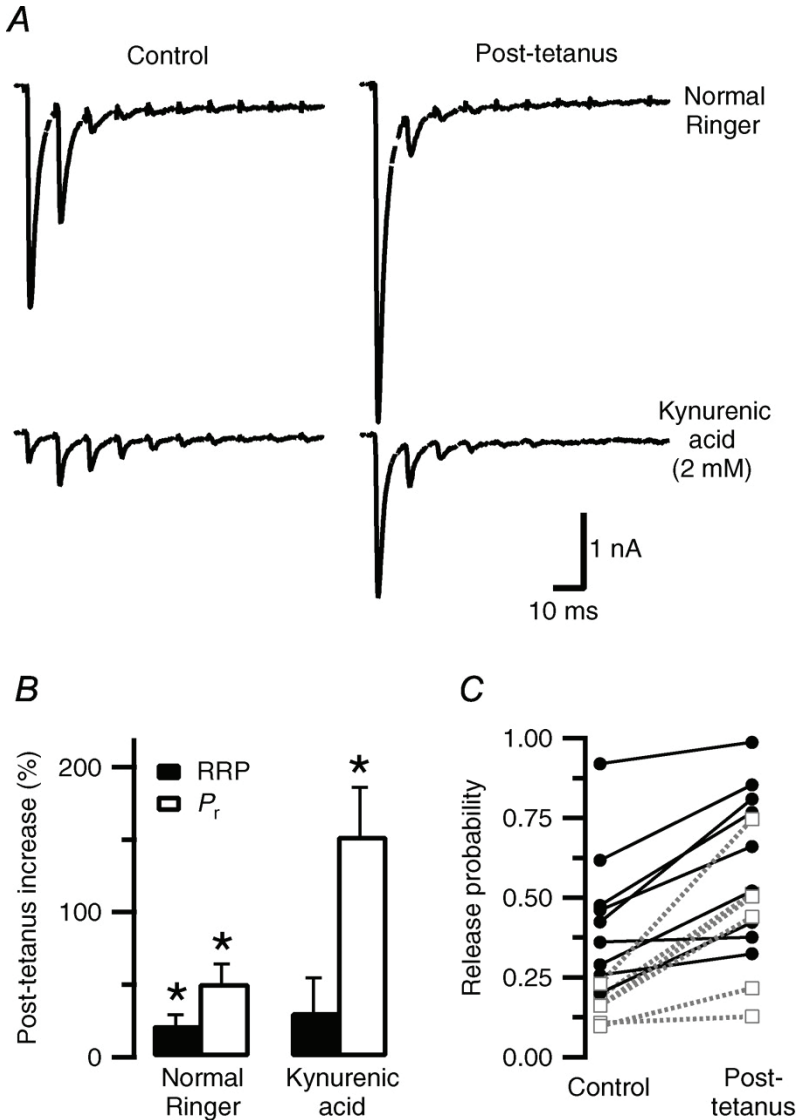


Figure 3. Readily releasable pool.

The size of the readily releasable pool (RRP) of vesicles was estimated from a high frequency train. EPSC peak amplitudes were summed and corrected for replenishment. Replenishment was estimated from the responses to the last stimuli and was assumed to be constant. Release probability (P_r) was calculated by dividing the first EPSC amplitude by the RRP estimate. A, top, EPSCs in response to 100 Hz stimulus trains before ('control') and after ('post-tetanus') a 20 Hz tetanus of five minutes. Bottom: Same stimulation in the presence of 2 mM kynurenic acid. B, Average increase in the RRP and P_r in normal Ringer ($n = 9$) and in

kynurenic acid ($n = 6$) *C*, Release probability of the individual experiments. black lines are the data points measured in normal Ringer solution. Grey broken lines were measured in the presence of *kynurenic acid*.

Decay of the PTP

In a minority (5 of 19) of the experiments in which decay of the potentiation of evoked EPSC amplitudes after the tetanus was monitored, a fast and a slow component could be discerned. The fast component had a time constant of less than one minute and may be an augmentation phase. These experiments showed particularly large increases in EPSC amplitude after the tetanus (>116%). In the other experiments, the fast component was less apparent and the decay could be approximated by a single exponential function with a time constant of 9 ± 2 min ($n = 14$).

After the tetanus, the frequency of spontaneous release decayed much faster than the amplitude of the evoked release. In four cells, evoked and spontaneous release were measured in consecutive trains within the same cell. In each case the decay time constant of spontaneous release was smaller than for evoked release. To compare their time courses, in these four experiments both the normalized, averaged amplitude of evoked release and the normalized, average frequency of spontaneous release were fit with a single exponential function. The time constants were 9.1 minutes for evoked release and 2.3 minutes for spontaneous release (Fig. 4*A,B*). In Fig. 4*C* the decay phase of the traces shown in Fig. 4*A* and *B* is displayed on semi-logarithmic scales to illustrate the difference in their decay.

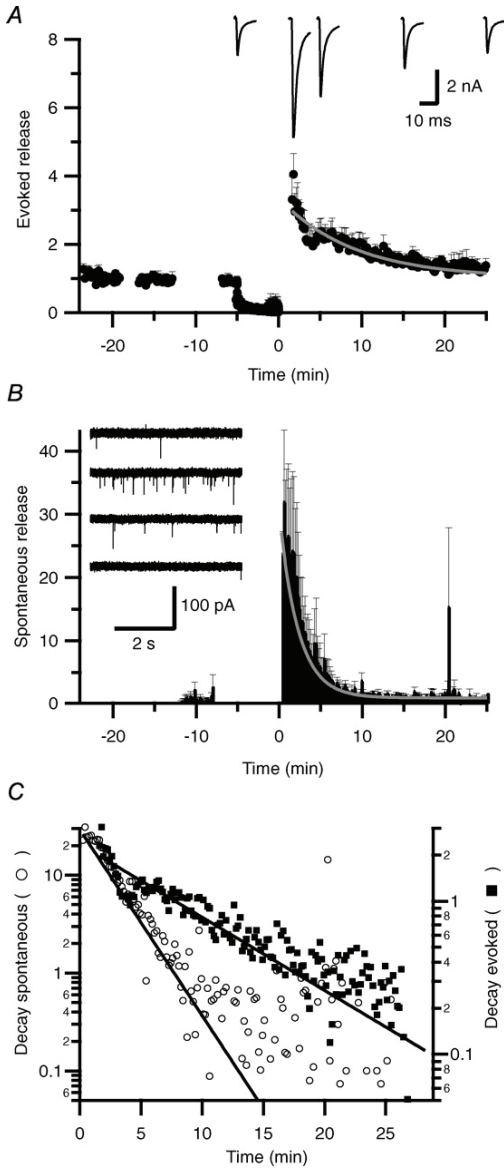


Figure 4. Decay of post-tetanic potentiation.

A, The evoked EPSC amplitudes of four cells were normalized to baseline and the average was plotted versus time after the tetanus ($n = 4 + SEM$). A single exponential function back to baseline was fit through the data (grey line). Time constant was 9.1 min. Example traces can be seen in the inset, from left to right: last EPSC before the tetanus and 1.4, 5, 15 and 25 minutes after the tetanus. *B*, In the same cells as shown in *A*, a second tetanus was given, but now only the spontaneous release was monitored. Spontaneous release was binned (bin size 10 seconds), normalized to baseline, and fitted with a single exponential

function. Time constant was 2.3 min (grey line). Example traces, before the tetanus and 1.4, 5 and 15 minutes after the tetanus, can be seen in the inset. C, semi-logarithmic plot of the decay of spontaneous (○) and evoked (■) release following the tetanus. The single exponential fits shown in A and B are shown as black lines.

Induction characteristics of the tetanus

Since the decay time constant of potentiation in the neuromuscular junction depends on the frequency and duration of the tetanus (Van der Kloot & Molgó, 1994), we investigated whether the induction characteristics were the same for both types of release. We varied the number of stimuli in a 20 Hz tetanus between 100 and 6000 and measured the amount of PTP after the stimulus. Fig. 5A shows an exceptionally long experiment, in which five different tetani could be presented. The amount of potentiation clearly depended on the number of stimuli in the tetanus. On average, evoked release was already elevated after 500 stimuli and it was close to maximal at 2000 stimuli (Fig. 5B). Spontaneous release was probably still far from maximal following the longest stimulus train (Fig. 5C). In contrast to PTP in the endplate (Lev-Tov & Rahamimoff, 1980), the decay time constant of evoked release did not depend on the number of stimuli.

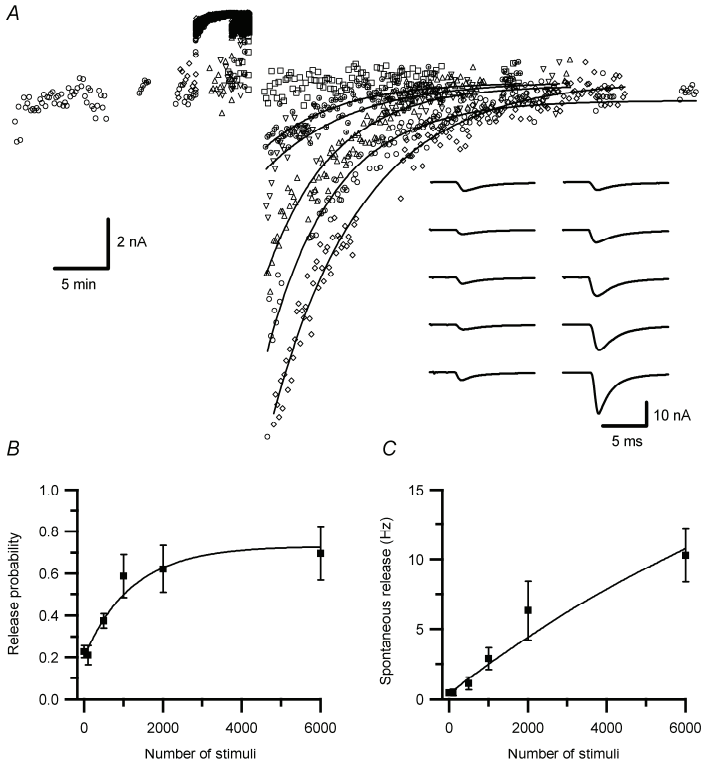


Figure 5. Induction characteristics.

The number of stimuli in a 20 Hz tetanus was varied between 100 and 6000. After each tetanus, the cell was stimulated at a frequency of 0.1 Hz until the EPSCs had returned to baseline. A, EPSC amplitudes before, during and after the tetanus are plotted. In A, five tetani of different duration were applied: 100 (□), 500 (⊕), 1000 (∇) and 2000 stimuli (Δ). The experiment was started (○) and ended (◇) with a train of 6000 stimuli. The inset: examples of the EPSCs. Left traces were measured before, right traces after the tetanus, which contained from top to bottom, 100, 500, 1000, 2000 and 6000 stimuli, respectively. B, Plot of the average release probability versus the number of stimuli in the tetanus. ($n = 6$ for 0 and 6000 stimuli, $n = 3$ for the other stimuli). Release probability was calculated by dividing the EPSC amplitude by the pool size estimate. C, Plot of the average spontaneous release frequency in the first minute after the tetanus. In B and C, the data were fitted with an exponential function (solid lines).

Presynaptic [Ca²⁺] dynamics

In several preparations, it has been shown that PTP depends on residual calcium (Zucker & Regehr, 2002). We therefore compared changes in the presynaptic calcium concentration, measured with fura-2 in pre-loaded terminals, with the EPSC amplitudes after induction of PTP (Fig. 6). During the tetanus, the high-affinity calcium indicator fura-2 approached saturation rapidly. Therefore, the concentrations during the tetanus reached the μM range and could not be accurately measured. After the tetanus, the calcium concentration decayed back to baseline bi-phasically. The rapid phase was not accurately measured. One to two min after the tetanus, the average calcium concentration was increased to 210 ± 60 nM from a resting concentration of 41 ± 5 nM. It subsequently decreased to resting levels with a time constant of 8.5 ± 2.1 minutes (Fig. 6B; $n = 4$). The corresponding EPSC amplitudes showed normal potentiation (Fig. 6C). In the same experiments, the time constant of PTP decay was 5.2 ± 1.0 minutes. If the EPSC amplitude was plotted against $[\text{Ca}^{2+}]$, the average slope of the best line fit was 35 ± 13 pA/nM ($n = 4$; Fig. 6D). A fit with a power law function, yielded on average an exponent of the power function that was close to 1 (0.72 ± 0.16 ; $n = 4$; Fig. 6E), confirming that the relation between the residual $[\text{Ca}^{2+}]$ and PTP was close to linear. Since both the amount of PTP and its decay time constant did not differ significantly from undialysed terminals, we conclude that the calcium measurements did not interfere with PTP induction.

The decay of the presynaptic calcium concentration and of the PTP had a similar time course (Fig. 6D,F), suggesting that residual calcium plays an important role in the increase of transmitter release. To test this hypothesis, we interfered with the normal presynaptic calcium dynamics by pre-loading the terminal with the slow calcium buffer EGTA. At a concentration of 1 mM, EGTA decreased the EPSC amplitudes by $27 \pm 13\%$ ($n = 5$) compared to the cell-attached configuration, in agreement with earlier results (Borst & Sakmann, 1996). The resting calcium levels were similar in the presence of EGTA (40 ± 12 nM; $n = 5$). After the tetanus the calcium concentration was significantly lower (70 ± 10 nM) than in the absence of EGTA. The average calcium concentration decayed to baseline much faster in the presence of EGTA compared to cells filled with only fura-2 (Fig. 6B; $n = 5$). In two experiments, no PTP was observed. In the other 4 experiments, potentiation of both evoked (Fig. 6C) and spontaneous release (not shown) were still largely intact. Both the decay of PTP and of residual calcium were clearly faster in the presence of EGTA (Fig. 6F,G). The observation that both sped up in parallel suggests that residual calcium and PTP are causally related. A comparison of all experiments in which calcium concentration and PTP time course were monitored indeed showed that the slow phase of PTP decay depended on residual calcium (Fig. 6G).

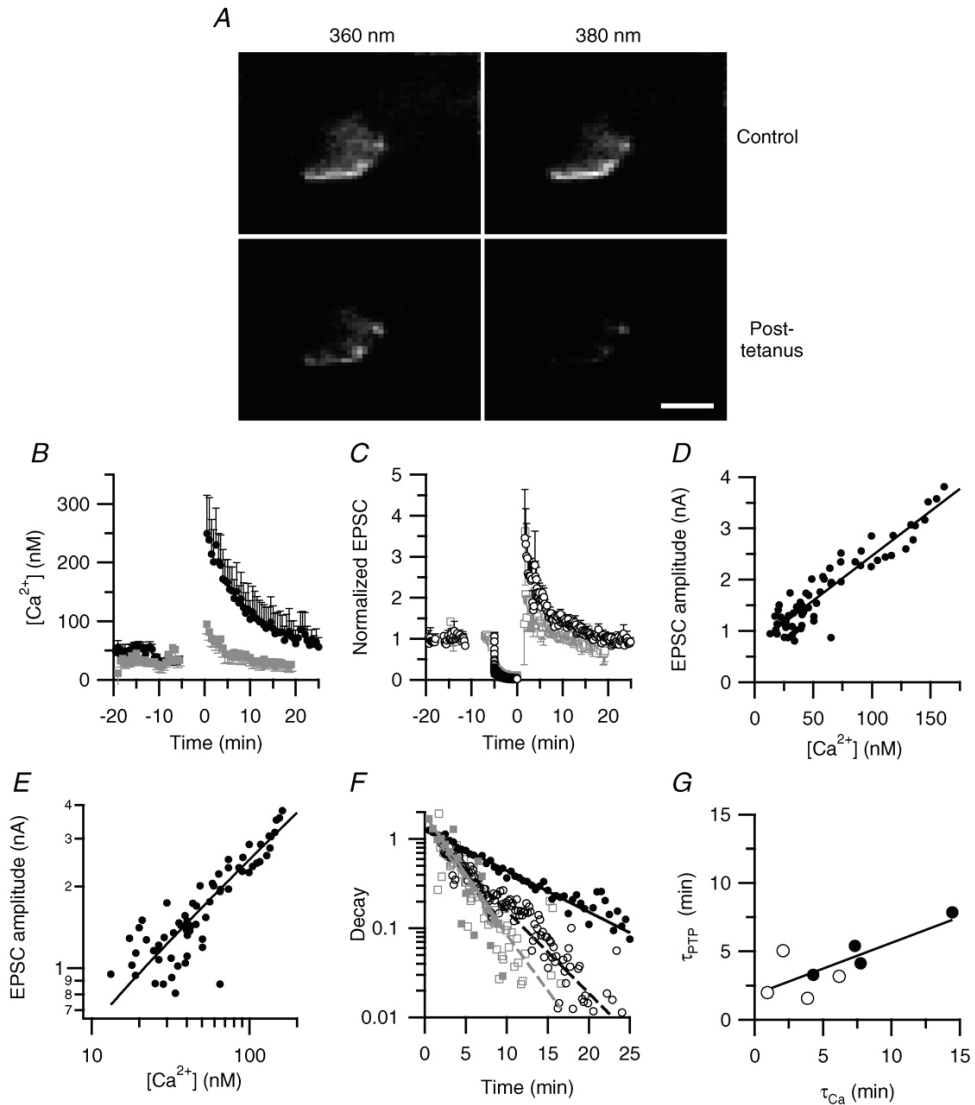


Figure 6. Relation between residual calcium and PTP time course.

A, A terminal was filled with 50 μ M fura-2. Images were obtained at 360 (isosbestic wavelength; left) and at 380 nm (calcium sensitive wavelength; right). At the excitation wavelength of 380 nm, fura-2 fluorescence decreases upon calcium binding. Calibration bar 10 μ m. The last pair of images before (top) and the first after the tetanus (bottom) are shown. *B*, Average calcium concentration for cells filled with fura-2 (\bullet , $n = 4$), or with fura-2 plus EGTA (\blacksquare , grey, $n = 5$). During the tetanus ($t = -5$ to 0 min) the high affinity calcium dye approached saturation in both conditions (data points not shown). *C*, Average normalized

EPSC amplitudes for cells filled with fura-2 (○) or fura-2 plus EGTA (□, grey). D, Relation between EPSC size and $[Ca^{2+}]$ during the decay phase of PTP for an individual experiment. Solid line has a slope of 17 pA per nM $[Ca^{2+}]$ ($r = 0.93$). E, Same data as in D, now shown on a double-logarithmic plot. Solid line is fit of the relation between EPSC amplitude and residual calcium with a power function: EPSC amplitude = $K_1[Ca^{2+}]^m + K_2$, where K_1 and K_2 are scaling constants. Best fit was obtained for $m = 0.55$. F, Semi-logarithmic plot of the decay of calcium and EPSC size. Symbols correspond to the symbols used in figures 6B and C. Both the $[Ca^{2+}]$ and the EPSC sizes are normalized to their respective average values during the time period when the first three EPSCs after the tetanus were measured (1.5-2 min after the tetanus). Solid black line is fit of $[Ca^{2+}]$ in 50 μ M fura-2 with a single exponential function with time constant 9.4 min. Solid grey line is fit of $[Ca^{2+}]$ in 50 μ M fura-2 plus 1 mM EGTA, with time constant 3.3 min. Broken black line is fit of EPSC decay in the absence of EGTA, with time constant 4.7 min. Broken grey line is fit of EPSC decay in the presence of EGTA, with time constant 3.5 min. G, Relation between PTP decay and residual calcium. A linear correlation ($r = 0.78$) was found (solid line; $p < 0.05$).

Since the potentiation of the evoked responses decayed not much more rapidly than the decay of residual calcium, the decay of the potentiation of the spontaneous events must have been more than three fold faster than residual calcium. A possible explanation for the difference in the decay of evoked and spontaneous release potentiation is that the relative increase in calcium concentration is much larger for the spontaneous events, which are normally triggered at the resting calcium concentration, than for the evoked events, which are normally triggered by a calcium concentration in the μ M range (Bollmann *et al.*, 2000; Schneggenburger & Neher, 2000). From the Theory section we concluded that as long as the fractional increases in the calcium concentration triggering release are small, as expected for the summation of residual calcium with action potential-evoked transients, the decay of potentiation becomes a linear function of residual calcium (Eq. 6), whereas for large fractional increases, as in the case of the difference between basal calcium and residual calcium, the decay is faster, due to the non-linear dependence of transmitter release on calcium (Eq. 10). However, a simple calculation shows that a direct activation of the phasic calcium sensor provides an insufficient explanation for the observed potentiation. The average increase in calcium after the tetanus was only about 170 nM. If phasic release is driven by brief calcium transients with an amplitude of about 8.9 μ M (Bollmann *et al.*, 2000), an increase of at most 9% ($((8.9+0.17)/8.9)^{4.4} \times 100\%$) is predicted. We therefore also considered whether changes in the apparent affinity of the calcium sensor for release would be compatible with the observed differences in the decay of spontaneous and evoked release after the tetanus (see Theory section for details). This simulation reproduced

some key features of our experimental findings. A 20% change in the K_d was needed to reproduce the observed amount of PTP. The resulting change in F was too large for the linear approximation (Eq. 6) to be valid, therefore the apparent PTP decay time constant will be somewhat smaller than the decay time constant of residual calcium (Fig. 7A), as was also experimentally observed (Fig. 6). The residual calcium leads to a relatively large change in $[Ca^{2+}]$ for spontaneous release. As a result, the observed decay time constant will be clearly smaller than of the evoked release (Fig. 7A), as was also experimentally observed (Fig. 4). We therefore find that an increase of the affinity of the calcium sensor for calcium of about 2 μM per 170 nM residual calcium would be compatible with both the amount of PTP we observed and the differences in decay of spontaneous and evoked release (Fig. 7). However, our experiments do not allow us to discriminate between a change in K_d or m of the calcium sensor and an increase in calcium influx or calcium buffer depletion, which would selectively potentiate evoked release, thereby protracting its decay phase.

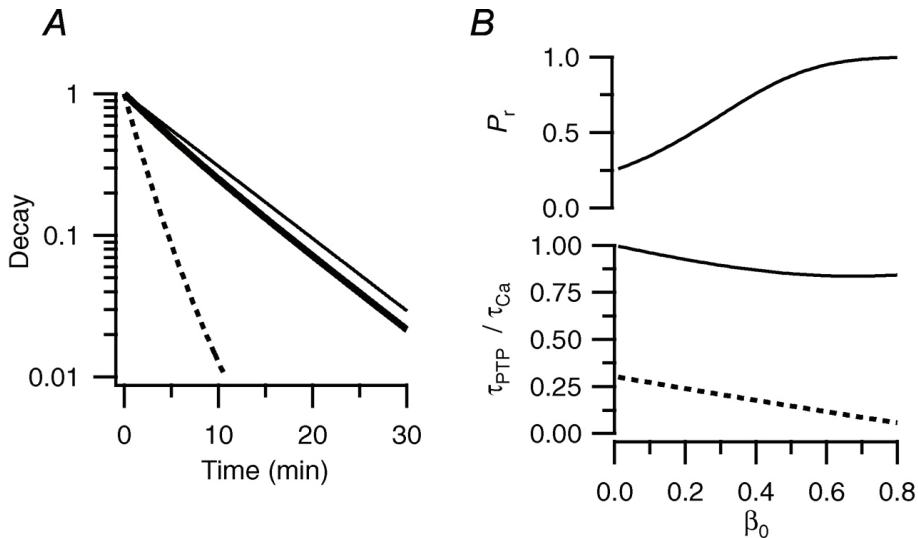


Figure 7. Simulation of PTP decay.

A, Simulation of the decay of evoked and spontaneous release according to a release model based on the Hill equation (equation 3; see Theory section for details). A good fit of the curve in Fig. 2D of (Meinrenken et al., 2003), which describes the probability that a vesicle of the readily-releasable pool is released as a function of the peak calcium concentration reached during an action potential, can be obtained with $K_d = 11.4 \mu\text{M}$ and $m = 4.4$ (results not shown). For a release probability of 0.25, a concentration of 8.9 μM is then needed (Bollmann et al., 2000). Basal calcium concentration was 40 nM. In addition, for the simulation it was

assumed that F , which is the ratio of K_d and $[Ca]$, depended linearly on the residual calcium. As a result, a decrease of F after the tetanus recovered with the same time course as residual calcium. Solid thin line gives the decay of residual calcium (time constant 8.5 min). Solid thick line is the decay of evoked release (apparent time constant 7.3 min). Broken grey line is the decay of spontaneous release (apparent time constant 2.0 min). Decays were normalized to the respective amplitudes at $t = 0$. To increase P_r twofold, as was experimentally observed during PTP, the change in F after the tetanus, (β , Eq. 4) would have to be about 0.2 (i.e., F would have to be about 20% smaller than control) directly after the tetanus, which translates as an increase in the apparent affinity of the calcium sensor of about 2 μM . B, Top: release probability of releasable vesicles (P_r) as a function of the fractional change in F directly after a tetanus (β_0). Bottom: Simulation of the relation between the ratio of the apparent time constant for decay of PTP and the time constant for decay of residual calcium (τ_{PTP}/τ_{Ca}) and β_0 . Solid line is computed for evoked release, broken line has been computed for spontaneous release. Simulations were performed as described in A, with residual calcium immediately after the tetanus in each case 170 nM, while K_d was varied to get the appropriate changes in F . F decayed with the same time course as residual calcium. For large values of β , evoked release saturated and -in contrast to what was experimentally observed- release plateaued after the tetanus. To be able to describe the decay of PTP satisfactorily by a single exponential function, the fit was therefore restricted to the period starting 5 min after the tetanus.

DISCUSSION

Cells in the MNTB show post-tetanic potentiation when stimulated with a tetanus of 500 or more action potentials at 20 Hz. The EPSCs returned to baseline in minutes. This enhancement of the evoked responses was accompanied by an increase in the frequency of spontaneous EPSCs. We show that the major mechanism was an increase in the release probability and that the time courses of the decay of PTP and of the residual calcium were similar, but that the spontaneous release decayed about threefold faster.

Physiological relevance of the stimulation protocol

A 25 s tetanus at 20 Hz was sufficient to induce PTP. During *in vivo* recordings, spontaneously recorded activities are almost as high (Kopp-Scheinflug *et al.*, 2003b). A comparison is not straightforward. Firstly, we recorded at room temperature, since the rapid, large synaptic currents are difficult to measure at physiological temperatures (Borst *et al.*, 1995). In the rabbit superior cervical ganglion, both the time course and the amplitude of PTP were shown not to be highly temperature-dependent (Zengel *et al.*, 1980). Secondly, we recorded in brain slices from animals a few days before the onset of hearing and it is not known what the electrical activity of this synapse is at this age. *In vivo* recordings before the onset of hearing are therefore needed to assess the physiological relevance of the stimuli used in this paper.

PTP is due to an increase in release probability

PTP was accompanied by an increase in the frequency but not the amplitude of spontaneous EPSCs. Both clearance of glutamate from the synaptic cleft (Otis *et al.*, 1996) and recovery from desensitization of glutamate receptors (Joshi *et al.*, 2004) most likely are complete within seconds after the tetanus, so they probably did not affect the measurements of the amplitudes of the spontaneous EPSCs during the first minute after the tetanus. The lack of a change in spontaneous EPSC size indicates that PTP was not caused by increases in vesicle filling (Ishikawa *et al.*, 2002) or increases in the postsynaptic sensitivity to glutamate. PTP was largely unaltered when synaptic transmission was reduced by about 95% by a glutamate antagonist, arguing against the involvement of a retrograde messenger (Bao *et al.*, 1997; Kushmerick *et al.*, 2004). We tested two possible mechanisms for the increase in the number of vesicles that were released by an action potential, an increase in the readily-releasable pool (RRP) and an

increase in the release probability of the vesicles in the readily-releasable pool (P_r). Measurements of the size of RRP suggested a modest increase following the tetanus. From these experiments we conclude that PTP in the MNTB is mostly due to an increase in the release probability of the vesicles in the RRP. This increase was quite large, following a five min, 20 Hz tetanus, P_r was approximately doubled. This increase may even have been underestimated, due to saturation of the postsynaptic receptors.

Role of changes in action potential waveform following a tetanus

The prespike, the capacitatively coupled presynaptic action potential measured in postsynaptic voltage clamp recordings (Forsythe, 1994), was decreased following the tetanus. The amplitude of the prespike, which is a measure of the rate of rise and fall of the presynaptic action potential, decreased by about 25%. This change will affect both amplitude and time course of the calcium influx during an action potential. In an earlier study, we tested the effect of changes in action potential shape, as occur during high-frequency trains. Halving the rate of rise and fall, which leads to halving of the prespike amplitude, results in a small increase of the calcium influx of about 8% and an increase in release of about 20% (Borst & Sakmann, 1999b). We therefore conclude that the changes in presynaptic action potential probably were smaller than in the earlier study and therefore resulted in an even smaller change in the calcium influx.

Effect of residual calcium

The decay of the presynaptic calcium concentration following a tetanus was much slower than after a single action potential, after which clearance takes only a few hundred milliseconds (Helmchen *et al.*, 1997). The slower decay following a tetanus could be due to a reverse action of the $\text{Na}^+/\text{Ca}^{2+}$ exchanger, which may allow calcium ions to enter the cell when pumping out the sodium ions that accumulate in the presynaptic terminal during a tetanus (Lev-Tov & Rahamimoff, 1980; Zhong *et al.*, 2001). It could also originate from an intracellular source, such as mitochondria (Billups & Forsythe, 2002), which may release calcium following a tetanus (Tang & Zucker, 1997; Yang *et al.*, 2003).

The observation that the time course of the decay of the residual calcium after the tetanus largely matched the decay of the PTP suggests that the two are causally related. Recently, it was observed that the time course of the decay of calcium after a brief stimulus and short-term facilitation also matched at the calyx of Held (Felmy *et al.*, 2003). Although residual calcium has generally been implicated in PTP, the precise

relation between the two is still largely unclear. Similar to what we observed, at the crayfish neuromuscular junction (Delaney *et al.*, 1989) and the chick ciliary ganglion (Brain & Bennett, 1995) the time courses of PTP decay and residual calcium match. Our conclusion that residual calcium and PTP are causally related at the calyx of Held is strengthened by the experiment in which we added the calcium buffer EGTA to the terminal. Under these conditions, the residual calcium decay and the PTP sped up in parallel and the linear correlation between PTP decay and residual calcium decay still held true. Similar results have been obtained in *Aplysia* (Kretz *et al.*, 1982). We conclude that it is therefore likely that residual calcium caused the increase in release probability.

Different decay of potentiation of spontaneous and evoked release

The potentiation of spontaneous release decayed about three times more rapidly than the evoked release. Since the latter followed the decay of residual calcium, the spontaneous release must have decayed much more rapidly than residual calcium. This is also observed at the crayfish neuromuscular junction (Zucker & Lara Estrella, 1983; Delaney *et al.*, 1989). In contrast, at the frog neuromuscular junction (Zengel & Magleby, 1981) and the *Aplysia* sensory-motor neuron synapse (Eliot *et al.*, 1994), decay of spontaneous and evoked release have a similar time course.

In the Theory section, we have explored possible causes for the difference in the decay of spontaneous and evoked release. In general, we observed that as long as changes in the calcium concentration, the affinity (K_d) and the power exponent (m) of the calcium sensor are relatively small, the time course of potentiation will largely follow the time course of the changes in these parameters. If any of these parameters shows a clear change ($>10\%$), this linear approximation is no longer valid. From our data it is clear that residual calcium after the tetanus is much larger than the resting calcium concentration. Firstly, a potentiation of calcium influx or a depletion of calcium buffers would selectively affect evoked release. In addition, the results of simulations (Fig. 7) indicate that changes in the residual calcium differentially affect the time course of evoked and of spontaneous release. The relative change in the calcium signal that triggers spontaneous release will be much larger after the tetanus than the relative change in the calcium signal that triggers evoked release. For small changes, the potentiation is predicted to follow the time course of residual calcium (Eq. 6), for large changes potentiation is predicted to decay more rapidly (eq. 10), as experimentally observed.

The potentiation of spontaneous release will only decay clearly faster than the potentiation of evoked release if the power law of the calcium dependence has an

exponent that is larger than one. This condition provides a possible explanation for the observed difference in the dependence of the decay of spontaneous release in the crayfish and in the frog neuromuscular junction. Asynchronous release at the crayfish neuromuscular junction depends on at least the third power of presynaptic calcium concentration increases (Ravin *et al.*, 1997), whereas the calcium dependence of asynchronous release in the frog neuromuscular junction appears to be much more shallow (Angleton & Betz, 2001).

From our simulations we conclude that residual calcium can result in the observed differences in the decay of the potentiation of spontaneous and evoked release at the calyx of Held, both as a direct effect and as an indirect effect. The possible indirect effects include calcium buffer depletion (Felmy *et al.*, 2003), a facilitation of calyceal calcium channels (Borst & Sakmann, 1998b; Cuttle *et al.*, 1998) or an activation of second messengers, which may change the K_d of the calcium sensor (Hori *et al.*, 1999; Sakaba & Neher, 2001b; Wu & Wu, 2001; Kaneko & Takahashi, 2004). We will next discuss these different possibilities in more detail.

Direct activation of the calcium sensor

Our results confirm earlier results showing that a moderate, sustained increase in presynaptic calcium concentration is both a necessary and sufficient condition to induce PTP (Zucker & Regehr, 2002). Measurements of the calcium sensitivity of transmitter release at the calyx of Held (Bollmann *et al.*, 2000; Schneggenburger & Neher, 2000) suggest that the increases that we observed during the decay phase of the PTP are sufficient to affect evoked or spontaneous release. In the experiments of Bollmann *et al.* (Bollmann *et al.*, 2000), a uniform raise of the calcium concentration to 0.5 μM resulted in an increase in the frequency of small EPSCs that was clearly larger than the increases we observed in the first minute after the tetanus. Although smaller increases than to 0.5 μM were not studied, this suggests that the increases in spontaneous EPSCs that we observed could be due to a direct activation of the calcium sensor that is responsible for phasic release. We emphasize that a direct activation of the calcium sensor due to residual calcium cannot be the major cause of PTP. With a 'typical' calcium concentration of 8.9 μM seen by the vesicles that are released during an action potential (Bollmann *et al.*, 2000), a linear summation with the residual calcium of 170 nM will lead to a potentiation of only about 9%, even if it is assumed that the relation between calcium and release is described by a power law with a power m of 4.4. Nevertheless, Felmy *et al.* (Felmy *et al.*, 2003) showed that sub-micromolar elevations of the calcium concentration can lead to larger increases in evoked release than the amount of PTP observed in the present study. They suggested that buffer

depletion leads to supra-linear addition of residual calcium with the calcium transients during an action potential. Candidates for this calcium buffer are still being investigated (Felmy & Schneggenburger, 2004).

Role of changes in presynaptic calcium currents

An earlier study reported post-tetanic depression (PTD) rather than PTP at the calyx of Held (Forsythe *et al.*, 1998). This PTD was due to inactivation of calcium currents. In dual whole-cell recordings, we also observed depression instead of potentiation following a tetanus. The use-dependent rundown of release that we observed in presynaptic whole-cell recordings could be related to washout of a cytoplasmic factor. This rundown precluded a direct measurement of the action potential-driven calcium influx during PTP.

The calyceal calcium currents facilitate calcium-dependently (Borst & Sakmann, 1998b; Cuttle *et al.*, 1998). They activate more rapidly in the presence of residual calcium. A change in calcium influx during an action potential following the tetanus cannot be solely responsible for PTP at the calyx of Held, since spontaneous release showed a prolonged increase as well. Direct measurements of the calcium influx during an action potential after establishment of PTP are necessary to quantify the contribution of facilitation and inactivation of calcium currents conclusively.

Involvement of second messengers

Calcium could indirectly affect release by activating a second messenger. For example, protein kinase C (PKC) is a good candidate because it is involved in PTP in the hippocampus (Alle *et al.*, 2001; Brager *et al.*, 2003), because its activity depends on Ca^{2+} and because PKC activation has been shown to increase release probability at this synapse without a large effect on RRP (Hori *et al.*, 1999; Wu & Wu, 2001). Munc13 could also be involved, largely for the same reasons as PKC (Hori *et al.*, 1999). An increase in cAMP will also increase the release probability in the calyx of Held (Sakaba & Neher, 2001b; Kaneko & Takahashi, 2004). Since cAMP results at the same time in a substantial increase of the RRP, whereas we observed only a modest increase, this second messenger cannot be exclusively involved in PTP.

If any of these second messengers acts at a late 'maturation' step, thereby decreasing the fraction of 'reluctant' vesicles (Wu & Borst, 1999; Sakaba & Neher, 2003b), the apparent calcium sensitivity of these vesicles is expected to increase. Our simulations showed that apart from a change in calcium influx or a depletion of calcium buffers, a

calcium-dependent change in K_d or m of the calcium sensor may also lead to a differential decay of the potentiation of spontaneous and of evoked release, similar to what we experimentally observed. Therefore, apart from pharmacological experiments, experiments in which the calcium sensitivity of release during PTP is measured would aid in the further delineation of the mechanisms that govern PTP at the calyx of Held synapse.

Chapter 4

An increase in calcium influx contributes to post-tetanic potentiation at the rat calyx of Held synapse

Ron L. P. Habets and J. Gerard G. Borst

J Neurophysiol. 2006 Dec;96(6):2868-76

ABSTRACT

We studied the contribution of a change in presynaptic calcium influx to post-tetanic potentiation (PTP) in the calyx of Held synapse, an axosomatic synapse in the auditory brainstem. We made whole-cell patch-clamp recordings of a principal cell following loading of the presynaptic terminal with a calcium dye. After induction of PTP by a high-frequency train of afferent stimuli, the Fluo-4 fluorescence transients evoked by an action potential became on average $15 \pm 4\%$ larger ($n=7$). Model predictions did not match the fluorescence transients evoked by trains of brief calcium currents unless the endogenous calcium buffer had low affinity for calcium, making a contribution of saturation of the endogenous buffer to the synaptic potentiation we observed in the present experiments less likely. Our data therefore suggest that the increase of release probability during PTP at the calyx of Held synapse is largely due to an increase in the calcium influx per action potential.

The calyx of Held synapse, a fast relay in the auditory brainstem, displays several forms of short-term synaptic plasticity. Depending on the stimulus conditions, the response to a second stimulus may be increased (paired-pulse facilitation, [PPF]) (Forsythe & Barnes-Davies, 1993), or decreased (short-term depression, [STD]) (Borst *et al.*, 1995). In addition, following a high-frequency train of stimuli, both a several minute-long decrease (post-tetanic depression, [PTD]) (Forsythe *et al.*, 1998) or increase (post-tetanic potentiation, [PTP], Chapter 3) (Korogod *et al.*, 2005) in the synaptic responses may occur. The accessibility of this synapse to patch-clamp recordings has allowed great progress in identifying different underlying mechanisms that contribute to these forms of short-term plasticity (von Gersdorff & Borst, 2002). The four different forms of short-term plasticity that occur at the calyx have in common that they are largely presynaptic phenomena. A change in the output of a synapse can be due to an increase in the size of the readily-releasable pool (RRP), which is typically defined as the pool of vesicles that can be released by a very large stimulus or to a change in the release probability of vesicles in the readily-releasable pool. PTP is accompanied by a large increase in the release probability (Chapter 3, Korogod *et al.*, 2005). In addition, we also observed a small increase in the RRP (Chapter 3). The PTP decayed with a similar time course as the presynaptic calcium increase. However, based on the measured affinity of the phasic calcium sensor (Bollmann *et al.*, 2000; Schneggenburger & Neher, 2000; Lou *et al.*, 2005), by itself this increase in presynaptic calcium would be insufficient to cause a substantial increase in the activation of the phasic calcium sensor. In this paper we further explore the mechanisms that underlie the increase in release probability during PTP at the calyx of Held synapse. We focus on possible changes in the calcium influx for several reasons. Firstly, small changes in calcium influx lead to large changes in release. Release typically is proportional to the third or fourth power of the calcium influx (Schneggenburger & Neher, 2005). Therefore, even relatively small changes in calcium influx would make substantial contribution to PTP. Secondly, the calcium currents at the calyx of Held facilitate calcium-dependently and this increase may contribute to PPF (Borst & Sakmann, 1998b; Cuttle *et al.*, 1998; Inchauspe *et al.*, 2004; Ishikawa *et al.*, 2005). Since PTP cannot be observed while the terminals are in whole-cell patch-clamp configuration (Chapter 3, Korogod *et al.*, 2005), we used a fluorometric method to investigate a possible contribution of changes in calcium influx to PTP.

MATERIALS & METHODS

Preparation of slices

Preparation of slices and electrophysiological measurements were done as described previously (Chapter 3). Animal procedures were in accordance with guidelines provided by the animal committee of the Erasmus MC. In brief, seven to ten day old Wistar rats were decapitated without prior anesthesia. The brainstem was dissected and immersed in ice-cold saline containing (in mM): 125 NaCl, 2.5 KCl, 3 MgSO₄, 0.1 CaCl₂, 1.25 NaH₂PO₄, 0.4 ascorbic acid, 3 myo-inositol, 2 pyruvic acid, 25 D-glucose, 25 NaHCO₃ (Merck); pH 7.4. Transverse slices of 200 µm thickness were cut with a vibratome (Vibratome, St. Louis, MO).

Electrophysiological recordings

Normal Ringer solution had the same composition as the solution that was used for slicing, except that the concentration of CaCl₂ and MgSO₄ were 2 and 1 mM, respectively. Neurons were visualized with an upright microscope (BX-50; Olympus, Tokyo, Japan), equipped with infrared differential interference contrast optics. Axons originating from the cochlear nucleus were stimulated (0.5 ms, 0.03-0.5 mA) in the midline by a bipolar electrode (Frederic Hear & Co, Bowdoinham, ME). Test frequency was increased compared to earlier experiments (0.5 vs. 0.1 Hz) (Chapter 3) to allow collection of more fluorescence data in the same time period. At this frequency there was already some synaptic depression (von Gersdorff *et al.*, 1997). PTP was elicited by a 5 min, 20 Hz tetanus. Cells were selected when extracellular recordings indicated postsynaptic action potential firing (Borst *et al.*, 1995). Electrophysiological recordings were made at room temperature with an Axopatch 200B amplifier (Axon Instruments, Union City, CA). Pipette solutions contained (in mM): 125 K-gluconate, 20 KCl, 10 Na₂-phosphocreatine, 4 MgATP, 0.3 Na₂GTP, 10 HEPES (Sigma) and 0.05-0.2 calcium sensitive dye (Molecular Probes, Eugene, OR) or 0.5 EGTA for pre- or postsynaptic recordings, respectively. Calcium currents were pharmacologically isolated by substituting 20 mM TEA-Cl (Fluka, Buchs, Switzerland) for 20 mM NaCl and adding 1 µM tetrodotoxin (Alomone labs, Jerusalem, Israel) and 0.1 mM 3,4-diaminopyridine to the Ringer solution. In these experiments, the internal solution contained (in mM) 125 Cs-CH₃SO₃, 20 CsCl, 10 Na₂-phosphocreatine, 4 MgATP, 0.3 Na₂GTP, 10 HEPES (Sigma). In some experiments Cs-CH₃SO₃ was replaced with Cs-Gluconate. Series resistance was 8-30 MΩ (compensated 80-98%, prediction was set to 80%). Leak subtraction was done with the P/-8 method. Holding potential in voltage clamp

experiments was -80 mV. Potentials were corrected for a -11 mV junction potential. Postsynaptic series resistance (<15 M Ω) was electronically compensated by 80-98% with a lag of 5 μ s. Signals were low-pass (10 kHz) filtered with a 4-pole Bessel filter. Only cells with a membrane resistance higher than 100 M Ω were accepted for analysis. Signals were sampled at 20-50 kHz with a Digidata 1320A (Axon Instruments). Data acquisition and analysis was done with pClamp 8 (Axon Instruments) or Igor 5 (Wavemetrics, Lake Oswego, OR).

Imaging

Terminals were pre-filled with fura-2, Fluo-4, rhod-dextran or Oregon Green BAPTA-5N (OGB-5N) for 10 min via the patch pipette. Only cells in which a G Ω outside-out patch formed after retraction were selected for analysis. The tissue was illuminated through a 40X objective (NA 0.8, Olympus, Tokyo, Japan) by a monochromator (Polychrome IV; 8 nm bandwidth, TILL Photonics, Martinsried, Germany). Excitation intensity was about 0.1 mW, when measured under the objective. Emission light was filtered through an appropriate bandpass filter and detected with a cooled photomultiplier tube (PMT; H7422-40, Hamamatsu, Hamamatsu City, Japan). Excess background fluorescence was removed by a 1 mm pinhole at the image plane of the microscope. PMT signals were amplified and low-pass filtered (2 kHz) with an 8-pole Bessel filter (Model 3382, Krohn-Hite, Brockton, MA) before digitization (Digidata 1320A, Axon Instruments). For fura-2, calcium concentrations were calculated as described in Chapter 3. For non-ratiometric dyes, responses evoked by an action potential (ΔF_{AP}) are given as a percentage of the basal fluorescence of the terminal, which was calculated as the difference between the fluorescence in the absence of stimuli and the fluorescence from a nearby region. In the case of PTP experiments, responses are expressed relative to the basal fluorescence before the tetanus ($\Delta F_{AP}/F_0$).

Data analysis

PTP

The amount of PTP was calculated as the percentage increase of the average amplitude of the first ten EPSCs after tetanic stimulation relative to the average amplitude of the last ten EPSCs before the tetanus.

APW trains

To test the relation between calcium influx and fluorescence changes, terminals were voltage clamped using a train of 10 action potential waveforms (APWs) at 100 Hz, as described earlier (Borst & Helmchen, 1998). Since clearance will start as soon as the influx starts, we corrected the amplitude of fluorescence changes for clearance during the rising phase assuming a similar time course for clearance as after the rising phase. In experiments in which terminals were loaded with a single dye, decay of the fluorescence between stimuli was fitted with a single exponential function. Its time constant was set to the time constant of a fit of the decay at the end of the train and its offset (value at $t=\infty$) was set to the baseline level before the first stimulus. To calculate the amplitude of the fluorescence change triggered by an APW, the fit that described the decay of the calcium transient elicited by the preceding APW was extrapolated to the time point where the increase of the fluorescence due to the actual APW was half-maximal. The fit of the decay following the actual APW was back-extrapolated, again to the time point where the increase of the fluorescence due to the actual APW was half-maximal. The amplitude was then taken as the difference between both fits at that point. In experiments in which two dyes were loaded, decays were fit with a double exponential function and fits were extrapolated to the peak value rather than the midpoint of the rising phase. Slow calcium-activated currents were subtracted before integration of the calcium currents.

Simulations

To assess the influence of the kinetics of the dye and the endogenous calcium buffer on the measured fluorescence transients, these transients were simulated using a single compartment model (Helmchen *et al.*, 1997). This model assumes spatial equilibrium at all time points. Even though diffusion of Ca^{2+} is disregarded, in the absence of significant buffer depletion, a single-compartment model may accurately describe the effect of the kinetics of calcium dyes on volume-averaged calcium transients at the calyx of Held (Helmchen *et al.*, 1997; Meinrenken *et al.*, 2003). We refer to (Meinrenken *et al.*, 2003) for a discussion of its limitations. Standard equations for buffering were solved numerically, by forward Euler finite difference using an adaptive step size. Calcium influx during an action potential was either provided by the response of a two-state Hodgkin Huxley model of calyceal calcium currents to a previously recorded action potential (Borst & Sakmann, 1998a), or the simultaneously measured calcium influx in presynaptic voltage clamp recordings was used, after filtering, truncation of outward currents and subtraction of slow calcium-activated currents. In the case of the

modeled calcium influx, total Ca^{2+} influx during an action potential was 0.91 pC, leading to an increase of the total calcium concentration to 12 μM in the calyx volume of 0.4 pl (Helmchen *et al.*, 1997). The standard model solution contained: free Ca^{2+} at a starting concentration of 50 nM; endogenous buffer concentration 1.3 mM, forward Ca^{2+} binding rate $5 \cdot 10^8$ per Msec (Klingauf & Neher, 1997), off rate 16000 s^{-1} (calcium-binding ratio 40, calculated as described in (Helmchen *et al.*, 1997); no ATP and 50-200 μM of fura-2, on-rate $4 \cdot 10^8$ per Msec, off rate 103 s^{-1} ; Fluo-4, on-rate $7.1 \cdot 10^8$ per Msec, off rate 369 s^{-1} (Naraghi, 1997) or Oregon Green BAPTA-5N (OGB-5N), on-rate $2.5 \cdot 10^8$ per Msec, off rate 8000 s^{-1} (Faas *et al.*, 2005). Removal of Ca^{2+} from the cytoplasm was modelled as a linear, non-saturable clearance mechanism. To match the experimentally observed decays, its rate constant was set to 800 (Figure 1) or 400 s^{-1} (Figure 4). In the simulations shown in Figure 1, a concentration of 50 μM was assumed, to account for loss of dye into the axon during the PTP experiments.

Simulated fluorescence transients were resampled to 50 kHz and digitally filtered with a binomial (Gaussian) filter to 2 kHz before analysis. To be able to compare the onset of simulated and measured responses in current clamp recordings, the measured prespike was aligned with the inverted first derivative of the simulated action potential after correcting for the delay introduced by the Bessel filtering.

Data are given as mean \pm standard error of the mean (SEM). Statistical comparisons were done using Student's *t*-test.

RESULTS

Rapid calcium transients at the calyx of Held synapse

PTP at the calyx of Held synapse rapidly washes out during presynaptic whole-cell recordings (Chapter 3, Korogod *et al.*, 2005). To prevent washout of PTP we therefore switched to fluorometric methods and pre-loaded dyes into the terminal during whole-cell recordings. Dyes were preloaded for 10 min to a final concentration of 200 μM (Figure 1A), after which the presynaptic pipette was withdrawn. Release was estimated from the size of the glutamatergic EPSCs in postsynaptic whole-cell recordings. We optimized fluorometric measurements by using dyes with a relatively low basal fluorescence and by using a cooled, high-quantum-efficiency PMT for detection. As a result, not only the amplitude of the fluorescence transient that was triggered by an action potential (ΔF_{AP}) could be accurately measured, but its rise time could also be resolved. The time course of the transients differed between dyes. Rise times of transients in the presence of OGB-5N, a low affinity dye (K_d 32 μM), were 0.32 ± 0.03 ms. Their decay was well approximated by a single exponential function with a time constant of 57 ± 8 ms ($n=5$; Figure 1B). In the presence of Fluo-4, a high affinity calcium dye (K_d 350 nM), 20-80% rise times were 0.68 ± 0.06 ms and decay time constants were 295 ± 42 ms ($n=7$; Figure 1C). Even in the absence of a presynaptic whole-cell recording, it was still possible to get information about the timing of the presynaptic action potential using the prespike in the postsynaptic recordings. The prespike is the capacitatively coupled presynaptic action potential (Forsythe, 1994). Its positive peak corresponds to the time when the speed of repolarization is maximal. For both dyes, the rise started around this time, which is shortly after the onset of the presynaptic calcium current (Borst & Sakmann, 1998a).

Single compartment model

The ΔF_{AP} transients shown in Figure 1 were compared with the predicted transients for a single compartment model that featured apart from the calcium dye, an endogenous calcium buffer, calcium influx and a linear clearance mechanism (see Methods for details). As long as the off-rate of the endogenous buffer was high (>5000 s^{-1}), the time course of the simulated and measured responses overlaid well for both the OGB-5N and the Fluo-4 transients (Figure 1D). If the off-rate of the endogenous buffer was lowered to 5000 s^{-1} or less, while adjusting its concentration to keep the endogenous binding ratio constant, the endogenous buffer was no longer able to 'track' the calcium influx and a prominent overshoot in the simulated volume-averaged calcium concentration at

the end of the repolarization phase became apparent in the simulations (Figure 1D). This component resulted in a bi-phasic decay of the OGB-5N transients. At 5000 s^{-1} , the fast component was already sufficiently large (>5% of the peak amplitude) to be well above the detection threshold in the measured transients. Since such a component was not present, this suggests that the endogenous buffer has a high unbinding rate for Ca^{2+} . This high off-rate implies that its K_d , which is the ratio of off-rate and on-rate, has to be large as well. Even if its on-rate were close to the diffusion limit, $\sim 1.10^9$ per Msec, its K_d would have to be $>5\text{ }\mu\text{M}$. At lower on-rates, the K_d would have to be correspondingly larger. These simulations therefore suggest that the endogenous buffer has a low affinity for calcium, enabling it to rapidly follow changes in the calcium concentration. The lack of a large overshoot in the volume-averaged calcium concentration, in combination with the rapid kinetics means that the rise phase of the OGB-5N transients largely reflects the integral of the calcium currents (Sabatini & Regehr, 1998). This is not the case for the Fluo-4 transients. Fluo-4 has a much smaller off-rate than OGB-5N and as a result, the rising phase of the Fluo-4 transients probably largely reflects the transfer of calcium ions between the endogenous buffer and Fluo-4 (Sabatini & Regehr, 1998). The around 5-fold slower decay can be explained by the much larger calcium binding ratio of this high-affinity dye (Helmchen *et al.*, 1997). Because of the inverse relation between total binding ratio (i.e. the sum of the contributions of the endogenous and the exogenous buffers) and the time constant of the decay of the fluorescence transients (Neher, 1995; Helmchen *et al.*, 1997), this indicates that on average Fluo-4 captures at least 80% of inflowing calcium ions.

In summary, the simulations suggest that the large majority of the endogenous calcium buffer of the calyx of Held has low affinity for Ca^{2+} ($K_d >5\text{ }\mu\text{M}$) and that at the concentration used in the PTP experiments, Fluo-4 will capture most inflowing calcium ions.

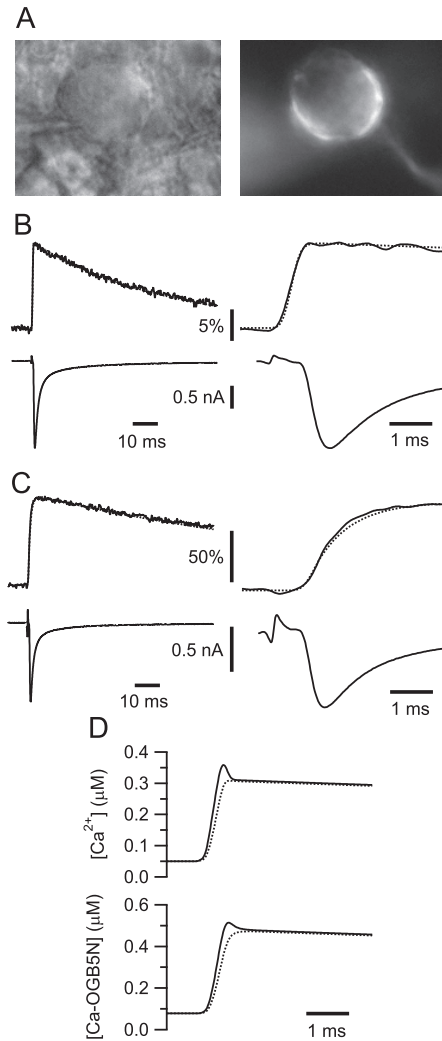


Figure 1. Fluorescent calcium transients at the calyx of Held synapse.

A: Nomarski (left) and fluorescent CCD image (right) of a calyx of Held filled with OGB-5N. B: Top traces: presynaptic OGB-5N fluorescence transients during an action potential, recorded with a photomultiplier tube. Bottom traces: excitatory postsynaptic currents. The right panel shows the same traces as the left panel at higher time resolution to emphasize the relation between the prespike and the presynaptic calcium transient. Responses are the average of 100 traces. Stimulation artifacts have been truncated. Broken line in top traces is the

response predicted from the single compartment model scaled to the same peak amplitude. In the simulations, dye concentration was $50 \mu\text{M}$, for the other parameters see Methods. C: Same as B except terminal was pre-loaded with Fluo-4. D: Effect of off-rate of the endogenous buffer on fluorescence transients. Lowering the off-rate of the endogenous buffer in the simulations from the control value of 16000 s^{-1} (broken line) to 10000 s^{-1} (continuous line), while keeping the on-rate at $5 \cdot 10^8$ per Msec and the endogenous binding ratio at about 40 results in a clear overshoot in the volume-averaged $[\text{Ca}^{2+}]$ (top traces), which is reported as a rapid component in the decay of the simulated OGB-5N transient (lower traces).

Calcium transients during PTP

We used the fluorometric signals to test for a change in the calcium transients after the induction of PTP. Unfortunately, it was no longer possible to induce PTP after prolonged calcium imaging. Probably, this was due to a phototoxic effect on the terminal. Only when light exposure was restricted to a short baseline period before the tetanus was it possible to induce PTP. Following a 5 min, 20 Hz tetanus, the EPSCs in the terminals that had been preloaded with Fluo-4 increased by $98 \pm 22\%$ ($n=7$), similar to intact terminals (Chapter 3). The PTP was accompanied by a clear increase in the amplitude of ΔF_{AP} (Figure 2A). The amount of PTP and the increase in ΔF_{AP} were correlated (Figure 2F). On average the fluorescence transient increased by $15 \pm 4\%$ ($n=7$). There was a small increase ($0.24 \pm 0.11 \text{ ms}$) in the time to onset of ΔF_{AP} . A clear example is shown in Figure 2B. This increase correlated well ($r=0.99$) with an increase in the delay of the EPSCs in the same experiments (Figure 2C), indicating that the increased delay following PTP induction was due to an increased delay until presynaptic calcium channels opened, rather than changes downstream of Ca^{2+} entry. Apart from the small increase in the delay of ΔF_{AP} , its kinetics were very similar after the tetanus: both its rise time ($p=0.75$; paired t-test) and its decay ($p=0.24$) did not change significantly (Figure 2C). The lack of a change in the kinetics of the fluorescence transients argues against a change in clearance after the induction of PTP. In most experiments, the decay of PTP matched the decay of the increase in ΔF_{AP} (Figure 2D-2E). In the experiment shown in Figure 2D the decay of PTP also matched the increase in basal fluorescence, as previously observed (Chapter 3, Korogod *et al.*, 2005). However, in most experiments this relation could not be reliably assessed, since basal fluorescence was generally not stable during the control period, probably due to washout of extracellular dye.

Surprisingly, in the presence of the low-affinity dyes rhod-dextran or OGB-5N, in only one out of six synapses a large increase in the size of the EPSC was observed. This was

accompanied by a clear increase in ΔF_{AP} . In the other five synapses, EPSCs increased by only $29 \pm 3\%$ and ΔF_{AP} changed little after the tetanus ($-1 \pm 4\%$).

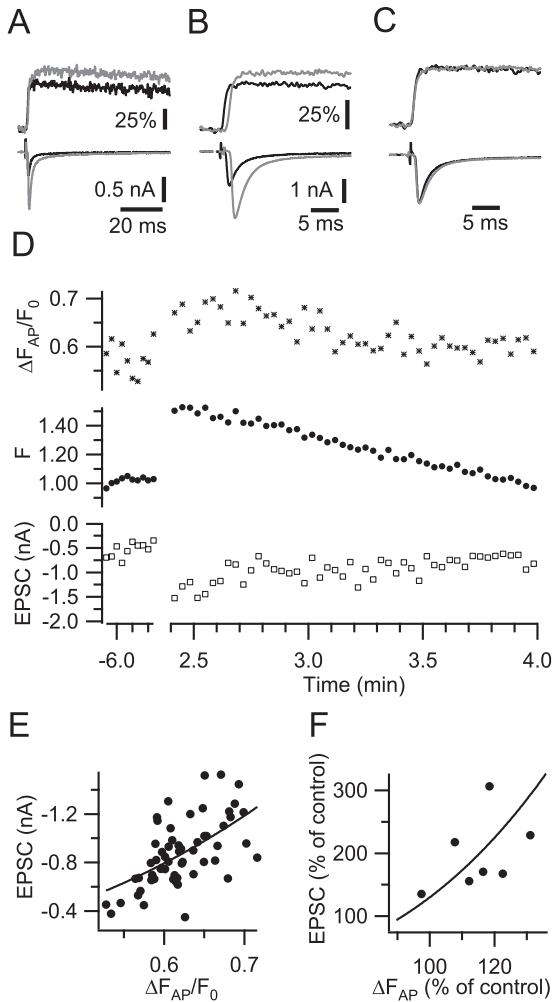


Figure 2. Relation between fluorescence transients and postsynaptic currents during PTP at the calyx of Held synapse.

A: EPSCs (bottom traces; average of 10) before (black) and after (grey) tetanization and accompanying fluorescence transients (top traces) of a terminal pre-loaded with 200 μM Fluo-4. The fluorescence level before the action potential was subtracted to illustrate the difference in amplitude before and after PTP induction. Fluorescence transients are shown as $\Delta F_{AP}/F_0$. *100%. B: Responses from a different synapse as in A, which showed a clear increase in delay

of both EPSCs and fluorescence transients during PTP. C: Same transients as in B, except scaled to the same peak amplitude and shifted in time until rising phase of EPSCs matched. D: Amplitudes of fluorescence transients evoked by an action potential relative to the basal fluorescence before the tetanus ($\Delta F_{AP}/F_o$; top traces), basal fluorescence (F ; middle traces) and amplitude of EPSCs (lower traces) before and after a 5 min, 20 Hz tetanus. Time points are given relative to the end of the tetanus. E: EPSC amplitude plotted against the calcium transient amplitude $\Delta F_{AP}/F_o$. Solid line is the fit with a power law $EPSC=A*(\Delta F_{AP}/F_o)^m$, where the scaling variable A was -3 , and m was 2.6 . Data in A, D, E are from the same experiment. F: Relation between EPSC amplitude following a tetanus and the amplitude of Fluo-4 transients. Each point represents a different experiment. The solid line is given by the function $EPSC_{after}/EPSC_{before}=1.3*(\Delta F_{after}/\Delta F_{before})^3$, where the factor 1.3 represents the relative pool size following PTP induction and the factor 3 the power relation between calcium signals and EPSC sizes.

Relation between calcium influx and fluorescence signal

The increase in the Fluo-4 transients following induction of PTP could be due to an increase in calcium influx, an increase in the fraction of inflowing calcium ions that are captured by the dye, or a combination of the two. A possible increase in the captured fraction of inflowing calcium ions could be due to a decrease in the calcium clearance or due to a decrease in competing endogenous buffers. Our earlier conclusion that the endogenous buffer most likely has low affinity and that Fluo-4 captures most of the calcium ions at the concentration used in the PTP experiments suggests that an effect on calcium influx is more likely than a selective depletion of endogenous buffers. To test the relation between the size of the calcium influx and the calcium signals at different presynaptic Ca^{2+} levels, we voltage clamped the presynaptic terminals with trains of ten action potential waveforms (APWs) at 100 Hz after pharmacologically isolating the calcium currents. This allowed us to directly compare the calcium influx per action potential with the fluorescence signals. Both in the presence of Fluo-4 and in the presence of OGB-5N, the calcium currents facilitated during the train (Figure 3A-3B). In the presence of Fluo-4, the influx per APW increased by around 20% at the end of the train, in agreement with earlier results (Borst & Sakmann, 1998b). In the presence of OGB-5N, the facilitation was more transient (Figure 3D), which is in line with the lack of an increase in ΔF_{AP} following a tetanus in most of the PTP experiments in which OGB-5N was used. The absence of calcium channel facilitation during long trains in the presence of OGB-5N may have contributed to the reduced PTP in the experiments described above. The train of APWs led to clearly resolvable fluorescent transients (ΔF_{APW}), consisting of a rapid rising phase followed by an exponential decay

(Figure 3A-3B). The time constant of this decay changed little during the train, both for terminals filled with OGB-5N (200 μM) and with Fluo-4 (100 μM). The amplitude of the fluorescence increase following the first and the last APW were similar for the OGB-5N transients (Figure 3A, inset), but the last APW evoked a smaller fluorescence transient than the first APW in the terminals filled with Fluo-4 (Figure 3B, inset), despite the larger calcium influx (Figure 3D). To take into account the changes in the calcium influx during the train, we calculated the ratio between fluorescence change and calcium influx ($\Delta F/\Delta Q$). In the presence of the low affinity dye OGB-5N, $\Delta F/\Delta Q$ largely remained the same, with a small increase during the first APWs and a small decrease towards the end of the train (Figure 3D). In contrast, in the presence of the high-affinity dye Fluo-4, $\Delta F/\Delta Q$ gradually decreased during the train, as Ca^{2+} accumulated. These experiments provide more evidence for our earlier conclusion that the large majority of the endogenous buffer has low affinity for Ca^{2+} . As a result the increase in the calcium concentration during the train leads to little saturation of both the endogenous buffer and OGB-5N, resulting in little changes in $\Delta F/\Delta Q$. At the same time the gradual decrease in the availability of Fluo-4 leads to a gradual decrease in $\Delta F/\Delta Q$.

Although these experiments are in agreement with our earlier conclusion that the endogenous buffer has low affinity for Ca^{2+} , they do not provide positive evidence that we would be able to detect the presence of a low concentration of an endogenous high-affinity calcium buffer. We therefore repeated these experiments in the presence of both OGB-5N (200 μM) and fura-2 (50 μM). The decay of the OGB-5N transients now clearly became bi-phasic (Figure 3C). If the decay of the response to a single APW was fitted with two exponential functions, the fast time constant ranged between 1-2 ms, whereas the slow time constant was >100 ms ($n=4$; not shown). Because of the different spectral properties of the two dyes, we could also measure the fura-2 fluorescence transients within the same experiment. The presynaptic calcium concentration increased from a basal level of about 100 nM to about 160 nM after the first APW ($n=4$). The rising phase of the fura-2 transients was much slower than of the OGB-5N transients, and it largely matched the fast component in the decay of the OGB-5N transients (Figure 3C). As calcium accumulated to a maximum level of about 1 μM at the end of the train, the relative contribution of the fast phase decreased from $81 \pm 5\%$ to $6 \pm 3\%$ ($n=4$) following the last APW. The $\Delta F/\Delta Q$ for OGB-5N showed a clear increase during the train, which we interpret as being due to the saturation of the competing other exogenous calcium buffer fura-2, since $\Delta F/\Delta Q$ of fura-2 became much smaller at the same time.

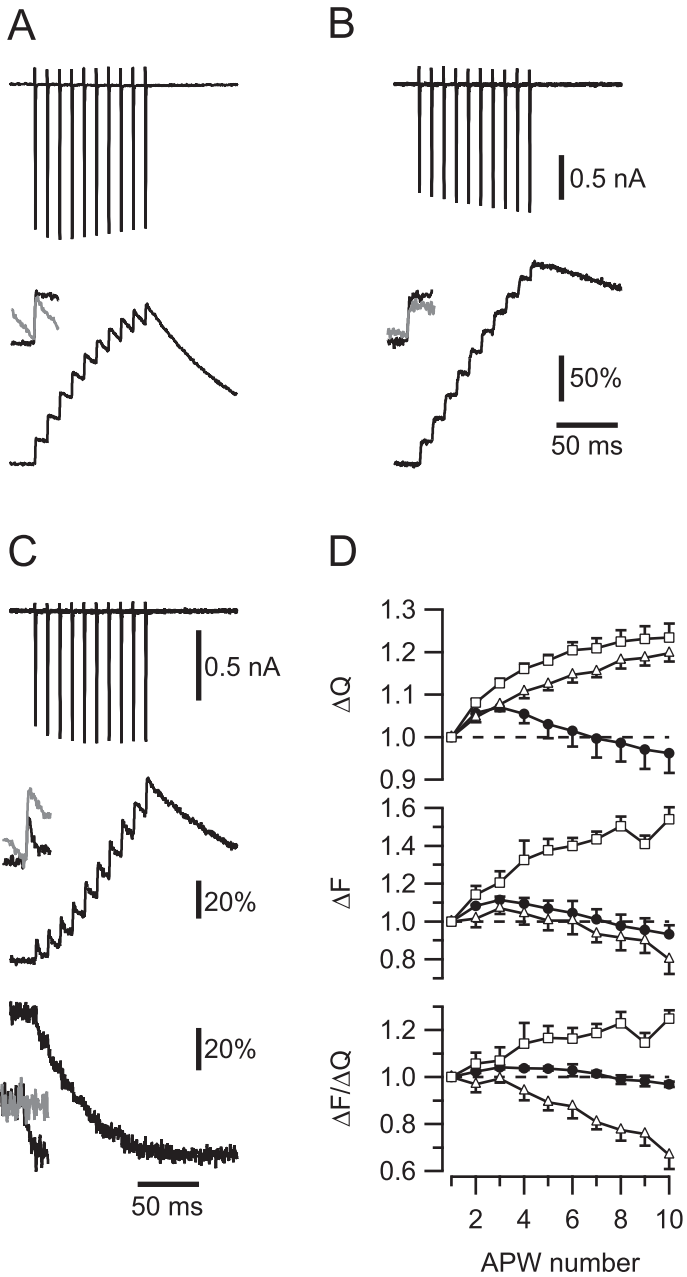


Figure 3. Calibration of fluorescence transients.

A: Example traces of a terminal which was filled with OGB-5N (200 μM) and was voltage clamped with ten action potential waveforms (APW) in the presence of blockers of Na^+ and K^+ channels. Top trace shows the calcium currents, bottom trace shows the fluorescence responses

(average of 10 responses) of the terminal. Inset shows the first (black) and the last (grey) fluorescence transient overlaid, enlarged to illustrate the difference in time course. B: Same as A, except the terminal contained Fluo-4 (100 μM). C: Same as in A and B, except the terminal contained both OGB-5N (200 μM , middle traces) and fura-2 (50 μM ; lower traces). D: Calcium influx per APW (top), fluorescence changes (middle) and the ratio between the two (lower panel) during the train, for terminals filled with OGB-5N (filled circles; 200 μM ; $n=3$), Fluo-4 (open triangles; 100 μM ; $n=3$) or both OGB-5N (200 μM) and fura-2 (open squares; 50 μM ; $n=4$). Responses are given relative to the response to the first APW.

Train simulations

Our interpretation of the fluorescence signals during trains of APWs does not take diffusion or heterogeneities in calcium influx or calcium buffering into account. To test whether the binding kinetics and relative affinities of the different endogenous and exogenous calcium buffers provided a sufficient interpretation of the observed signals we repeated the simulations of the single compartment model for trains of APWs. In these simulations we used the measured calcium currents illustrated in Figure 3 (after filtering, truncation of outward currents and subtraction of slow calcium-activated currents) as inputs and added the exogenous calcium buffers using the same low-affinity endogenous buffer as in Figure 1. During these trains the volume-averaged calcium concentration rose to about 0.6 μM in the presence of a high affinity calcium dye (Fluo-4, or fura-2 in combination with OGB-5N) and about 1.3 μM in the presence of OGB-5N. Both the simulated fluorescence transients (Figure 4A-4C) and the resulting $\Delta F/\Delta Q$ (Figure 4D) were qualitatively similar to the data illustrated in Figure 3. The simulations also confirmed the validity of the interpretation of the experiments in which we added both a high- and a low-affinity dye. The low-affinity dye is able to report how the calcium transfers from the low-affinity buffers to the high-affinity dye. Due to its slow equilibration, the high-affinity dye is not able to report subtle changes in the time course of the calcium influx, as may happen following PTP induction. The contribution of the high-affinity dye becomes less pronounced as calcium accumulates and the dye saturates. As a result, the low-affinity dye faces less competition and $\Delta F/\Delta Q$ will increase during the train. The experiments and simulations with two different exogenous dyes confirm that even small concentrations (<50 μM) of a slowly equilibrating calcium buffer (off-rate <5000 s^{-1}), would lead to clear deviations from a single exponential decay for the OGB-5N transients, in contrast to what was observed in Figures 1 and 3A.

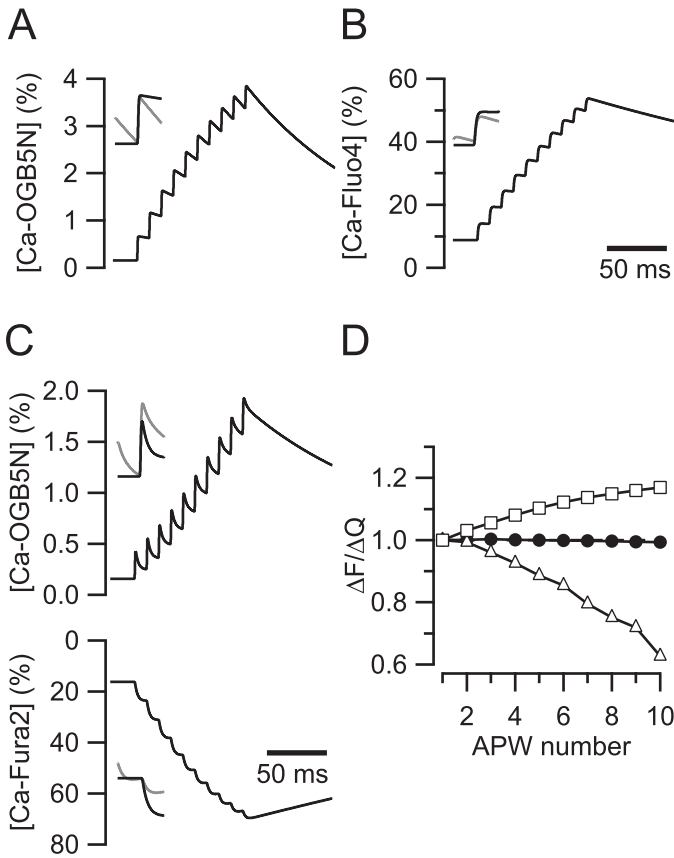


Figure 4. Simulations of fluorescence transients.

Calcium currents shown in Figure 3 were taken as inputs for calculating the fluorescence transients in a single-compartment model of the calyx of Held. Parameters are given in Methods. Terminal contained OGB-5N (200 μM ; A), Fluo-4 (100 μM ; B) or a combination of OGB-5N (200 μM) and fura-2 (50 μM ; C). Responses are given as percentage of total dye concentration. Insets show overlay of fluorescence transients evoked by the first (black) and the last APW (grey), enlarged to emphasize the difference in time course. D: Ratio between calcium influx and amplitude of the fluorescence transient, relative to the first APW. Black circles, OGB-5N; Open triangles, Fluo-4; Open squares, OGB-5N plus fura-2.

DISCUSSION

By choosing dyes with low background fluorescence and by using a low-noise photomultiplier, we were able to record the calcium signals that were evoked by an action potential in a single presynaptic terminal at much higher time resolution and with a much better signal-to-noise ratio than in earlier studies of the calyx of Held (Helmchen *et al.*, 1997; Schneggenburger *et al.*, 1999; Billups & Forsythe, 2002). The signal-to-noise ratio was also much higher than in our earlier study, in which we used fura-2 (Chapter 3). This allowed us to compare the calcium transients evoked by an action potential before and after induction of PTP. We show that PTP at the calyx of Held synapse is accompanied by a clear increase in these calcium transients. The most likely cause for this increase is an increase in calcium influx during an action potential. In this Discussion we review the evidence for this conclusion and we discuss the significance of our findings for the mechanism of PTP at the calyx of Held synapse.

Increased calcium transients during PTP

We observed a clear increase in the Fluo-4 transients following PTP induction. On average, the transients increased by around 15%. There are three possible causes for the observed increase in the Fluo-4 signal. It could be due to an increase in the calcium influx, a decrease in calcium clearance or it could be due to a decrease in the endogenous calcium buffers that compete with the Fluo-4. We have several arguments that support our conclusion that the increased Fluo-4 signal was due to increased calcium influx. A decrease in Ca^{2+} clearance is unlikely since the time course of the Fluo-4 signal was not changed after PTP induction. Following the induction of PTP, the presynaptic calcium concentration is elevated by around 100 nM and the decay of PTP largely matches the decay of this increase (Chapter 3). This increase in residual calcium could lead to a partial depletion of endogenous calcium buffers. At other terminals, fluorometric evidence for a high-affinity endogenous buffer component has been obtained (Sinha *et al.*, 1997; Jackson & Redman, 2003; Collin *et al.*, 2005; Lin *et al.*, 2005) and partial depletion of the endogenous calcium buffer has been proposed to be responsible for most of the short-term facilitation of release at the calyx of Held synapse (Felmy *et al.*, 2003). We therefore analyzed the measured calcium transients in detail, to investigate whether under the conditions in which we observed the increase in calcium transients, we could find fluorometric evidence for a high-affinity endogenous calcium buffer, whose depletion could be partially responsible for the observed increase in the calcium transients.

Analysis of calcium transients suggests low endogenous buffer affinity

A comparison of amplitude and time course of different calcium dyes with model predictions indicated that under our experimental conditions the large majority of the endogenous buffer has low affinity ($>5 \mu\text{M}$) for Ca^{2+} . The OGB-5N transients that were evoked by a single action potential decayed mono-phasicly. Simulations (Figure 1D) and experiments (Figure 3C) suggested that the presence of even small amounts ($<50 \mu\text{M}$) of a high-affinity endogenous calcium buffer would lead to clear deviations from a mono-exponential decay. In presynaptic voltage clamp experiments we compared calcium influx during action-potential waveform stimuli and the resulting fluorescence changes at different Ca^{2+} concentrations. If the endogenous buffer has low affinity, both the amplitude and the time course of the low-affinity OGB-5N transients are predicted not to change, as long as the calcium clearance mechanism is linear and not saturated. The low-affinity buffer OGB-5N initially showed a small increase in the fraction of calcium ions that it captured per stimulus, followed by a small decrease as Ca^{2+} accumulated during the train (Figure 3D). The increase of a few percent for the OGB-5N signal could be due to saturation of a small component of the endogenous buffer with a higher affinity for Ca^{2+} than the dye. Alternatively, it could be due to small errors in the quantification of the calcium influx, due to incorrect estimate of calcium-activated currents or gating currents, or small errors in the quantification of the fluorescence step, due to incorrect correction for clearance during the rising phase of the transients. Apart from this small increase, both the amplitudes and the time course of the OGB-5N transients closely followed the prediction of the model with a low-affinity endogenous buffer and a linear clearance mechanism, up to a level of at least $1 \mu\text{M}$. This concentration was much higher than the increase in residual calcium observed after PTP induction at the calyx of Held (Chapter 3, Korogod *et al.*, 2005). A linear clearance mechanism has also been observed at the crayfish neuromuscular junction (Tank *et al.*, 1995).

In contrast, in the presence of a low-affinity endogenous buffer, a high-affinity dye like Fluo-4 is expected to show a gradual decrease in the fraction of inflowing calcium ions that it captures during the train, as less and less dye will be available to compete with the endogenous buffer. At other terminals it was not possible to directly measure the calcium influx during trains of action potentials, but nevertheless qualitatively similar results have been obtained, a decrease in signals during the train for high-affinity dyes, but increases or no change for low-affinity dyes (David *et al.*, 1997; Kreitzer & Regehr, 2000; Koester & Johnston, 2005).

From the analysis of the time course and amplitudes of the calcium transients we therefore conclude that the endogenous calcium buffer in these experiments had a low affinity for Ca^{2+} . A similar conclusion was also reached along different lines by

(Bollmann & Sakmann, 2005). At cerebellar terminals (Sabatini & Regehr, 1998) or in chromaffin cells (Xu *et al.*, 1997) the endogenous buffer also has low affinity for Ca^{2+} . Our data cannot exclude the washout during dye loading of a high-affinity mobile buffer. The absence of PTP in experiments in which the terminals were loaded with low-affinity dye indicates that calcium buffering is of importance for the induction of PTP. Possibly these buffers interfered with PTP induction by limiting the maximal Ca^{2+} increase during the tetanus more effectively than the low-affinity buffer fluo-4. Alternatively, the low-affinity buffers shortened the decay time of the PTP to the extent that it was missed in our recordings, which did not start until more than one minute after the tetanus to allow for pool recovery. At later developmental stages, high-affinity calcium binding proteins such as calretinin or parvalbumin may make a larger contribution to calcium binding (Lohmann & Friauf, 1996; Felmy & Schneggenburger, 2004) and this might explain why longer stimulation is needed to induce PTP in older animals (Korogod *et al.*).

Increased calcium influx during PTP

If the endogenous buffer is low, this means that the increase in the Fluo-4 transients after PTP induction was not due to selective depletion of a high-affinity endogenous calcium buffer. We therefore conclude that this increase must have been due to an increase in calcium influx. Although the Fluo-4 concentrations we used were low (<200 μM) and comparable to the buffer concentrations we used in our previous study in which we focussed on residual calcium (Chapter 3), due to the low endogenous buffer capacity of the calyx of Held at young ages (Helmchen *et al.*, 1997), the calcium dye nevertheless captured most of the incoming calcium ions (>80%) in the PTP experiments. This means that in these experiments, the ‘overload’ condition was almost reached, meaning that under these conditions the dye provided a sensitive indication for calcium influx (Neher, 1995). Changes in the endogenous buffer will therefore have comparatively little effect on the measured Fluo-4 transients and it is hard to come up with a scenario for which these effects are larger than the effects that residual calcium will have on the availability of Fluo-4 after PTP induction. This means that the increase of 15% has to be viewed as a lower estimate for the increase in calcium influx.

What caused the increase in calcium influx?

The increase in calcium influx can be due to a facilitation of the calcium currents (Borst & Sakmann, 1998b; Cuttle *et al.*, 1998) or to a change in the action potential shape. We

did observe a change in the prespike (Figure 2A-2B), suggesting that a broadening of the action potential may have contributed to the increased calcium influx (Borst & Sakmann, 1999b). We were not able to address this conclusively, because of the inability to evoke PTP in presynaptic whole-cell recordings and because the Fluo-4 transients were too slow to detect changes in the time course of the calcium influx. Facilitation of calcium currents very likely contributed to the observed changes in the calcium influx. A few action potential waveforms were sufficient to induce a facilitation of the calcium influx that was comparable to the increases that we observed in the Fluo-4 signal after PTP induction (Figure 3). In contrast, in the presence of OGB-5N, a train of action potential waveforms did not give a sustained facilitation of the calcium influx and no increase in the calcium signals following a tetanus was observed in most current clamp experiments that used OGB-5N as the dye. Since PTP was reduced in the presence of OGB-5N, whereas in the fluo-4 experiments it was comparable in size to the PTP observed in intact terminals, these experiments suggests that the increase of the calcium influx that we observed in the Fluo-4 voltage clamp experiments best matches the situation in the undialysed terminals. Interestingly, an increase of around 15% in calcium signals during action potential trains was also observed in granule cell terminals of the cerebellum (Kreitzer & Regehr, 2000).

Our experiments provide further evidence for the key role that the modulation of calcium channels plays in the regulation of short-term plasticity. Facilitation of calcium currents is also important for short-term facilitation of transmitter release at the calyx of Held (Taschenberger *et al.*, 2002; Inchauspe *et al.*, 2004; Ishikawa *et al.*, 2005) and inactivation of calcium currents contributes to synaptic depression (Forsythe *et al.*, 1998; Xu & Wu, 2005). The facilitation of calcium currents depends on an interaction with the high-affinity calcium-binding protein neuronal calcium sensor 1 (NCS-1)(Tsujiimoto *et al.*, 2002) and this protein has also been implicated in short-term facilitation of transmitter release at the neuromuscular junction or the hippocampus (Rivosecchi *et al.*, 1994; Sippy *et al.*, 2003), although as of yet there is no evidence that it exerts its effects via calcium channels at these synapses. The regulation of calcium channels by calcium binding proteins like NCS-1 or other members of this family is complex and they may have both Ca^{2+} -dependent and Ca^{2+} -independent effects on both inactivation and facilitation of calcium channels (Burgoyne *et al.*, 2004; Few *et al.*, 2005). It would be interesting to test to what extent these differential effects could explain why following a long tetanus calcium currents inactivate during presynaptic whole-cell recordings, leading to PTD (Forsythe *et al.*, 1998), whereas the opposite appears to be true when synapses are intact.

The observed increase in calcium influx most likely played a significant role in the increase in release probability following the tetanus. A third power relation between volume-averaged calcium signals and release has been observed in previous

experiments at the calyx of Held synapse (Borst & Sakmann, 1999b; Wu *et al.*, 1999) and combined with the pool size increase of around 30% that we observed in our earlier experiments following PTP induction (Chapter 3), this would be sufficient to account for most if not all of the PTP (Figure 2F). This conclusion depends on the assumption that even if the time course of the calcium influx would change, the third power relation between influx and release would remain valid. Although this may be true for the changes in the time course of calcium influx due to action potential changes during high-frequency trains (Borst & Sakmann, 1999b), both lower (Bollmann & Sakmann, 2005) and higher (Fedchyshyn & Wang, 2005) values for this power relation have also been observed when the time course of the calcium transients were changed. Therefore, our experiments cannot exclude that local buffer saturation or changes downstream of Ca^{2+} may provide additional contributions, as suggested by other experiments in the same preparation (Felmy *et al.*, 2003; Awatramani *et al.*, 2005; Lou *et al.*, 2005).

In earlier experiments we observed that the potentiation of evoked release decayed similarly to residual calcium, whereas increases in the frequency of spontaneous release decayed more rapidly (Chapter 3). An attractive feature of the possibility that the increased calcium influx was due to the interaction of a high-affinity calcium binding protein such as NCS-1 with the presynaptic calcium channels is that it provides a simple explanation for this observation, since a regulation of calcium influx by residual calcium will preferentially affect evoked release over spontaneous release. The more rapid decay of spontaneous release could be due to supralinear effects of a direct activation of the calcium sensor for release by residual calcium (Chapter 3).

Chapter 5

Dynamics of the readily-releasable pool during post-tetanic potentiation in the rat calyx of Held synapse

Ron L. P. Habets and J. Gerard G. Borst

J Physiol. 2007 Jun 1;581(Pt 2):467-78

ABSTRACT

The size of the readily releasable pool (RRP) of vesicles was measured in control conditions and during post-tetanic potentiation (PTP) in a large glutamatergic terminal, called the calyx of Held. We measured excitatory postsynaptic currents evoked by a high frequency train of action potentials in slices of 4-11-day-old rats. After a tetanus the cumulative release during such a train was enlarged by approximately 50%, indicating that the size of the RRP was increased. The amount of enhancement depended on the duration and frequency of the tetanus and on the age of the rat. After the tetanus, the size of the RRP decayed more slowly ($t_{1/2} = 10$ versus 3 min) back to control values than the release probability. This difference was mainly due to a very fast initial decay of the release probability, which had a time constant compatible with an augmentation phase ($\tau \approx 30$ s). The overall decay of PTP at physiological temperature was not different from room temperature, but the increase in release probability (P_r) was restricted to the first minute after the tetanus. Thereafter PTP was dominated by an increase in the size of the RRP. We conclude that due to the short lifetime of the increase in release probability, the contribution of the increase in RRP size during post-tetanic potentiation is more significant at physiological temperature.

INTRODUCTION

Synaptic terminals can increase the release of the number of vesicles per action potential after repetitive stimulation. Release can be enhanced because the release probability (P_r) has become higher or because the number of vesicles available for release, the so-called readily-releasable pool (RRP), is larger (Zucker & Regehr, 2002). Both mechanisms have been proposed to be responsible for short-term synaptic plasticity (Stevens & Wesseling, 1999; Rosenmund *et al.*, 2002; Kalkstein & Magleby, 2004); for review see: (Zucker & Regehr, 2002). Short-term plasticity has been classified based on duration. Post-tetanic potentiation (PTP) has the longest duration and augmentation has a duration intermediate between facilitation and potentiation (Magleby & Zengel, 1976). The RRP is a functionally defined pool of vesicles that most likely consists of the docked vesicles observed in electron microscopic studies (Schikorski & Stevens, 2001).

The size of the RRP has been thoroughly investigated in the calyx of Held synapse, a large glutamatergic nerve terminal originating from the globular bushy cells of the cochlear nucleus. The axons of the bushy cells cross the midline and terminate onto the glycinergic principal cells in the medial nucleus of the trapezoid body (MNTB). During a short high-frequency train of action potentials, excitatory postsynaptic currents (EPSCs) in the postsynaptic cell depress. This depression has several causes (Schneggenburger *et al.*, 2002; von Gersdorff & Borst, 2002), of which depletion of synaptic vesicles from the RRP is the most important one at frequencies higher than 100 Hz (Xu & Wu, 2005). Measuring how many vesicles are released during such a train therefore provides an estimate of the RRP size. Depletion of the RRP by high frequency stimulation was confirmed by subsequent depolarizing steps, flash photolysis of caged calcium or hypertonic sucrose application (Schneggenburger *et al.*, 1999; Wu & Borst, 1999; Bollmann *et al.*, 2000; Wu & Wu, 2001). When the size of the RRP is calculated by dividing the cumulative EPSC of a train by the miniature EPSC size, estimates for the size of the RRP at the calyx of Held vary from 600 to 800 vesicles. Larger numbers are obtained by capacitance measurements, deconvolution of EPSCs and quantal analysis (Sakaba & Neher, 2001a; Scheuss & Neher, 2001; Sun & Wu, 2001). Calyx of Held terminals contain around 500 release sites with 2-6 docked vesicles per active zone (Sätzler *et al.*, 2002; Taschenberger *et al.*, 2002). This number of docked vesicles corresponds well with the estimated number of vesicles in the physiologically defined RRP. During an action potential 200 (Borst & Sakmann, 1996) to 400 (Taschenberger *et al.*, 2002) vesicles are released from the terminal, leading to an average P_r of 0.2 per vesicle (Schneggenburger *et al.*, 1999).

In contrast to depression during the tetanus, EPSCs in the principal cells of the MNTB potentiate to around 200 % of control after repetitive stimulation. This potentiation of the EPSCs decays back to baseline with a time constant of 1-9 minutes (Chapter 3, Korogod *et al.*, 2005), which defines this form of synaptic plasticity as PTP. The majority of PTP could be explained by an increase in the P_r of the vesicles in the RRP (Chapter 3, Korogod *et al.*, 2005), but we also found a small but significant increase of the size of the RRP (Chapter 3). An increase in the RRP has also been observed following application of forskolin, an activator of adenylate cyclase (Sakaba & Neher, 2001b; Kaneko & Takahashi, 2004), but it is unclear under what physiological stimulus conditions the RRP size increases. In this study we measured the RRP size with short trains of action potentials and examined its size before and after tetanic stimulation of different lengths and frequencies.

MATERIALS & METHODS

Preparation of slices

Animal procedures were in agreement with the guidelines of the animal committee of the Erasmus MC. Wistar rats were decapitated at postnatal day 4-11 (P4-11) and the brainstem was dissected in ice-cold saline containing (mM): 125 NaCl, 2.5 KCl, 3 MgSO₄, 0.1 CaCl₂, 1.25 NaH₂PO₄, 0.4 ascorbic acid, 3 myo-inositol, 2 pyruvic acid, 25 D-glucose, 25 NaHCO₃ (Merck); pH 7.4 when bubbled with carbogen (95% O₂, 5% CO₂). Coronal slices of 200 μm were cut with a vibratome (Leica, Bensheim, Germany), while the tissue was submerged in ice-cold oxygenated saline. Slices were transferred to a holding chamber containing artificial cerebrospinal fluid (aCSF), which had the same composition as the slicing solution, except that the concentrations of CaCl₂ and MgSO₄ were 2 and 1 mM, respectively. Slices were incubated for 30 minutes at 37 °C. Thereafter, they were either kept at room temperature or at 37 °C for experiments performed at physiological temperature.

Electrophysiological recordings

For electrophysiological measurements slices were transferred to a recording chamber on an upright microscope (BX-50; Olympus, Tokyo, Japan). Oxygenated aCSF was continuously perfused over the slice at 2 ml min⁻¹. In most experiments kynurenic acid (2-4 mM, Tocris, Bristol, UK) was added, to reduce postsynaptic receptor saturation and desensitisation. At the concentration range used (2-4 mM), the rapidly dissociating, competitive glutamate receptor antagonist kynurenic acid reduced the EPSCs by 93-96%, indicating that it prevented released glutamate from binding to most of the available AMPA receptors, thus also largely preventing saturation and desensitization (Diamond & Jahr, 1997; Wu & Borst, 1999; Sakaba & Neher, 2001c; Wong *et al.*, 2003). As a result, the paired-pulse ratio at a stimulus interval of 10 ms increased both at room temperature and at physiological temperature. Neurons were visualized with infrared differential interference contrast optics. The axons of the calyces of Held were stimulated (0.1 ms, 0.03-0.5 mA) at the midline by a bipolar electrode (FHC, inc., Bowdoinham, ME, USA). Cells were selected when extracellular recordings indicated postsynaptic action potential firing (Chapter 3). Whole-cell voltage clamp recordings were made with an Axopatch 200B amplifier (Molecular Devices, Union City, CA, USA) and low-pass (2-10 kHz) filtered with a 4-pole Bessel filter. Signals were digitized at 50 kHz with a Digidata 1320A (Molecular Devices). Pipette solutions contained (in mM): 125 K-gluconate, 20 KCl, 10 Na₂-phosphocreatine, 4 MgATP, 0.3 Na₂GTP, 10

Hepes (Sigma) and 0.5 EGTA. Holding potential for all experiments was -80 mV. Potentials were corrected for a -11 mV junction potential. Series resistance (<15 M Ω) was electronically compensated by 80-98% with a lag of 5 μ s. Cells with a membrane resistance lower than 100 M Ω were rejected from analysis. Data acquisition and analysis was done with pCLAMP (Molecular Devices) or Igor (Wavemetrics, Lake Oswego, OR, USA).

Data analysis

The RRP size was calculated from the sum of the EPSC amplitudes evoked by a train of action potentials with a frequency of 50, 100, 200 or 400 Hz, depending on the maximal frequency at which the terminals fired action potentials without failures. Such short trains of action potentials have been shown to fully deplete the RRP (Wu & Borst, 1999). After six EPSCs the depletion and replenishment of vesicles was considered to have reached a steady state and the rest of the cumulative EPSC plot was fitted with a line, which was back-extrapolated to the start of the stimulus train to correct for replenishment during the train (Elmqvist & Quastel, 1965; Schneggenburger *et al.*, 1999). This yielded an RRP estimate in nanoamps, which was converted to number of vesicles by dividing it by the mean amplitude of spontaneous release events of the same cell. This method of calculating the RRP size assumes that the RRP can be depleted by high-frequency trains of action potentials, for which experimental evidence has been obtained (e.g. Wu & Borst, 1999). In addition, it assumes that replenishment is constant. Although this assumption is most likely incorrect (e.g. Sakaba & Neher, 2001a), as long as the steady-state component is small, the errors in the estimate of RRP can be expected to be small as well. An estimate of the P_r of the vesicles in the RRP was obtained by dividing the amplitude of the first EPSC of a train by the RRP size. This method assumed that the P_r of vesicles in RRP is homogeneous. Since this assumption is most likely incorrect (e.g. Wu & Borst, 1999), the reported P_r values may overestimate the true release probabilities. The increase in PTP or RRP size was calculated by dividing the difference before and after the tetanus by the pre-tetanus value. Averaged traces were fitted with a bi-exponential function. Processes with a time constant of at most 30 s were regarded as an augmentation phase. The mean pre-tetanus value was subtracted from data plotted on a semi-logarithmic axis.

Spontaneous release events were identified using Clampfit 9.0 (Molecular Devices) by a template made of averaged, manually selected, spontaneous EPSCs.

The amplitude of the prespikes, which could be observed preceding the EPSC in the postsynaptic recordings (Forsythe, 1994), was quantified as the difference between the negative and positive peak. Prespike amplitudes and EPSC amplitudes were divided by

their respective mean value before the tetanus (except for Fig. 5C, where the data were normalized to the peak). Data are given as means \pm standard error of the mean (S.E.M.). Statistical comparisons were done using Student's t-test, unless otherwise noted.

RESULTS

Induction criteria for a change in the RRP

High frequency stimulation in the calyx of Held results in PTP (Chapter 3, Korogod *et al.*, 2005). This potentiation results from two different processes, an increase in the RRP and an increase in the probability that a vesicle from this pool is released (P_r). Although the latter has been extensively investigated (Chapter 3 & 4, Awatramani *et al.*, 2005; Korogod *et al.*, 2005; Lou *et al.*, 2005), the increase in the RRP has received less attention. We started by looking at the induction criteria for an increase in the RRP. We stimulated the axons of the calyces with 100 Hz tetani of different lengths. Before and after this stimulation the EPSC amplitude was measured at 0.1 Hz (Fig. 1A) and an estimate of the size of the RRP and P_r was obtained with a short high frequency train (Fig. 1B). The RRP was enlarged by $13 \pm 4.5\%$ ($P = 0.81$) after 100 stimuli and reached a plateau after 500 stimuli ($52 \pm 7.1\%$, $P < 0.05$, Dunnett's t-test, Fig. 1C). The increase in P_r after 100 Hz stimulation (Fig. 1D) was similar to our previous measurements after 20 Hz stimulation (Chapter 3).

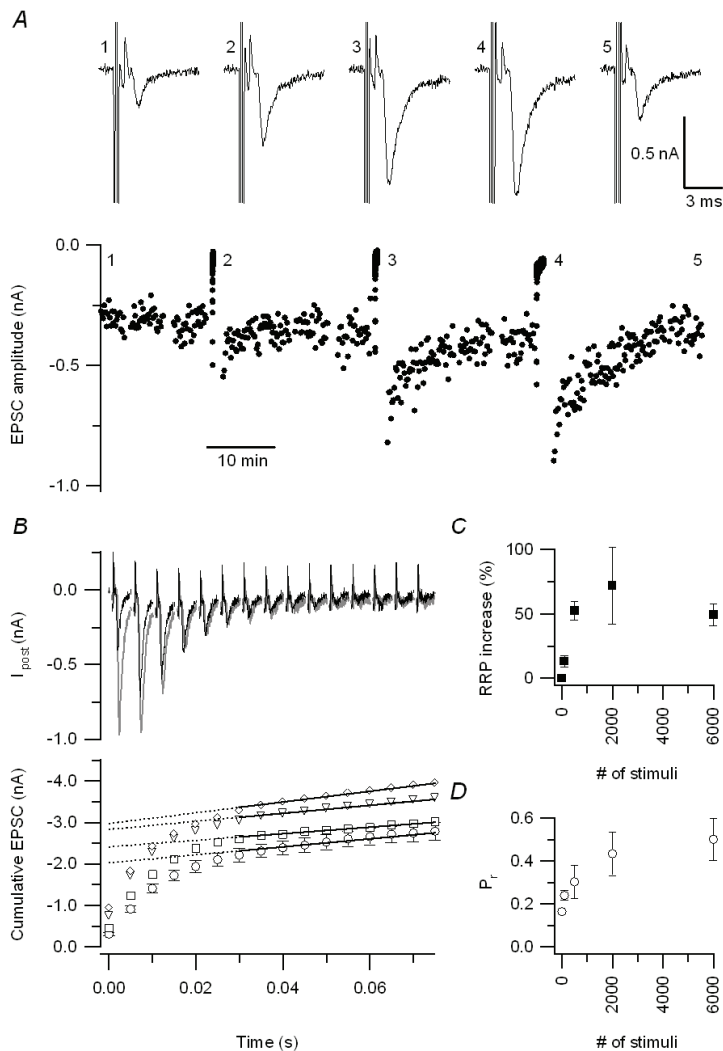


Figure 1. Induction criteria for PTP at 100 Hz

Axons were stimulated in the midline and EPSCs were recorded in the presence of 2 mM kynurenic acid. The experiments were conducted at RT in slices of 9-10 day old rats. *A*, EPSC amplitudes were measured at 0.1 Hz before and after a 100 Hz tetanus of 500, 2000 and 6000 stimuli. Top, example traces, numbers indicate corresponding time point in the bottom graph. *B*, Six minutes before and one minute after the tetanus the size of the RRP was probed with a short 200 Hz train (25 stimuli). Black traces in the top panel show the first 15 EPSCs in such a train under control conditions, while grey traces show the same, one minute after a tetanus (6000 stimuli at 100 Hz). Stimulation artefacts were blanked, but prespikes are

shown. In the bottom panel the EPSC amplitudes of the 200 Hz trains are plotted cumulatively. The amplitudes after a tetanus of 500 stimuli (squares), 2000 (triangles) and 6000 (diamonds) are shown together with the average of the control trains (circles \pm SEM). An estimate of the RRP size was obtained by extrapolation to the first EPSC of a line that was fitted through the last 18 points in the curve. Traces and amplitudes shown in A and B are from the same experiment. C, The mean (\pm SEM) increase in the RRP estimate of all experiments ($n=3$) is shown as a function of the number of stimuli in the tetanus. The increase without stimulation is set to zero. D, P_r plotted versus the number of stimuli in a 100 Hz tetanus. The mean P_r was calculated by dividing the first EPSC amplitude of a train by the estimate of the RRP.

Dynamics of the increase in pool size

In the experiments summarized in Fig. 1, a bi-exponential decay of PTP was present in 3 of 5 cells (as judged by eye, e.g. Fig. 1A). We previously reported a fast and slow component of decay for a subset of experiments following 20 Hz stimulation (Chapter 3). To assess the contribution of the increase in RRP size and in P_r to the two phases of decay, we continuously stimulated the terminal with short high frequency trains with an inter-stimulus interval of 1 min (Fig. 2A and D). These experiments were followed by a second experiment where PTP was quantified in a more standard fashion, by analysing the change in EPSC amplitude during 0.1 Hz stimulation. PTP was more prolonged when the RRP was continuously measured, indicating that these short high frequency trains sustained the potentiation. The size of the RRP estimate in Fig. 2E increased during the baseline period, probably for the same reason. This stimulation protocol enabled us to measure changes in the RRP and changes in P_r simultaneously during the decay of PTP. We found that the P_r was already greatly increased 20 seconds after a 100 Hz tetanus. The P_r returned to baseline levels with a half decay time of 3.0 ± 1.4 min ($n=5$). The RRP did not reach its maximum until after 1 min, and decreased more slowly to baseline ($t_{1/2}=10 \pm 2.4$ min, $n=5$; Fig. 2, E and F). The decay of the mean P_r increase was well described with a double exponential function ($\tau_{\text{fast}} \approx 0.5$ min, $\tau_{\text{slow}} = 11$ min; Fig. 2C), which indicates that there might be an augmentation phase shortly after the tetanus. The dynamics of the mean RRP size were fitted with a fast increase ($\tau \approx 0.3$ min) and a slow decrease ($\tau = 15$ min) after the tetanus (Fig. 2C). During RRP depleting trains, the steady state release from terminals depends on replenishment of

Dynamics of the readily-releasable pool during post-tetanic potentiation in the rat calyx of Held synapse vesicles (Kushmerick *et al.*, 2006). The amount of depression is therefore inversely proportional to the replenishment rate. Twenty seconds after the tetanus the action potentials in the presynaptic terminals failed in response to high frequency stimulation (Fig. 2A). This hampered a correct analysis of depression and replenishment. At 80 seconds post-tetanus the amplitudes of the EPSCs at the end of the 200 Hz train were similar to control (Fig. 2B).

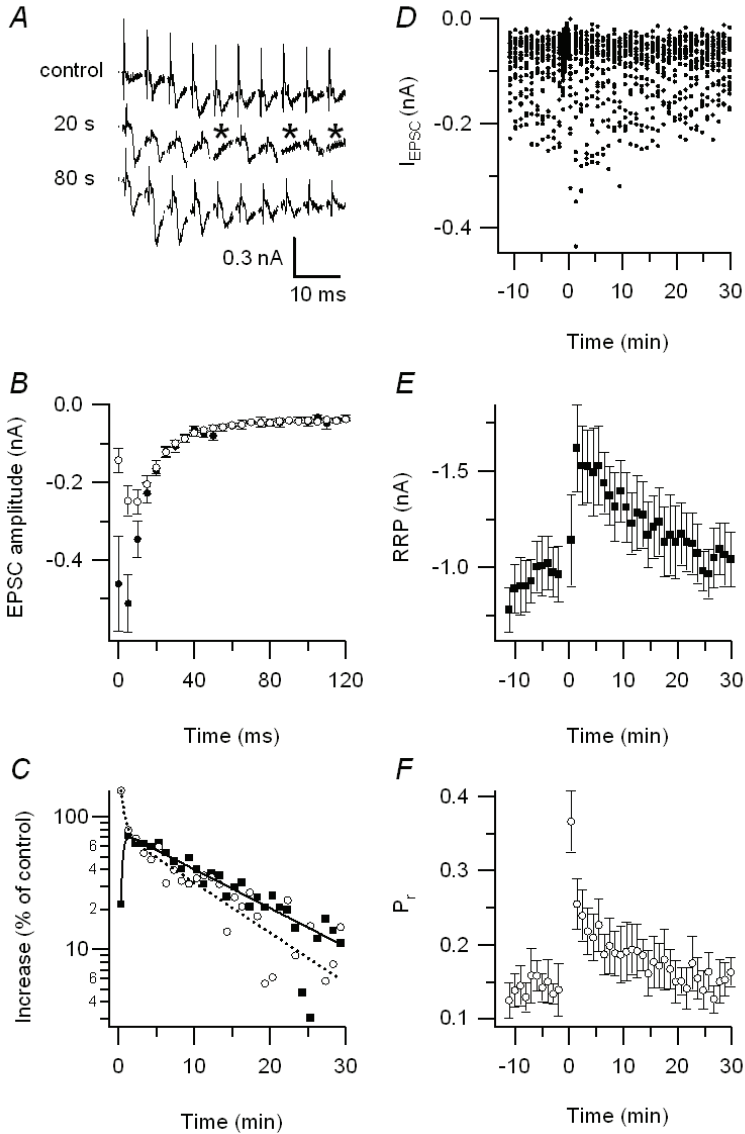


Figure 2: Dynamics of the RRP during PTP

The RRP size was continually probed with short trains of action potentials in the presence of 2 mM kynurenic acid. A, the first 10 traces of a train, before (top), 20 seconds after (middle) and 80 seconds after a 100 Hz tetanus of 1 minute. Asterisks indicate presynaptic action potential failures. Stimulation artefacts were blanked. B, mean amplitudes during the 200 Hz trains of 4 experiments. Open circles are from the test train before the tetanus, filled circles are

from a test train 80 seconds after the tetanus. C, semi-logarithmic plot of the P_r (open circles) and RRP size (filled squares) after the tetanus. The values correspond to the values in figures E and F, but are presented as the change from baseline for comparison of the contribution of both decays to PTP. Double exponential functions were fitted through the mean RRP values ($n=5$, continuous line) and mean release probabilities ($n=5$, dotted line). D, EPSC amplitudes of the experiment with continuous measurement of the RRP before and after the tetanus ends ($t=0$). E, time plot of the mean RRP estimates. F, Time plot of the release probabilities.

Age and frequency dependence of a change in the number of releasable vesicles

The size of the RRP and the number of active zones increase with age in the calyx of Held (Taschenberger *et al.*, 2002) and PTP is more easily induced in younger rats (Korogod *et al.*, 2005). We therefore compared the contribution of a change in the RRP to PTP at different neonatal ages (Fig. 3). In slices from 4-day-old rats, just after formation of the calyceal synapse (Hoffpauir *et al.*, 2006), PTP could be induced with a 20 Hz tetanus of 5 min. The change in RRP size was maximal at P4 and declined with age until around P10. The age dependence could arise from the more rapid calcium clearance at the older ages (Chuhma & Ohmori, 2001).

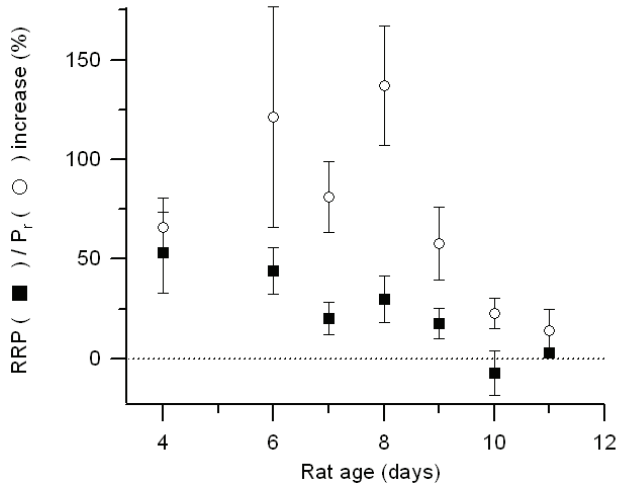


Figure 3: Age dependence of the increase in RRP and P_r

The increases in RRP size (filled squares) and P_r (open circles) are plotted for the different ages of the rats. Only experiments with a 20 Hz tetanus of 5 min are shown. The animals used were 4 ($n=2$), 6 ($n=2$), 7 ($n=13$), 8 ($n=7$), 9 ($n=7$), 10 ($n=3$) or 11 ($n=5$) days old.

The data in Fig. 3 apply to increases in the RRP induced by a 20 Hz tetanus of 6000 stimuli. PTP at this stimulation frequency is almost completely absent in slices from 10-day-old animals (Fig. 4A and B). Three different stimulation frequencies (20, 50 and 100 Hz) were applied to the afferent fibres of 9-10-day-old rats. Increasing the stimulus frequency resulted in more PTP for this age group. On average the P_r increased from 0.15 ± 0.02 before tetanization to 0.21 (20 Hz, $n=4$), 0.25 (50 Hz, $n=2$) and 0.35 (100 Hz, $n=9$) 1 min after the tetanus (Fig. 4C). The change in RRP size was significantly larger after a 100 Hz tetanus than after a 20 Hz tetanus (Fig. 4D, one-tailed t-test, $P < 0.01$). This indicates that in older animals an increase comparable to the values shown in Fig. 3 for younger ages can be achieved by stimulation at higher frequencies. The increase in P_r was the dominant mechanism of PTP at 1 min after the tetanus for all frequencies tested.

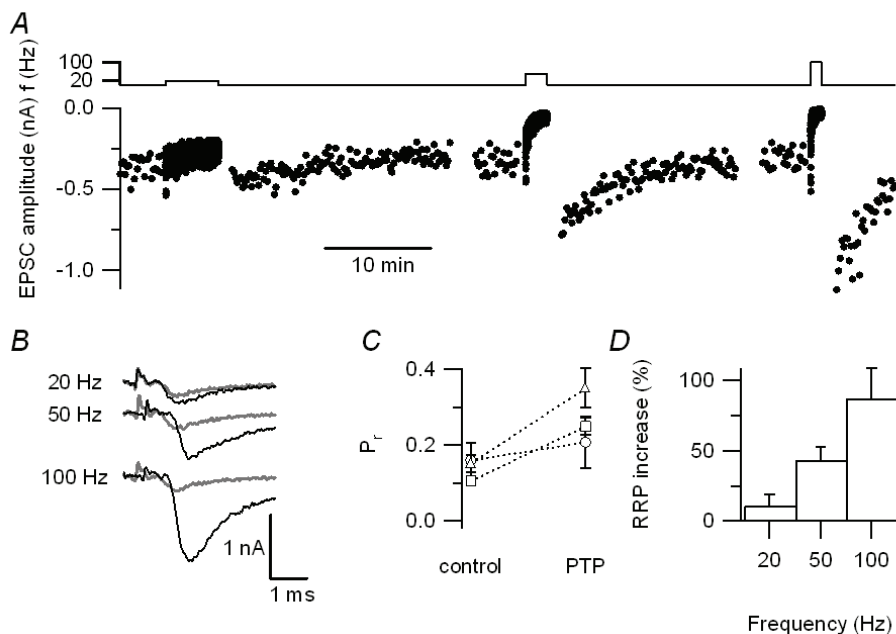


Figure 4: Frequency dependence of PTP

A, EPSC amplitudes measured in a principal cell from a P10 rat. The cell was tetanized with 6000 stimuli of three different frequencies, as indicated in the top graph by bars. From left to right: 20 Hz, 50 Hz and 100 Hz. *B*, example traces before (grey) and after (black) the 20 Hz (top), 50 Hz (middle) and 100 Hz (bottom) tetanus. *C*, mean release probabilities from P9 and P10 slices. PTP was induced with a 20 Hz (circles), 50 Hz (squares) or 100 Hz (triangles) tetanus. *D*, increase in the size of the RRP for the three different frequencies tested. Experiments were conducted in the presence of kynurenic acid.

PTP at physiological temperature

Experiments on PTP in mammals are often performed at room temperature, although synaptic transmission during and after trains of action potentials depends strongly on temperature (Klyachko & Stevens, 2006). We therefore set out to measure the effect of temperature on PTP at the calyx of Held. At the neuromuscular junction the decay of PTP is accelerated at higher temperature (Rosenthal, 1969; Zengel *et al.*, 1980) and we first wanted to see whether this was also true at the calyx of Held synapse. At physiological temperature (PT) the fast rise time and large size of the EPSCs in the principal cells of the MNTB can lead to voltage escape (Borst *et al.*, 1995). The competitive antagonist kynurenic acid, in addition to reducing postsynaptic receptor

saturation and desensitization, improved the voltage-clamp on the postsynaptic cell by reducing the rise time and amplitude of the EPSCs (Wong *et al.*, 2003). Kynurenic acid was less effective in reducing the EPSC amplitude at PT (37 °C) compared to room temperature (RT). EPSCs were reduced to 3.6 ± 0.3 % (n=7) in 2 mM kynurenic acid at RT (24 °C), while the EPSC amplitude was 7.1 ± 0.9 % (n=5) of control in 4 mM kynurenic acid at PT. A difference in inhibition of the EPSCs at PT versus RT has also been observed for γ -DGG (Kushmerick *et al.*, 2006), which is a glutamate antagonist with a somewhat lower affinity compared to kynurenic acid (Wong *et al.*, 2003).

At all frequencies tested (20, 50 and 100 Hz), PTP decayed somewhat faster at PT ($t_{1/2} = 2.7 \pm 0.3$ min; n=20) than at RT ($t_{1/2} = 3.6 \pm 0.4$ min; n=17), although the difference was not significant. Figure 5A shows the mean EPSC amplitudes obtained at RT when the terminals were stimulated with a 100 Hz tetanus (n=9). A clear biphasic decay is apparent and the data points after the tetanus could be fitted with a double exponential function with time constants of 0.3 ± 0.4 min and 8.1 ± 3.6 min. Figure 5B shows the mean EPSC amplitude at PT (n=5). The amount of PTP was not significantly smaller at 37 °C than at RT and the decay looked similar. To compare the decay phases, the relative amplitudes are plotted on semi-logarithmic axes in Fig. 5C. Example traces of individual EPSCs can be seen as insets in Fig. 5A and 5B for RT and PT, respectively. The EPSC kinetics were clearly faster at higher temperature, as has been reported previously at the calyx of Held synapse (Borst *et al.*, 1995; Kushmerick *et al.*, 2006; Postlethwaite *et al.*, 2007).

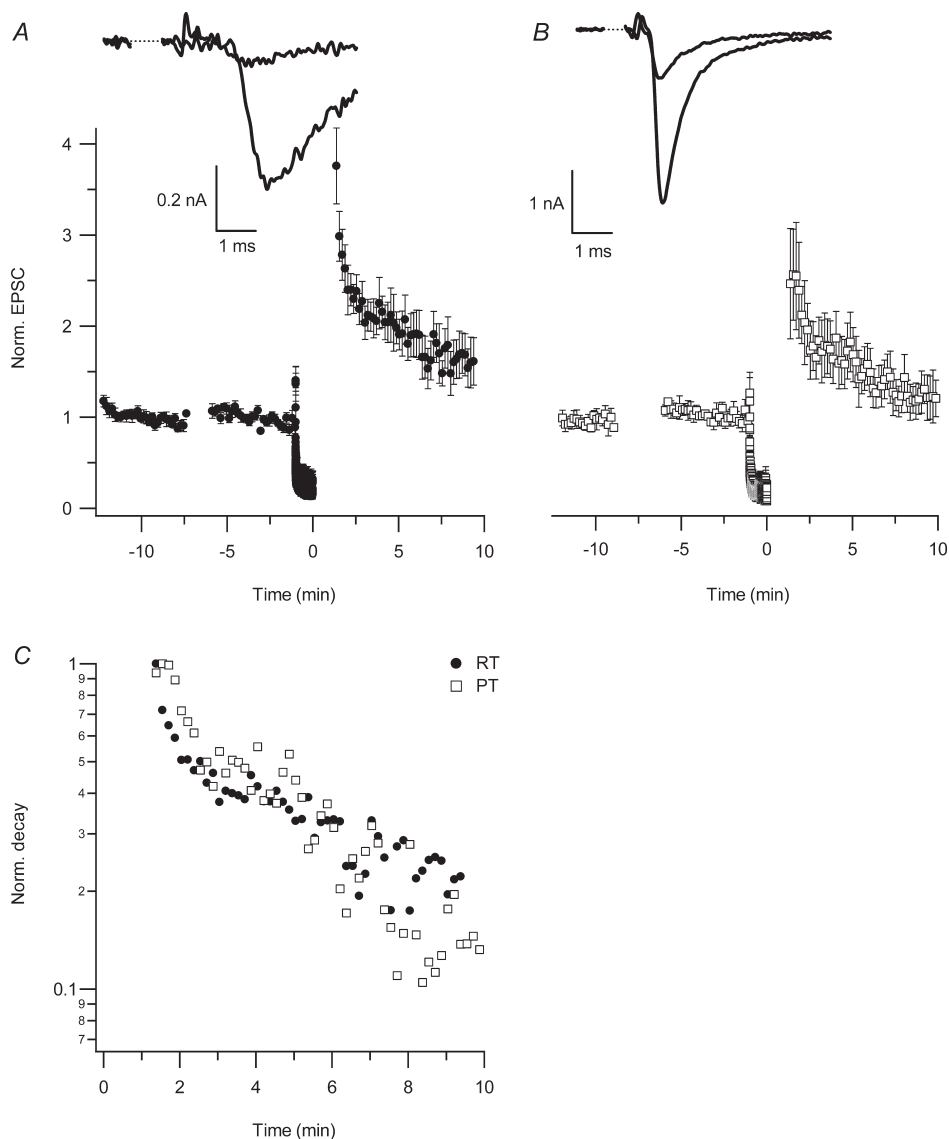


Figure 5: Temperature dependence of PTP

A, Normalized EPSC amplitudes at RT ($n=9$). Axons were stimulated at 0.1 Hz, in the presence of 2 mM kynurenic acid. At $t=-1$ minute, the cell was stimulated with a 100 Hz tetanus of 1 minute. Inset shows example currents before (black) and after (grey) the tetanus, with the stimulation artefacts blanked. B, Same as in A, only these experiments were done at PT in the presence of 4 mM kynurenic acid ($n=5$). C, To compare the decay of PTP at RT

(filled circles) to the decay at PT (open squares), the EPSC values from graphs A and B were normalized to the maximum and plotted on a semi-logarithmic scale.

Temperature has a profound effect on the filling of the RRP in the calyx of Held (Kushmerick *et al.*, 2006) and other synapses (Dinkelacker *et al.*, 2000; Pyott & Rosenmund, 2002). We therefore set out to explore the contribution of a change in pool size to PTP at PT. Before the application of kynurenic acid, the amplitude of spontaneous EPSCs was 43 ± 2 pA (n=7) at RT and 76 ± 5 pA (n=5) at PT (data not shown). These values are comparable to results by Kushmerick *et al.* (2006). Based on these findings we calculated the number of vesicles in the RRP by dividing the cumulative EPSC amplitude of a train by the spontaneous release amplitude. Our estimates for the number of releasable vesicles in the RRP at both temperatures were 781 ± 187 (RT, n=7) and 623 ± 45 (PT, n=5), which was not significantly different from each other and comparable to previous estimates based on this method (Schneppenburger *et al.*, 1999; Wu & Borst, 1999). We repeated the experiment shown in Fig. 2 at 37 °C (Fig. 6). Because the terminals follow high frequency stimulation more easily at PT, we increased the frequency of the test trains, which were given every 60 seconds, to 400 Hz. One experiment was excluded because it did not result in an increase of the EPSC amplitude after the tetanus. Figure 6C shows the mean cumulative EPSC amplitudes of three experiments. This figure shows that the mean RRP size 20 seconds after the tetanus (filled triangles) was not larger than the estimate from the last train before the tetanus (open circles). A clear increase in P_r is apparent when comparing the first response of a train after the tetanus with the first response of a train before the tetanus (Fig. 6A, B and C). Eighty seconds after the tetanus (open squares, Fig. 6C) P_r was back to baseline while the RRP was increased. On average, increasing the temperature from 24 to 37 °C made the increase in P_r more transient (Fig. 6E). The dynamics of the RRP were also somewhat faster at PT (Fig. 6D), but this might be attributed to a slow decrease in RRP size during the baseline at PT, in contrast to the slow increase we observed at RT (Fig. 2E).

In a previous study (Chapter 4) we found a contribution of an increase in calcium influx to the increase in P_r . We hypothesised that this increase in calcium influx could be due to facilitation of the calcium current or due to broadening of the action potential. Action potential broadening is often linked to inactivation of potassium channels (Geiger & Jonas, 2000). Recovery from inactivation of these channels (Rodríguez *et al.*, 1998) and thereby return of the action potential shape to control is much faster at higher temperatures. This could explain why the decay of P_r is much faster at 37 degrees Celsius. We therefore examined the prespike (Forsythe, 1994), which resembles an inverted first derivative of the action potential (Borst *et al.*, 1995). Despite

some rundown during the recording and the noisiness of this small signal, analysis of the prespikes at the time points shown in Fig. 6A and C indicates that the timecourse of the decrease in normalized prespike amplitude resembled the decay of P_r after the tetanus (Fig. 6B and F).

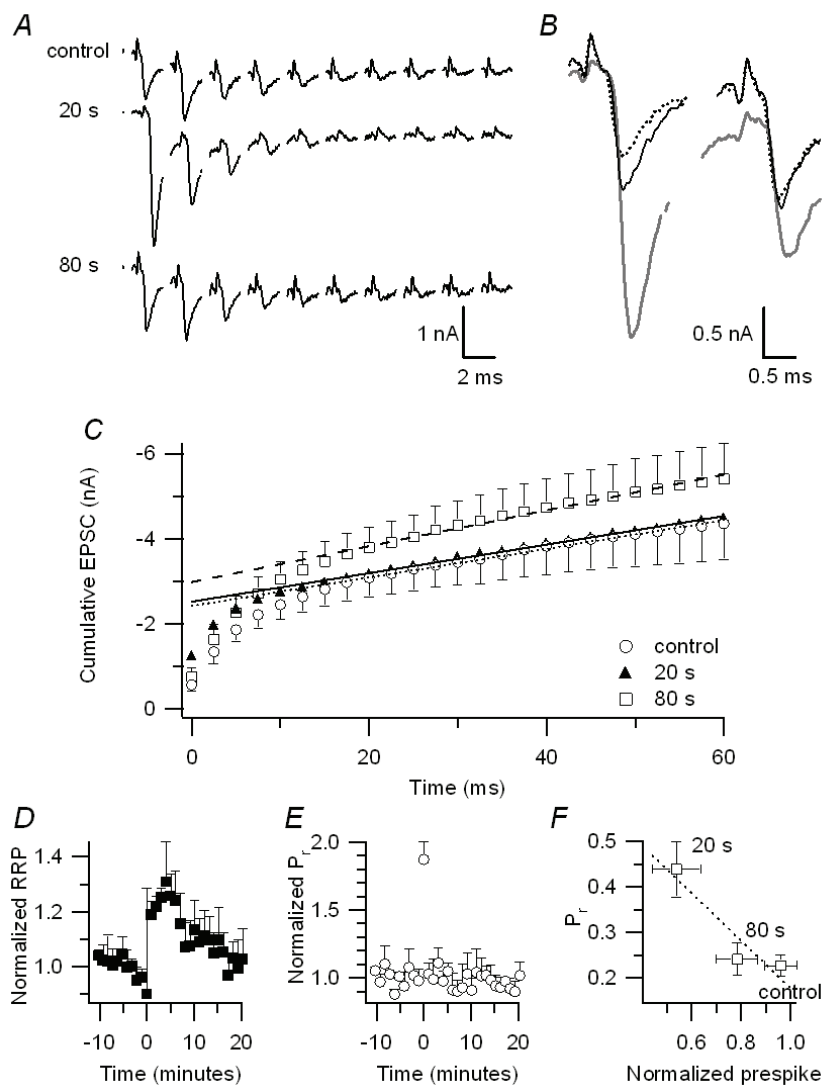


Figure 6: RRP dynamics at physiological temperature

The size of the RRP was continuously probed at 37 °C, with short 400 Hz trains in 4 mM kynurenic acid. Data of cells stimulated for 20 s to 1 min with a 100 Hz tetanus were pooled.

A, the first 10 EPSCs of a train of 25 are shown for the last train before the tetanus (top) and for trains 20 s (middle) and 80 s (bottom) after the tetanus. B, enlargement of the first two EPSCs of control (dotted trace), 20 s (grey) and 80 s (black continuous) trains shown in A. Traces were aligned on their prespikes C, cumulative EPSC plots show the mean values of three experiments at control (open circles), 20 s (filled triangles) and 80 s (open squares) after the tetanus. Error bars for the values 20 s after the tetanus are omitted for clarity. The cumulative release curves were fitted with lines (dotted line for control; solid line, 20 s after the tetanus; dashed line, 80 s after the tetanus). D, the mean normalized RRP estimates from the experiments shown in C are plotted versus time after the tetanus. The RRP was probed with 1 minute intervals. E, mean normalized P_r was calculated by dividing the first EPSC amplitude from a train by the RRP estimate. F, EPSCs are preceded by a small prespike which resembles the first derivative of the action potential (examples shown in B). The mean P_r of the first EPSC is plotted versus the mean amplitude of the prespike for the three time points shown in A ($n=3$). The prespike amplitudes were normalized to the mean pre-tetanus value.

In a previous study (Chapter 4) we found a contribution of an increase in calcium influx to the increase in Pr. We hypothesized that this increase in calcium influx could be due to facilitation of the calcium current or due to broadening of the action potential. Action potential broadening is often linked to inactivation of potassium channels (Geiger & Jonas, 2000). Recovery from inactivation of these channels (Rodríguez *et al.*, 1998) and thereby return of the action potential shape to control is much faster at higher temperatures. This could explain why the decay of Pr is much faster at 37°C. We therefore examined the prespike (Forsythe, 1994), which resembles an inverted first derivative of the action potential (Borst *et al.*, 1995). Despite some rundown during the recording and the noisiness of this small signal, analysis of the prespikes at the time points shown in Fig. 6A and C indicates that the time course of the decrease in normalized prespike amplitude resembled the decay of Pr after the tetanus (Fig. 6B and F).

To compare the contribution of the change in RRP at RT and at PT we plotted the increase in RRP versus the increase in EPSC amplitude 1 min after the tetanus (PTP). The fit through the data was steeper for the data obtained at PT for 20 Hz (Fig. 7) and 50 Hz tetanization (data not shown). The steepness of the fits indicate that 1 min after the tetanus, more than 50% of PTP can be explained by an increase in the RRP at PT, while this percentage is considerably smaller (<19%) at RT. The difference in contribution of the RRP between PT and RT was less clear for data obtained with a 100 Hz tetanus, probably because the dataset was smaller for this frequency. We conclude that the contribution of the RRP enlargement to PTP is more significant at PT compared to RT.

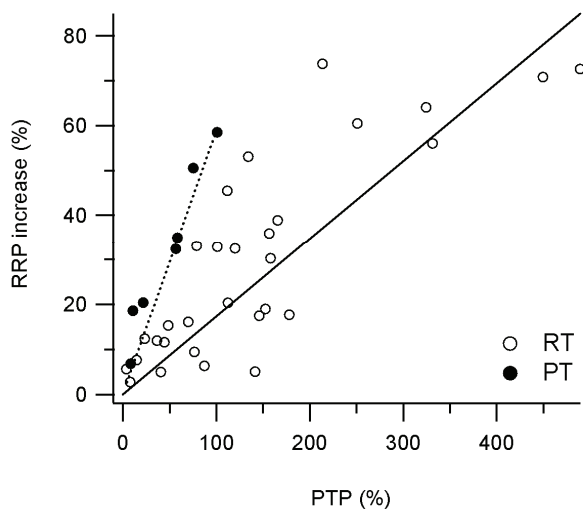


Figure 7: Contribution of the RRP increase to PTP

The RRP increase 1 min after the tetanus of all cells stimulated with a 20 Hz tetanus was plotted against the amount of PTP. Data at RT (open circles) were fitted with a line through zero and a slope of 0.17 (continuous line). A similar fit through the data at PT (closed circles, dotted line) resulted in a slope of 0.59. Experiments with depressed EPSCs are not shown, but were included in the fit.

DISCUSSION

We measured the pool of vesicles that is immediately ready for release in the calyx of Held and found that it is enlarged after as few as 500 stimuli at 100 Hz. Furthermore, we could measure the RRP during PTP and its return to pretetanus levels. We saw that the increase in the RRP was longer lasting than the increase in P_r and that this difference was even larger at PT. At PT, P_r was increased for less than 80 s, thereafter it was the RRP increase that resulted in larger EPSCs.

Physiological relevance

The calyx of Held is part of the auditory network responsible for detecting interaural intensity differences. In young-adult mice the mean spontaneous firing rate is about 40 Hz (Kopp-Scheinflug *et al.*, 2003a), which is in the same order as the stimulation frequencies used in this study. Although our experiments are conducted at ages before the onset of hearing, it is conceivable that there is spontaneous activity at similar rates as in adult animals. Our experiments show that a higher stimulation frequency is necessary to induce a similar amount of PTP in older animals. This would indicate that PTP induction is still possible in animals that are past the onset of hearing. The function of the calyx of Held synapse is considered to be that of a sign inverting relay (but see: Kopp-Scheinflug *et al.*, 2003b; Schneggenburger & Forsythe, 2006). For this function fast and reliable transmission is important. Increasing the size of the RRP can increase the output of the synapse, thereby alleviating depression due to vesicle depletion, although for high frequencies the steady-state output was not increased (Fig. 1B, 2B, and 6C) and it is not yet known whether PTP is induced by the high firing rates of the adult calyx of Held synapse.

PTP at physiological temperature

We observed a biphasic decay of PTP at RT and found that the decay of P_r was dominated by an augmentation phase. At PT only the augmentation phase of P_r was detectable. Therefore, the overall decay of PTP at PT was dominated by the decay of the RRP size, which was only slightly accelerated. A moderate sensitivity of PTP for temperature is consistent with previous studies, in which a Q_{10} of around 2 for the decay of PTP was found (Zengel *et al.*, 1980; Fisher *et al.*, 1997) in contrast to a Q_{10} of 4-5 for augmentation (Magleby & Zengel, 1976; Klyachko & Stevens, 2006). The decay of P_r correlated with the amplitude of the prespike in the experiments conducted at PT.

The prespike (Forsythe, 1994) is proportional to the inverted first derivative of the action potential (Borst *et al.*, 1995) and a reduction of the prespike amplitude indicates a broadening of the action potential. The reduction of the prespike after the tetanus was larger than in our previous study (Chapter 3). This is due to the fact that we started measuring sooner (20 s) after the tetanus in this study. Indeed at a comparable time after the tetanus (80 s) the prespike had already recovered to 78% (PT, Fig. 6) and 80% (RT, data not shown) of control. Broadening of the action potential contributes to the augmentation phase of PTP, because changes in the action potential shape have been shown to have a profound effect on neurotransmitter release (Borst & Sakmann, 1999b; Geiger & Jonas, 2000; Fedchyshyn & Wang, 2005). We showed that during PTP, calcium influx is increased and that this increase is sufficient to explain the increase in release probability (Chapter 4). Action potential broadening is one of the mechanisms that could underlie increased calcium influx during PTP. The contribution of a presynaptic post-tetanic hyperpolarization (Kim *et al.*, 2007) to changes in action potential waveforms and release probabilities remains to be investigated under conditions that preserve PTP.

Temperature accelerates vesicle mobilization to the RRP (Pyott & Rosenmund, 2002; Kushmerick *et al.*, 2006) and this accelerated replenishment in combination with calcium dependent vesicle recruitment transiently overfills the RRP in chromaffin cells (Dinkelacker *et al.*, 2000). Unlike chromaffin cells, the size of the RRP in the calyx of Held was not significantly different at both temperatures, in agreement with the results of Kushmerick *et al.* (2006). PTP at the calyx of Held is dependent on residual calcium, which is apparently not very sensitive to changes in temperature. Residual calcium at other synapses has a moderate temperature dependence (Regehr *et al.*, 1994; Dinkelacker *et al.*, 2000).

RRP increase

A change in the number of vesicles immediately ready for release has been proposed as a mechanism for short term plasticity in a number of other synapses (Byrne & Kandel, 1996; Rosenmund *et al.*, 2002; Kuromi & Kidokoro, 2003; Zhao & Klein, 2004). After repetitive stimulation, no change or partial depletion of the RRP has been observed in hippocampal cultures (Stevens & Wesseling, 1999) and frog neuromuscular junction (Kalkstein & Magleby, 2004), respectively. In contrast to a study by Korogod *et al.* (2005), we found a 30% increase of the number of vesicles in the RRP during PTP at the calyx of Held (Chapter 3). In the present study we show that this difference is not due to differences in the stimulation protocol since we found an even bigger

enlargement of the pool with a similar tetanus (100 Hz, 5 s) as used in their experiments. Our measurements in P₄ animals also exclude that the age of the rats caused the difference. We think that the time point at which the pool size was measured provides a more likely explanation. Korogod *et al.* (2005) measured 20 seconds after the tetanus. At this time point, we also did not observe an increase in the RRP, while another 60 seconds later the RRP was significantly overfilled.

The P_r of vesicles in the readily-releasable pool of the calyx of Held is heterogeneous (Wu & Borst, 1999; Sakaba & Neher, 2001a). Both differential calcium sensitivities of the vesicles and positional heterogeneity may contribute to this heterogeneity (Wölfel & Schneggenburger, 2003; Sakaba *et al.*, 2005; Wadel *et al.*, 2007). During a train of short stimuli the vesicles with high P_r are depleted by 80-100% (Wu & Borst, 1999; Sakaba, 2006). We found that mainly the first four responses of a stimulus train were enlarged during PTP (Fig. 2B). These first four EPSCs are predominantly composed of vesicles from the pool with high P_r (Sakaba & Neher, 2001c). We therefore think that the increase in RRP during PTP is an increase of the number of vesicles with high P_r. It seems likely that residual calcium, the long-lasting increase in the presynaptic Ca²⁺ concentration after a tetanus, is involved in this increase. PTP at the calyx of Held synapse depends on residual calcium (Chapter 3, Korogod *et al.*, 2005). Since the RRP increase decayed with a similar time course to the residual calcium after a tetanus, the most parsimonious explanation is that the residual calcium was responsible for the increased pool size during PTP. The age dependence of the increase in RRP size may then have its origin in the calcium extrusion, which is faster in older animals (Chuhma & Ohmori, 2001). This view is supported by the observation that PTP can be induced in older animals by stimulation at higher frequency. We assumed constant replenishment in all our measurements of the RRP, which is most likely not correct. If the two pools of vesicles identified at the calyx of Held represent different maturation steps in vesicle priming (Sakaba & Neher, 2003b) acceleration of the replenishment to the high P_r pool, due to residual calcium from the tetanus, could account for the observed increase in RRP size. A Ca²⁺/calmodulin dependent acceleration of replenishment of the high P_r pool has been shown in the calyx of Held (Sakaba & Neher, 2001a). Calmodulin is thought to regulate the RRP size during short-term plasticity via an interaction with Munc13 (Junge *et al.*, 2004), a protein involved in the modulation of transmitter release by phorbol esters in the calyx of Held (Hori *et al.*, 1999). Another possibility is that the cAMP-dependent guanosine exchange factor Epac is involved in the increase in the number of vesicles with high P_r (Sakaba & Neher, 2001b, 2003a; Kaneko & Takahashi, 2004). Many proteins that are involved in the docking or priming process could function as downstream effectors of Ca²⁺ and/or cAMP, including synapsins (Sun *et al.*, 2006), Munc18 (Toonen *et al.*, 2006), Rim (Calakos *et al.*, 2004), or Rab3 and other Ras-related GTPases (Owe-Larsson *et al.*, 2005; Schlüter *et al.*, 2006). These proteins

might aid in increasing the RRP size independently or in conjunction (Dulubova *et al.*, 2005) with each other.

Chapter 6

General Discussion

We investigated short term plasticity at the calyx of Held synapse and found that the responses in the postsynaptic neurons were potentiated after repetitive stimulation. This potentiation returned to control values in the order of minutes, characterizing this form of plasticity as post-tetanic potentiation. The decay of the potentiation often deviated from a single exponential function indicating that there are multiple underlying mechanisms with different decay times.

Pre- versus post-synaptic site of action

We showed that the amplitude of spontaneous release was unchanged after a tetanus. This indicates that the mechanisms involved in PTP are localized at the presynaptic terminal, rather than at the level of the postsynaptic receptors (Chapter 2)(Korogod *et al.*, 2005). This conclusion was reinforced by the finding that PTP was accompanied by an increase of the presynaptic calcium influx (Chapter 4). Most experiments were conducted with the postsynaptic cell voltage clamped to -80 mV. Under these conditions very little calcium flows into the postsynaptic cell, which would be a requisite for the involvement of a retrograde messenger in PTP (Bao *et al.*, 1997; Kushmerick *et al.*, 2004). In a few experiments, we held the postsynaptic cell in current clamp, or even stimulated it with depolarizing steps during the tetanus. No obvious increase or lengthening of PTP occurred (unpublished observations). The relative increase of the EPSC amplitude was very comparable between experiments conducted in the absence and presence of the competitive glutamate antagonist kynurenic acid, further arguing against a retrograde signal. Most types of transmitters that are found at the calyx of Held synapse, including noradrenalin, endocannabinoids, adenosine, 5-HT and GABA, inhibit release (Takahashi *et al.*, 1998; Leão & Von Gersdorff, 2002; Kimura *et al.*, 2003). PTP might arise from a use dependent disinhibition, although no such phenomenon has to date been described. The majority of the evidence thus points towards a presynaptic origin of PTP, as has also been observed at other synapses (Zucker & Regehr, 2002).

Residual calcium

The most obvious change accompanying PTP was a long lasting increase in the Ca²⁺ concentration. Such a long lasting increase in calcium concentration has been found with several forms of synaptic plasticity and is called residual calcium (Katz & Miledi, 1968; Zucker & Regehr, 2002). One to two minutes after the tetanus, the residual calcium had a concentration of around 210 nM (Chapter 3). With a baseline Ca²⁺

concentration of ~40 nM, this constitutes an increase of 170 nM. Comparable values have been found in the NMJ and in the hippocampal mossy fibre boutons (Delaney *et al.*, 1989; Zucker *et al.*, 1991; Regehr *et al.*, 1994; Zucker & Regehr, 2002). A calcium concentration of 210 nM is about half the concentration of what can be observed after a single action potential, which is cleared from the terminal within a second (Helmchen *et al.*, 1997; Kim *et al.*, 2005). The concentration of residual calcium, however, decayed back to baseline levels in minutes. It is therefore reasonable to assume that the residual calcium is either transported into the terminal after the tetanus, or stored in intracellular compartments, out of which it cannot be cleared as easily. One mechanism described to account for transport of calcium into the nerve terminal after the tetanus is sodium accumulation. Accumulation of sodium ions, which has as a consequence that the Na⁺/Ca²⁺ exchanger starts working in reverse mode, i.e. pumping Ca²⁺ in and Na⁺ out, has been observed at the NMJ after repetitive stimulation (Van der Kloot & Molgó, 1994). This would mean that extracellular Ca²⁺ would not be needed during the tetanus, but only after the tetanus. We did precisely that experiment; we rapidly changed from low to high extracellular Ca²⁺ during the tetanus and found that extracellular Ca²⁺ was necessary during the tetanus for both residual calcium and PTP (data not shown). Furthermore, accumulation of Na⁺ is less likely in the calyx of Held, because the sodium channels are not located in the terminal itself, but in the axonal heminodes (Leão *et al.*, 2005). We therefore think it is more likely that calcium is taken up by an intracellular compartment. The contribution of the endoplasmic reticulum to Ca²⁺ sequestration is very limited in the calyx of Held (Billups & Forsythe, 2002; Chuhma & Ohmori, 2002; Kim *et al.*, 2005). Other possible compartments involved in calcium sequestration could be the synaptic vesicles (Oheim *et al.*, 2006), the axon, or the mitochondria. The contribution of synaptic vesicles to Ca²⁺ clearance in the *Drosophila* NMJ is limited (Macleod *et al.*, 2004). It has never been tested whether the axon could function as a Ca²⁺ sink during tetanic stimulation, for the obvious reason that in most experiments it is the axon that is stimulated and a loss of function experiment would therefore be difficult. Mitochondria are the most likely candidates as compartments for calcium storage during tetanic stimulation (Tang & Zucker, 1997; Yang *et al.*, 2003; Verstreken *et al.*, 2005), and they are involved in clearance of Ca²⁺ at the calyx of Held (Billups & Forsythe, 2002; Kim *et al.*, 2005). Lee *et al.* (Lee *et al.*, 2008) recently found that blocking mitochondrial Ca²⁺ efflux by tetraphenylphosphonium (TPP⁺) completely blocked residual calcium after tetanic stimulation, while it blocked most but not all PTP. We therefore think that calcium is taken up by mitochondria during stimulation and slowly dissipates into the cytoplasm afterwards, resulting in the prolonged increase in the cytosolic calcium, which we call residual calcium.

Residual calcium decayed with a similar time constant as the EPSCs after the tetanus, which indicates that PTP and the minute-long increase in the Ca^{2+} concentration are related. To prove that residual calcium is indeed responsible for PTP, we tried to buffer the Ca^{2+} concentration during the tetanus with 1 mM EGTA (Swandulla *et al.*, 1991). This EGTA concentration was chosen because it has only little effect on evoked release (Chapter 3)(Borst & Sakmann, 1996). We found that the buffering capacity of 1 mM EGTA was not sufficient to buffer the calcium load during the tetanus, but it did reduce the residual calcium concentration after the tetanus (Chapter 3). In addition, the decay of residual calcium was accelerated in the presence of EGTA. This is unexpected, since increasing the calcium binding ratio of the terminal slows down the calcium decay of single action potentials (Chapter 4)(Helmchen *et al.*, 1997). Interestingly, the decay of residual calcium after the tetanus in our experiments with 200 μM fluo-4 (chapter 4) was also faster compared to our experiments with 50 μM fura (Fig. 6, chapter 3), while the calcium transient of a single action potential was slowed, as predicted by our single compartment model. A single compartment model apparently does not describe the dynamics of residual calcium very well. During a single action potential, calcium clearance is predominantly achieved by plasma membrane pumps and transporters, while during repetitive stimulation other compartments, such as mitochondria (discussed above), are also involved (Kim *et al.*, 2005). The faster decay of the residual calcium in the presence of EGTA was accompanied by a shortening of PTP, further strengthening the hypothesis that residual calcium is causing PTP at the calyx of Held synapse. Korogod *et al.* (Korogod *et al.*, 2005) found that application of a membrane permeable EGTA analogue also completely blocked PTP, but at a concentration that blocked most evoked release as well.

Direct effect of residual calcium on the calcium sensor for release

Residual calcium was postulated to exert its effect by summing with calcium influx during evoked release (Katz & Miledi, 1968; Felmy *et al.*, 2003). Because the calcium sensitivity for release is in the μM range (Augustine *et al.*, 1991; Llinas *et al.*, 1992; Heidelberger *et al.*, 1994; Bollmann *et al.*, 2000; Schneggenburger & Neher, 2000; Augustine, 2001) and the concentration of residual calcium is only a fraction of that, the contribution of summation of residual and microdomain Ca^{2+} to PTP is only minor (Chapter 3)(Zucker & Regehr, 2002). The increase in the frequency of spontaneous release on the other hand can be explained solely by the action of residual calcium on the calcium sensor. As discussed in chapter 3, the frequency of spontaneous release is on the order of what would be expected in the presence of a Ca^{2+} concentration of 200 nM. The increase in calcium current during PTP (Chapter 4) should not affect

spontaneous release, for the obvious reason that in the absence of an action potential the voltage gated calcium channels should not open (Awatramani *et al.*, 2005). Our conclusion that the frequency of spontaneous release is mainly enhanced due to a direct activation of the calcium sensor was supported by the observation that spontaneous release decayed faster to baseline levels after the tetanus than evoked release, as also found by Korogod *et al.* (2005; 2007). They observed that the PKC inhibitor Ro31-8220 blocked PTP of evoked responses, but did not affect PTP of spontaneous release, further strengthening our conclusion that residual calcium is solely responsible for augmenting spontaneous release during PTP. It would be interesting to see what would happen to PTP of spontaneous release when accumulation of residual calcium is prevented by blocking mitochondria with TPP⁺. An accelerated decay of spontaneous release is expected from the supra-linear relation between release and calcium (Theory section chapter 3). In this respect our data are in disagreement with a study by Lou *et al.* (Lou *et al.*, 2005), who postulate a sublinear dependence of release to calcium concentrations below 200 nM. An increase in the size of the RRP (chapter 4) will increase the spontaneous release of vesicles, but since this increase will only be around 30-50%, it is negligible to the 10- to 30-fold increase in spontaneous release that can be observed during the peak of PTP. Direct summation of residual calcium and microdomain calcium has been shown to be responsible for 30% of facilitation at the calyx of Held (Felmy *et al.*, 2003). The concentration of residual calcium during PTP is considerably lower and we therefore estimated that it can only be responsible for 9% of the observed PTP. It can, however, account for the increase in spontaneous release during PTP.

An increase in the calcium influx

Voltage-gated calcium channels are the main source of calcium influx during an action potential at the calyx of Held. There are two ways to increase calcium influx through these channels during short term plasticity; 1) changing the number of channels that open during the action potential, which happens when calcium channels facilitate (Borst & Sakmann, 1998b; Cuttle *et al.*, 1998) or 2) prolonging the time the channels are open, which can be accomplished by changing the shape of the action potential.

Changes in action potential shape

A change in the action potential was already observed in pioneering studies on PTP (Liley & North, 1953; Hughes, 1958; Lloyd, 1959). Since then, a decrease in the

amplitude and/or an increase in the width of the action potential during a high frequency train have been reported in the sensory neurones of *Aplysia* (Byrne & Kandel, 1996), crayfish neuromuscular junction (Wojtowicz & Atwood, 1985) and hippocampal granule cells (Geiger & Jonas, 2000). Changes in action potential often persist long after the stimulus train has ended and have profound influence on neurotransmitter release (Hochner *et al.*, 1986; Augustine, 1990). In contrast, at the ciliary ganglion of the chick, no changes in the shape of the action potential were found during post-tetanic potentiation (Martin & Pilar, 1964).

The EPSC at the calyx of Held synapse has a tenth order dependence on the amplitude of the action potential (Wu *et al.*, 2004). Part of this high order relationship stems from an approximately third power relationship between the action potential amplitude and the calcium influx (Wu *et al.*, 2004). Calcium influx in its turn is related to release of vesicles by a third to fourth order dependence (Borst & Sakmann, 1999b; Xu & Wu, 2005; Yang & Wang, 2006), depending on the calcium channel type that mediates the current (Wu *et al.*, 1999) and on the age of the rats (Fedchyshyn & Wang, 2005). These power law relationships between release and the calcium influx only hold true for very brief stimuli, since longer stimuli have been shown to deplete the RRP of vesicles (Wu & Borst, 1999). The shape of the calcium influx affects neurotransmitter release greatly because it directly shapes the local Ca^{2+} transient as seen by the vesicles in the readily releasable pool (Meinrenken *et al.*, 2003). In experiments where calcium was directly elevated by flash photolysis of caged calcium (DM-nitrophen), the EPSC amplitude had an exponential dependence on the peak of the calcium transient, while the half-width was linearly related to release (Bollmann & Sakmann, 2005).

We attempted to directly measure changes in action potential shape in whole cell voltage clamp, but unfortunately PTP was absent when the calyx of Held was dialyzed by the patch pipette solution during the tetanus. Korogod *et al.* (Korogod *et al.*, 2005, 2007) observed a similar inability to induce PTP in the calyx of Held when the terminal was recorded in the whole cell configuration, but interestingly, PTP returned when they retracted the pipette and challenged the terminal with a second tetanus. We chose to infer changes in the action potential shape from cell attached recordings of the terminal and from changes in the prespike (Forsythe, 1994), which resembles a scaled inverted action potential (Borst *et al.*, 1995). The latter turned out to be the more reliable estimate because it is less dependent on the access resistance of the recording. Also, it is easier to measure, because a presynaptic recording is not necessary. We found a clear reduction of the prespike after a tetanus (Chapter 3), which correlated with the fast decay of the release probability (Chapter 5). Since we also observed an increase in the calcium influx (Chapter 4), it is conceivable that the increase in release probability is

due to a broadened action potential. The rise phase of the action potential determines the number of calcium channels that activate during the action potential (Yang & Wang, 2006). Reducing the amplitude of the action potential therefore leads to less open calcium channels and less calcium influx. A smaller prespike however indicates that the rise and fall of the action potential are also slower. A slower rise of the action potential increases the number of activated calcium channels, while a slower decay keeps them open longer. Broadening of the action potential therefore leads to more calcium influx (Fedchyshyn & Wang, 2005; Yang & Wang, 2006). The net effect of a broader but smaller action potential is hard to predict but has been investigated experimentally (Borst & Sakmann, 1999b). A decrease in amplitude and a lengthening of the half-width of the action potential have been observed at the calyx of Held during a train of action potentials at 100 Hz (Borst *et al.*, 1995). The last action potential in a train of 50, henceforth called broad action potential, had an amplitude that was approximately 20% smaller compared to the first, while the half-width was increased by about 40% (Borst & Sakmann, 1999b; von Gersdorff & Borst, 2002). In experiments where the broad action potential was used as the waveform to voltage clamp the calyx of Held, the amplitude of the calcium current was smaller, but its duration was longer compared to a control action potential. The resulting calcium influx, calculated by integrating the calcium current, was increased by 8%. This increase in calcium influx resulted in 20% more transmitter release (Borst & Sakmann, 1999b). We observed an increase in the calcium influx of 15 % after a tetanus (chapter 4), which is almost twice as large as the increase in calcium influx due to a broad action potential. The mismatch is probably larger for two reasons. 1) The calcium influx after a tetanus is a lower estimate because partial saturation of the high affinity indicator by residual calcium results in a sub linear relation between calcium influx and fluorescent transient. 2) The calcium influx in chapter 4 was measured more than a minute after the tetanus. At this time the prespike had already recovered to approximately 75% of its original value, compared to a 50% reduction of the prespike resulting from the broad action potential (Borst, unpublished observations). In addition the increased calcium influx decayed in conjunction with PTP in most experiments, while the change in the prespike decayed much faster (Chapter 5), as also found in experiments where run down was prevented using perforated patch (Korogod *et al.*, 2007). This suggests that the increase in calcium influx during PTP can only be partially explained by a broadening of the action potential.

Calcium current facilitation

An additional increase in the calcium influx due to an action potential can be achieved when the calcium channels open more easily upon depolarization. Such facilitation of the calcium channels has been shown at the calyx of Held (Borst & Sakmann, 1998b; Cuttle *et al.*, 1998; Tsujimoto *et al.*, 2002; Inchauspe *et al.*, 2004; Ishikawa *et al.*, 2005). The amount of facilitation of the calcium currents is calcium dependent, since it is attenuated when residual calcium is strongly buffered. It has recently been shown that facilitation of calcium currents could account for all types of short term plasticity in cultured hippocampal neurons. Calmodulin, calcium binding protein 1, neuronal calcium sensor-1 and visinin-like protein-2 are all possible modulators of calcium channels (Cheng & Augustine, 2008) and calcium-dependent facilitation of the calcium channels was shown to be regulated by NCS-1 at the calyx of Held (Tsujimoto *et al.*, 2002). This protein has also been shown to be involved in short term plasticity in hippocampal cell cultures (Sippy *et al.*, 2003) and leads to impairments in memory formation in *C. elegans* (Gomez *et al.*, 2001). In our calibration experiments in chapter 4, the calyces of Held were voltage clamped with a train of identical action potential waveforms at 100 Hz. During such trains the amplitude of the calcium current increased. The initial amplitude and the degree of facilitation were different for the two dyes used. When the low affinity dye Oregon Green Bapta-5N was infused in the nerve terminals the calcium currents were large to begin with but facilitated little, while the reverse occurred with the high affinity dye Fluo-4. The 20 % increase in calcium influx due to facilitation of the calcium currents during the train of identical APWs could easily explain the increase in both the calcium influx and EPSC during PTP. In experiments where the calcium current was measured during and after tetanization the calcium current was inactivated (Forsythe *et al.*, 1998). These experiments were conducted while recording from the terminal in the whole cell configuration. As indicated before, PTP is absent under these conditions. Interestingly, when washout of presynaptic cytosol was prevented by using perforated patch, voltage clamped terminals showed no PTP and no change in the amplitude or kinetics of the calcium current (Korogod *et al.*, 2007). Since the same study showed that PTP could be induced in perforated patch when terminals were held in current clamp, this indicates that either voltage changes in the action potential underlie PTP (as discussed above) or that the procedure of voltage clamping itself prevents PTP. Notably, it is unclear at the moment whether PTP occurs when the axon is severed from the calyx, as is required for adequate voltage clamp (Borst & Sakmann, 1998a). It is possible that a long axon is needed to store calcium during the tetanus, as discussed above. Alternatively, the voltage command protocol used by Korogod *et al.* (Korogod *et al.*, 2007)(1 ms

depolarization to +30 mV) occluded facilitation of the calcium current, because this paradigm already activates most of the channels.

We tried to distinguish between changes in action potential shape and calcium current facilitation by looking at the rise phase of the calcium transient (Chapter 4). Action potential broadening, as discussed above, results in a smaller but broader calcium current, while facilitation of the calcium channels will enlarge the calcium current. The rise phase of the calcium transient, measured with a low affinity indicator, reflects the calcium current. Unfortunately PTP was absent in most experiments when the terminal was perfused with low-affinity dyes (Chapter 4). In experiments with the high affinity dye fluo-4, the rise phase did not reflect the calcium current (Habets, unpublished observations), probably because the calcium indicator was out-competed by the low affinity calcium buffers in the terminal. Figure 3 in Chapter 4 shows an example of how calcium is transferred from the low affinity dye OGB-5N to the high affinity fura-2. From the whole cell experiments it can be concluded that one should be cautious when interpreting data on PTP obtained from experiments where the terminals are dialyzed. Future research designed towards understanding the mechanisms of Ca^{2+} influx during short term plasticity could include measurement of PTP in α1A knock-out mice, which lack calcium current facilitation and in mice lacking the gene for neuronal calcium sensor-1, which has been shown to be responsible for facilitation of the calcium currents (Tsujiimoto *et al.*, 2002).

Calcium buffer saturation

Calcium buffer saturation has been postulated to be responsible for facilitation (Blatow *et al.*, 2003; Felmy *et al.*, 2003). In the experiments in chapter 4 we showed that the increase in the Ca^{2+} transient as reported by our high affinity dye, could not be due to buffer saturation. This means that an increase in the calcium influx is contributing to PTP. It does not necessarily exclude a role for buffer saturation. In Figure 3C of the same chapter, the effect of saturation of 50 μM high affinity buffer fura-2 was already measurable after a single action potential. It is not unlikely that, at 200 μM , the high-affinity dye that was used in the experiments in Figure 2 (Chapter 4), acts itself as a saturable buffer. This would explain why PTP was absent in terminals that were dialyzed with low affinity dyes, which are less easily saturated by residual calcium. In whole cell measurements or measurements during which the terminals were loaded with dyes, the soluble endogenous buffers are probably washed out of the terminal. Under these conditions we found some evidence that there is a small amount of endogenous buffer, with a K_d somewhere between 350 nM and 32 μM . It was shown

that BABTA, but not EGTA was able to rescue facilitation, when endogenous buffers are washed away (Rozov *et al.*, 2001). This is probably due to the speed at which Calcium binds to these buffers (slow for EGTA, fast for BABTA). Our experiments in which the terminals were loaded with 1 mM EGTA (Chapter 3, Fig. 6) therefore argue against a considerable involvement of buffer saturation. EGTA is too slow as a buffer to be saturated at this concentration (Rozov *et al.*, 2001), but effectively reduces residual calcium in the terminal (Chapter 3, Fig. 6B). This concentration of EGTA would thus reduce buffer saturation of endogenous buffers, without acting as a saturable buffer itself. In four out of six experiments there was normal PTP, indicating that buffer saturation does not play an important role in PTP. Buffer saturation is particularly important in terminals that have relatively high levels of fast high-affinity buffer, like calbindin or calretinin (Rozov *et al.*, 2001; Blatow *et al.*, 2003; Matveev *et al.*, 2004; Burnashev & Rozov, 2005). The calyx of Held has a low calcium buffering capacity at the ages used in our experiments (Helmchen *et al.*, 1997) and in the absence of parvalbumin, the predominant calcium binding protein at that age, the amount of facilitation is not changed (Muller *et al.*, 2007). At later developmental stages, the amount of calcium binding protein, especially calretinin, increases (Lohmann & Friauf, 1996; Felmy & Schneggenburger, 2004). We therefore conclude that the role of buffer saturation for PTP is limited and that the absence of PTP in terminals dialyzed with low affinity dye is not related to its buffering capacity after the tetanus. The observed lack of PTP in these experiments could result from a different Ca^{2+} concentration during the tetanus and its effect on Ca^{2+} influx.

Increase in the RRP

With the proposed function as a sign-inverting relay in mind it is hard to understand why the calyx of Held would increase its P_r during a tetanus. Assuming that this synapse has evolved to faithfully transmit the action potentials from the calyx to the MNTB principal cell during high frequency trains, increasing P_r will intensify depression rather than alleviate it (Billups *et al.*, 2005). Increasing the number of readily releasable vesicles would on the other hand be a far better mechanism to sustain synaptic transmission at high frequencies. We found a ~30-50 % increase in the cumulative release during a short high frequency train, indicating that the RRP is accordingly bigger. The experiments in chapter 5 were conducted to validate this assumption. Alternative explanations for the increase in the cumulative EPSC amplitude during short high frequency trains could be that depletion of the RRP was not complete before the tetanus. An increase in P_r could then look like an apparent increase in RRP size. To refute this last hypothesis, we searched for conditions in

which the RRP was increased without an increase in P_r . The opposite was found directly (20 s) after the tetanus. At that time P_r is much larger, while the RRP is still depressed from the tetanus. At room temperature, most stimulation protocols resulted in simultaneous increase in P_r and RRP after the tetanus. Only when we switched from room temperature to physiological temperature, did we find that the RRP could be significantly increased without a change in P_r (Chapter 5). Recently, a study by Lee *et al.* (2008) found that by using pharmacology, it is possible to separate changes in the RRP and changes in P_r during PTP at the calyx of Held synapse.

Only in a minority of reports a change in the RRP has been seen during short term plasticity (Byrne & Kandel, 1996; Rosenmund *et al.*, 2002; Kuromi & Kidokoro, 2003; Zhao & Klein, 2004). During augmentation, the RRP in hippocampal cultures, as probed by hypertonic sucrose application, was found to be unaffected (Stevens & Wesseling, 1999), while the RRP of the frog NMJ was depressed (Kalkstein & Magleby, 2004). Measuring the RRP is not straightforward, as is evident from the wide range of estimates for the size of the RRP in the calyx of Held (Schneggenburger *et al.*, 1999; Wu & Borst, 1999; Sakaba & Neher, 2001a; Scheuss & Neher, 2001; Sun & Wu, 2001). Most of the variability stems from the method to compare the quantal size with the EPSC size. When the quantal content is estimated by simply dividing the EPSC amplitude by the quantal size (Chapter 5)(Schneggenburger *et al.*, 1999; Wu & Borst, 1999), a lower estimate is obtained than by deconvolution of the EPSC (Sakaba & Neher, 2001a), capacitance measurements (Sun & Wu, 2001) or looking at the variance of the EPSCs (Scheuss & Neher, 2001). To circumvent errors due to incorrect calculation of the quantal content, in most cases we expressed the RRP as the cumulative EPSC amplitude (nA). This cumulative EPSC amplitude was clearly enlarged after the tetanus. A study by Korogod *et al.* (Korogod *et al.*, 2005) did not find such an increase during PTP in the same preparation. We think this discrepancy stems from a difference in the moment at which the pool size is probed, as discussed in chapter 5. Our measurements of the RRP relied on depletion of synaptic vesicles from the RRP. It has been shown that the P_r of vesicles in the readily-releasable pool of the calyx of Held is heterogeneous (Wu & Borst, 1999; Sakaba & Neher, 2001a). Some vesicles have high P_r and are depleted during a high frequency train of action potentials and some vesicles have low P_r and might be resistant for depletion (see discussion chapter 5). It is a matter of semantics whether or not these vesicles, which apparently can not be released by action potentials, can be called readily releasable, or whether they constitute precursors of readily releasable vesicles (Sakaba & Neher, 2003b). In the end our experiments show that for physiological stimuli the number of vesicles the terminal can draw upon is increased during PTP. PTP at the calyx of Held synapse depends on residual calcium (Chapter 3)(Korogod *et al.*, 2005). It is very likely that the residual

calcium is involved in enlarging the RRP (Wang & Kaczmarek, 1998) by speeding up recovery, although elevating the calcium concentration is not sufficient to increase the RRP (Felmy *et al.*, 2003; Awatramani *et al.*, 2005) and it was recently shown that the RRP was increased during PTP in the absence of residual calcium (Lee *et al.*, 2008). It has been shown that replenishment to the RRP can be increased by a Ca^{2+} /calmodulin dependent mechanism (Sakaba & Neher, 2001a; Hosoi *et al.*, 2007). Calmidazolium, an antagonist of calmodulin, indeed blocks the increase in RRP size during PTP at the calyx of Held (Lee *et al.*, 2008). Calmodulin regulates the RRP size during short term plasticity by interacting with Munc-13 (Junge *et al.*, 2004). Munc-13 has been shown to be involved in phorbol ester-mediated enhancement of vesicle release in the calyx of Held (Hori *et al.*, 1999; Lou *et al.*, 2008). Other proteins involved in the modulation of vesicle release like cAMP-dependent guanosine exchange factor (Epac) (Sakaba & Neher, 2001b; Kaneko & Takahashi, 2004), synapsins (Sun *et al.*, 2006), Munc-18 (Wierda *et al.*, 2007), Rim (Calakos *et al.*, 2004), or Rab3a (Schlüter *et al.*, 2006) may also be involved.

The mechanisms that produce PTP at the calyx of Held are still heavily debated. We and others (Lee *et al.*, 2008) consistently found that the RRP was increased during PTP, while Korogod and co-workers do not (Korogod *et al.*, 2005, 2007). In addition, the latter find a very similar increase in calcium influx and reason that this is only sufficient to explain an increase in EPSC amplitude of 50%. Unfortunately they do not report how much PTP was observed in the experiments that were used to estimate calcium influx. It is crucial to compare PTP at the same experiment because we showed that infusion of calcium dyes can affect the amplitude of PTP (Chapter 4). If the EPSCs shown in their Figure 2 are representative, their increase in EPSC amplitude would be exactly what they predict from their 15% increase in calcium current. Furthermore, both the paper by Korogod *et al.* (2007) and a recent publication by Lee *et al.* (2008) claim to have discovered the molecular substrate for PTP at the calyx of Held. Korogod *et al.* (2007) claim that PTP is a consequence of activation of protein kinase C. They find that PTP is occluded by phorbol esters, activators of PKC and Munc-13. In addition, antagonists of PKC, bisindolylmaleimide I (BIS-I) and R031-8220, block PTP of evoked release. In contrast, Lee *et al.* (2008) show that not only BIS-I and R031-8220 block PTP, but that bisindolylmaleimide V, an inactive analogue, also reduced PTP significantly at a concentration five times lower than used by Korogod *et al.* (2007). Chelerythrine, a PKC inhibitor that acts on the catalytic domain instead of the ATP-binding domain, had no effect on PTP in the publication of Lee *et al.* (2008), similar to Gö-6976 and calphostin (Korogod, 2006). Lee *et al.* (2008) further show in an elegant set of experiments that the increase in P_r and the RRP during PTP can be pharmacologically separated. Blockers of mitochondrial calcium influx (RU360) and

efflux (TPP⁺) reduce both residual calcium and the rapidly decaying component of PTP, which corresponded with the increase in P_r. The increase in the size of the RRP was unaffected by these drugs, indicating that PTP of the RRP is independent of residual calcium. The increase in the size of the RRP was abolished by inhibitors of the myosin light chain kinase pathway (ML-7, MLCKip, Blebbistatin, calmidazolium)(Lee *et al.*, 2008). In conclusion, I think that the RRP is increased during PTP, by a mechanism involving calmodulin and myosin light chain kinase, while the release probability is increased due to an increase in the presynaptic calcium influx.

Physiological significance of PTP

The calyx of Held is part of the auditory network responsible for detecting interaural intensity differences. In young-adult mice the mean spontaneous firing rate is about 40 Hz (Kopp-Scheinflug *et al.*, 2003a), which is in the same order of magnitude as the stimulation frequencies used in this study. Although our experiments are conducted at ages before the onset of hearing, it is conceivable that there is spontaneous activity at similar rates as in adult animals. The calyx of Held synapse is considered to be a sign-inverting relay (Schneppenburger & Forsythe, 2006) but see: (Kopp-Scheinflug *et al.*, 2003b; Joris *et al.*, 2008). For this function fast and reliable transmission is important. Increasing the size of the RRP can increase the output of the synapse and can alleviate depression due to vesicle depletion. It has been shown that the number of vesicles in the RRP can increase by manipulation with different pharmacological agents, but to date there was no detailed account on the size of the RRP during physiological stimulation. We looked at PTP during development because the ability of the principal cells to follow the presynaptic spikes depends on age (Taschenberger & von Gersdorff, 2000) and the size of the RRP increases with age (Taschenberger *et al.*, 2002). It could be that the increase in RRP after a tetanus is a way of coping with a demand for vesicles in younger animals. The experiments in chapter 2 show that before the formation of the calyx, the axon fibres have many collaterals. Figure 2 of that chapter also shows that activity in these collaterals can be sufficient to elicit postsynaptic action potential firing, meaning that activity could be a factor in determining on which cell the terminal forms. We therefore hypothesised that PTP might be involved in calyx formation. Unfortunately we could not reliably induce PTP in these axon collaterals (unpublished observations), which makes this hypothesis less likely. We have shown that PTP is dependent on residual calcium and it is reasonable to assume that the magnitude of residual calcium is dependent on the ability of the terminals to pump out calcium during the tetanus. Calcium extrusion from the calyces of Held is faster in older animals (Chuhma & Ohmori, 2001) and we therefore hypothesise that the age

dependence of PTP is a result from the increased ability to handle the calcium load during tetanic stimulation. This view is supported by the observation that PTP can be induced in older animals by stimulation at higher frequency. If this holds true for animals at ages past the onset of hearing, PTP could also have relevance for sound localization.

The extracellular calcium concentration used in our experiments (2 mM) is slightly higher than has been reported *in vivo* (Jones & Keep, 1988). It is unclear whether this has an effect on PTP since we did not test alternative calcium levels, but similar amplitudes of PTP have been reported at 1 mM extracellular calcium (Korogod *et al.*, 2007). Probably the optimal frequency for inducing PTP is higher at lower calcium levels, because less calcium flows in per action potential.

To take a further look into the physiological relevance of PTP, we conducted experiments at physiological temperature (PT) and compared them to experiments at room temperature (RT). The quantal content is similar at RT and PT because both EPSCs and miniature EPSC amplitudes are larger at PT compared to RT (Kushmerick *et al.*, 2006). At PT, the action potential in the calyx of Held terminal is much faster than at RT (Kushmerick *et al.*, 2006). At the same time, the calcium current is much larger, probably due to increased activation of the calcium channels (Borst & Sakmann, 1998a). The net effect is a slight reduction in the calcium current integral. The size of the RRP and the P_r are also very comparable at RT and PT. It was therefore not very surprising that PTP at PT and RT were remarkably similar. At other synapses there is a temperature dependence (Q_{10}) of 1 to 2 for PTP (Rosenthal, 1969; Magleby, 1973; Regehr *et al.*, 1994). A much larger temperature dependence has been reported for augmentation (Magleby & Zengel, 1976; Klyachko & Stevens, 2006). We also found that the major effect of temperature was on the fastest component of our potentiation, the decay of P_r .

Future experiments

Since it is now clear that PTP at the calyx of Held is governed by both an increase in P_r and an increase in the size of the RRP and that both mechanisms are regulated by separate molecular pathways, the relative contribution to calyx development and sound localization could be assessed in animals that lack genes involved in these pathways. The increase in RRP size was shown to be dependent on myosin light chain kinase (Lee *et al.*, 2008). Myosin light chain kinase-deficient mice die hours after birth, which is before calyces are formed. Lethality could be circumvented because the knock-in gene

is flanked by loxP sites and the mice can be rescued by expression of the cre recombinase (Somlyo *et al.*, 2004). One would need to find a cre expressing mouse line that has no expression in the cochlear nucleus and survives until after the onset of hearing. To my knowledge, mice lacking NCS-1 have not yet been generated, but the $\alpha 1A$ knock-out mice, lacking a subunit to make P/Q type calcium channels and thereby devoid of calcium current facilitation at the calyx, would be a good start to search for defects in PTP and sound localization.

Conclusion

We found that the output of the calyx of Held could be up-regulated for up to half an hour by prior activity in a process called PTP. PTP at the calyx of Held synapse was due to an increase in the Ca^{2+} concentration with a time course similar to PTP. The EPSCs in the principal cells during PTP were larger for two reasons. The number of vesicles that were immediately available for release was increased and the probability for a vesicle to be released was higher after the tetanus. At physiological temperature the increase in P_r was much briefer with a time course more consistent with augmentation. The change in P_r was caused by an increase in calcium influx due to action potential broadening and facilitation of the calcium currents.

Nederlandse samenvatting

Het brein is samengesteld uit vele miljarden zenuwcellen (neuronen), die met elkaar in verbinding staan en met elkaar communiceren zodat ze gespecialiseerde neuronale netwerken vormen. Deze maken specifieke taken mogelijk zoals beweging, spraak en taal, gedachten, sociale interactie, leren en geheugen.

Zenuwcellen communiceren met elkaar via actiepotentialen, elektrische stroompjes door de uitloper van de zenuwcel naar het zenuwuiteinde. De structuur tussen het zenuwuiteinde en het volgende neuron heet een synaps. Een actiepotentiaal die aankomt bij een synaps zorgt voor een reeks van chemische processen, waarbij een signaalstof (neurotransmitter) die in kleine blaasjes (vesicles) zit opgeslagen, uit het zenuwuiteinde vrij komt en door receptoren van het volgende neuron wordt opgevangen.

Er zijn verschillende manieren waarop het doorgeven van een actiepotentiaal beïnvloed kan worden. 1. Sommige neuronale netwerken zijn zo georganiseerd dat meerdere cellen gelijktijdig moeten vuren om in de ontvangende cel een actiepotentiaal te genereren, zodat een dergelijk netwerk integrerende eigenschappen zal vertonen. 2. In andere neuronale netwerken moeten de cellen ontheven worden van negatieve regulatie om de actiepotentiaal door te geven. 3. Weer andere netwerken leiden alleen tot doorgifte van de actiepotentiaal als de verzendende zenuwcel meerdere malen kort na elkaar gestimuleerd wordt. 4. Zulke repetitieve stimulatie kan resulteren in veranderingen in de afgifte van neurotransmitter zelf (synaptische plasticiteit) die op zichzelf een randvoorwaarde voor doorgifte van de actiepotentiaal kan zijn. Elk van de hier genoemde mechanismen zal het neuronale netwerk specifieke eigenschappen verlenen, zoals integratie, filtering of een andere vorm van informatieverwerking. Deze bewerkingen zorgen er gecombineerd met de specifieke manier waarop cellen in een neuronaal netwerk met elkaar verbonden zijn voor dat het neuronale netwerk specifieke taken als geheugenformatie, cognitie, etc. kan bewerkstelligen.

Korte termijn plasticiteit is een fenomeen waarbij de communicatie tussen twee zenuwcellen gedurende een korte tijd verandert. De mechanismen die aan plasticiteit ten grondslag liggen hebben vaak hun oorsprong in het zenuwuiteinde dat neurotransmitter afgeeft (presynaptisch). Deze zenuwuiteindes zijn vaak klein en daardoor moeilijk te bestuderen. Wij hebben onze metingen daarom gedaan in een presynaptisch zenuwuiteinde dat uitzonderlijk groot is, zodat we in staat waren om elektrische en optische metingen te doen voor, tijdens en na korte termijn plasticiteit. Deze zogenoemde calyx van Held (Figuur 1) is gelokaliseerd in de hersenstam van onder andere knaagdieren. Hij is betrokken bij de lokalisatie van geluid en functioneert

door het exciterende signaal van de gehoornucleus om te vormen tot een inhiberend signaal naar de andere kant van het brein toe. Deze omvorming vindt plaats in de mediale nucleus van het trapezoid lichaam (MNTB), waar de calyx van Held een synaps maakt op het cellichaam van de principale cellen. Deze cellen projecteren op hun beurt naar de laterale bovenste olijkern (LSO), waar de informatie van beide oren vergeleken wordt.

Er wordt slechts één calyx synaps gevormd per principale cel en het is van cruciaal belang dat die verbinding gemaakt wordt op de juiste cel in de MNTB. In hoofdstuk twee onderzochten we hoe die verbinding ontstaat bij ratten. We vonden dat de karakteristieke kelk-achtige vorm van de calyx pas drie tot vier dagen na de geboorte tot stand komt en dat de zenuwuitlopers, oftewel axonen, eerst kleine contacten maken met verscheidene cellen in de MNTB alvorens een grote “één op één” verbinding te maken. Deze kleine contacten zijn zeer dynamisch: er worden voortdurend nieuwe contacten gevormd of weggesnoeid. Ook na vorming van de calyx van Held blijven het axon en de calyx kleine verbindingen maken met naburige cellen. Deze verbindingen worden wel steeds zeldzamer naarmate de ratjes zich ontwikkelen tot volwassen dieren.

Er zijn verschillende vormen van synaptische plasticiteit gerapporteerd in de calyx van Held. Alle vormen hebben een korte duur en behoren daarom tot de korte termijn plasticiteit. In hoofdstuk drie beschrijven we een relatief langdurende vorm van korte termijn plasticiteit genaamd “post-tetanic potentiation” (PTP) die nog niet eerder ontdekt was bij deze synaps. We ontdekten deze vorm van plasticiteit nadat we de axonen van de calyces van Held langdurig (5 minuten) gestimuleerd hadden met hoog frequente stimulatie (20 Hz). Terwijl de respons op een actiepotentiaal verdubbelde na stimulatie, bleef de respons op spontaan fuserende neurotransmitter blaasjes (vesicles) constant. Hierdoor concluderen we dat er meer vesicles per actiepotentiaal worden afgegeven tijdens PTP en dat er dus geen veranderingen in de postsynaptische cel plaatsvinden. We ontdekten verder dat er een kleine toename was in de hoeveelheid neurotransmitter blaasjes die klaar ligt voor afgifte, maar dat de voornaamste reden voor PTP een toename in de kans van afgifte was. Deze toename in de zogenaamde “release probability” (P_r) tijdens PTP, was afhankelijk van een langdurige toename van de presynaptische calcium concentratie (residual calcium).

Afgifte van vesicles gevuld met neurotransmitter is een proces dat in zeer hoge mate afhankelijk is van calcium. Een toename van de afgiftekans (P_r) kan ontstaan doordat de vesicles makkelijker fuseren met de membraan, omdat de vesicles gevoeliger zijn voor calcium of doordat er meer calcium instroomt per actiepotentiaal. In hoofdstuk vier laten we zien dat gedurende PTP de calcium influx is toegenomen. Deze toename

is relatief klein (15%), maar door de hoge gevoeligheid van het afgifte proces voor calcium is dit toereikend om de toename in P_r te verklaren.

In hoofdstuk vijf hebben we de kleine toename in de hoeveelheid vesicles die klaar liggen om af te worden gegeven nader onder de loep genomen. Deze vesicles worden de “readily releasable pool” (RRP) genoemd en hun hoeveelheid kan worden gemeten door een korte hoogfrequente stimulus te geven. We vonden dat de toename in RRP zich anders gedraagt als de toename in afgifte waarschijnlijkheid (P_r). Kort (20 seconden) na de stimulus is de RRP nog niet toegenomen terwijl P_r al maximaal is. Ook de duur van de verandering in RRP en P_r verschillen van elkaar, wat vooral zichtbaar wordt als de metingen bij 37°C (fysiologische temperatuur) gedaan worden. In studies die mijn bevindingen opvolgen (Lee et al., 2008) is ook gevonden dat beide mechanismen, toename in RRP en toename in P_r , verschillend tot stand komen. De korte duur van de verandering in P_r bij fysiologische temperatuur benadrukt het belang van de toename in RRP aan post-tetanische potentiatie.

Samengevat vonden we dat post-tetanische potentiatie veroorzaakt wordt door een toename van het aantal klaarliggende vesicles (de RRP), en tevens door een toename van de afgiftewaarschijnlijkheid van deze vesicles. De afgiftewaarschijnlijkheid neemt toe doordat de influx van calcium per actiepotentiaal toeneemt en de toename in de RRP is van groter belang bij fysiologische temperatuur.

Dankwoord

Allereerst ben ik Gerard mijn dank verschuldigd voor zijn jarenlange supervisie en zijn vele inspanningen om dit boekje en mijn promotie te verwezenlijken. Verder wil ik diverse collega's bedanken voor de gelegenheid om met hen samen te werken en te leren. Omdat mijn promotie in Amsterdam aan de Universiteit van Amsterdam begon wil ik als eerste Albert de Roos en Bo de Lange bedanken, twee post-docs waarmee we het lab hebben opgezet en waarmee ik ook buiten het werk om veel plezier heb beleefd. Later heeft Ingrid Saarloos zich bij ons gevoegd als analiste waarmee ik verwoede pogingen heb ondernomen om hersenplakken in culture te houden en die te infecteren met "Semliki Forest virus". We werden hierbij geholpen door Hans van Hooft die tegelijkertijd hippocampale plakken kweekte. Ik wil Prof. Wadman bedanken voor zijn toewijding als promotor tijdens mijn aanstelling in Amsterdam. Mijn eerste project betrof het meten van micro calcium domeinen, wat een onmogelijke opgave bleek te zijn. Toch heb ik van dit project veel geleerd over "imaging" en microscopie, wat ik te danken heb aan Prof. Brakenhoff en Michiel Müller die me geholpen hebben om een twee-foton confocale microscoop in elkaar te zetten. In de categorie onuitvoerbaar projecten valt ook het infuseren van peptiden in de calyx van Held door de patch pipet. Ik wil Thomas Südhof van de universiteit van Texas Southwestern bedanken voor synaptotagmine peptiden en Kees Jalink en Jose van der Wal van het Nederlands kanker instituut voor hulp bij het maken van PH_{plc δ 1}-GFP peptiden. De synaptotagmine peptiden vertoonden geen fenotype en de fluorescentie van PH_{plc δ 1}-GFP kon worden waargenomen als een dikke blob in het uiteinde van mijn pipet, wat waarschijnlijk ook het lot van de synaptotagmine peptiden is geweest en daarmee het gebrek aan fenotype verklaart.

Eind 2001 verhuisde Gerard met het lab naar Rotterdam om een positie als hoogleraar te bekleden aan de afdeling neurowetenschappen van de Erasmus Universiteit, waar ik hem volgde om mijn experimenten aan de calyx van Held voort te zetten. In Rotterdam werd het bouwen van twee-foton opstellingen gelukkig door Kees Donkersloot van me overgenomen. Kees heeft alle trucs uit de doos gehaald om voor mij mogelijk te maken micro domein calcium verhogingen waar te nemen. Het mocht helaas niet baten. De fotomultipliers die eigenlijk voor de twee-foton opstelling bestemd waren, bleken echter uitstekend geschikt om met hoge temporele resolutie calcium influx te meten. De resultaten daarvan zijn te bewonderen in hoofdstuk drie, ook daarvoor mijn dank.

De volgende mensen hebben mij geholpen bij het genetisch manipuleren van de cochleaire nucleus door middel van injectie van het "Semliki Forest virus". Michael van der Reijden heeft aan mijn voordurende vraag naar meer, beter en geconcentreerder

virus altijd gehoor gegeven. Michael bedankt en “hang loose”. Hans van der Burg heeft me het opereren in ratjes bijgebracht en Kees Entius heeft nog een stuk van zijn vinger gedoneerd bij een poging om zelf een atlas voor acht dagen oude pups te zagen. Elize Haasdijk, Erika Goedknecht en Hilco Theeuwes hebben me enorm geholpen met immunohistochemie van de geïnjecteerde beesten.

Ik wil Sander Groffen en Matthijs Verhage van het center for neurogenomics and cognitive research te Amsterdam bedanken voor onze samenwerking aan Doc 2 AB dubbel knock-out muizen. Verder wil ik Bogdan Milojkovic and Chris de Zeeuw bedanken voor het gebruik van hun Leica vibratoom.

Ik wil Adrián, John en Heiko bedanken voor onze samenwerking met als vruchtbaar resultaat de experimenten zoals getoond in hoofdstuk 2. Ik wil ook de andere mensen in het lab van Gerard bedanken voor zinvolle of minder zinvolle discussies en voor de gezellige sfeer in de donkere “imaging” hokken. Vooral Liane wist altijd op het juiste moment een kopje thee te zetten en me daarmee af te leiden van het binnensmonds gevloek op het hierboven beschreven preparaat. Verder wil ik alle andere collegas van de afdeling neurowetenschappen waar ik door de jaren heen mee samengewerkt heb bedanken.

Ik wil Loes Nijs en Edith Klink bedanken voor de altijd aanwezige hulp met de paperassen en Loes ook speciaal voor de hulp met de referenties van hoofdstuk drie.

Verder wil ik Joris de Wit bedanken om als afvoerputje te fungeren als ik mijn gal wilde spuwen over de hierboven beschreven projecten en personen. Ik ben mijn familie, mijn ouders en schoonouders, mijn broers, schoon zussen en schoonbroer dankbaar voor hun interesse in mijn werk en voor alle hulp die mij in staat stelde dit proefschrift te realiseren. Ik wil karlijn bedanken voor het poseren tijdens het nemen van de fotos voor de cover, zodat de kermis exploitant niet op gekke ideeën zou komen. Als laatste wil ik mijn gezin bedanken. Guus en Noortje voor het inkleuren van donkere tijden en voor jullie aanstekelijke vrolijkheid en Claudia voor haar altijd aanwezige liefde en steun.

Curriculum Vitae

Ron Habets is op 27 maart 1973 geboren in Heerlen. Na zijn verblijf op basisschool “de heipaal” deed hij in 1992 eindexamen voortgezet wetenschappelijk onderwijs aan het Grotius college te Heerlen. In datzelfde jaar startte hij met de studie sterrenkunde aan de Universiteit van Amsterdam, waar hij in 1993 overstapte naar de studie biologie aan diezelfde universiteit. Tijdens zijn studie deed hij onderzoek bij dr. Maarten Kamermans op het Interuniversitair Oogheelkundig Instituut, naar adaptatie van de kegeltjes in de retina en de effecten daarvan op de communicatie naar de horizontale cellen. Daarna deed hij een tweede stage bij dr. Kees Jalink op het Nederlands Kanker Instituut, waar hij betrokken was bij een studie naar membraanlipiden en hun functie in intracellulaire signaal transductie. Hij studeerde in 1999 af op een scriptie met de titel “Learning and memory can be coupled to LTP through the use of transgenic animals “.

Datzelfde jaar trad hij in dienst als assistent in opleiding bij de Universiteit van Amsterdam onder leiding van dr. Gerard Borst en prof. Wytse Wadman waar hij een start maakte met zijn neurofysiologisch onderzoek waarvan de resultaten in dit proefschrift beschreven staan. Lopende het onderzoek verhuisde de onderzoeksgroep naar de Erasmus Universiteit in Rotterdam (promotor prof. JGG Borst).

In januari 2007 werd hij aangenomen als Post-doc bij het Vlaams Instituut voor Biotechnologie (VIB) in het lab van Patrik Verstreken aan de KU Leuven, waar hij momenteel als neurobioloog onderzoek doet naar afgifte en heropname van met neurotransmitter gevulde blaasjes in de fruitvlieg *Drosophila melanogaster*.

Ron woont samen met Claudia en ze hebben twee kinderen; Guus, 5 jaar en Noortje, 2 jaar.

Claudia Lipsch

Publications

1. Fahrenfort I, **Habets RL**, Spekreijse H & Kamermans M (1999) Intrinsic cone adaptation modulates feedback efficiency from horizontal cells to cones. *J Gen Physiol* **114**, 511-24.
2. van der Wal J, **Habets R**, Varnai P, Balla T & Jalink K (2001) Monitoring agonist-induced phospholipase C activation in live cells by fluorescence resonance energy transfer. *J Biol Chem* **276**, 15337-44.
3. **Habets RLP** & Borst JGG (2005) Post-tetanic potentiation in the rat calyx of Held synapse. *J Physiol* **564**, 173-87.
4. **Habets RLP** & Borst JGG (2006) An increase in calcium influx contributes to post-tetanic potentiation at the rat calyx of Held synapse. *J Neurophysiol* **96**, 2868-2876.
5. **Habets RLP** & Borst JG (2007) Dynamics of the readily releasable pool during post-tetanic potentiation in the rat calyx of Held synapse. *J Physiol* **581**, 467-78.
6. Rodriguez-Contreras A, van Hoeve JS, **Habets RLP**, Locher H & Borst JGG (2008) Dynamic development of the calyx of Held synapse. *Proc Natl Acad Sci U S A* **105**, 5603-8.
7. Kasprovicz J, Kuenen S, Miskiewicz K, **Habets RLP**, Smitz L & Verstreken P (2008) Inactivation of clathrin heavy chain inhibits synaptic recycling but allows bulk membrane uptake. *J Cell Biol* **182**, 1007-16.
8. Verstreken P, Ohyama T, Haueter C, **Habets RLP**, Lin YQ, Swan LE, Ly CV, Venken KJT, Camilli Pd & Bellen HJ (2009, submitted) Tweek, a novel player in synaptic vesicle endocytosis.
9. Groffen AJ, Martens S, Díez R, Cornelisse LN, Lozovaya N, Goriounova NA, **Habets RLP**, Borst JGG, Brose N, McMahon HT & Verhage M (2009, in preparation) DOC2B is a calcium sensor for spontaneous synaptic vesicle exocytosis.
10. **Habets RLP** & Verstreken P. (2009, in preparation) Acute inactivation of proteins in *Drosophila melanogaster* using FlAsH-FALI.

List of abbreviations

AMPA	= alpha-amino-3-hydroxy-5-methyl-4-isoxazole propionic acid
AP	= action potential
APW	= action potential waveform
BIS-I	= bisindolylmaleimide I
EPSC	= excitatory postsynaptic current
f	= frequency
F	= fluorescence
F _o	= baseline fluorescence
K _d	= dissociation constant
LSO	= lateral superior olive
mGLUR	= metabotropic glutamate receptor
MNTB	= medial nucleus of the trapezoid body
NCS-1	= neuronal calcium sensor 1
NMDA	= N-methyl-D-aspartic acid
NMJ	= neuromuscular junction
OGB-5N	= Oregon Green Bapta-5N
PMT	= photomultiplier tube
PPF	= paired pulse facilitation
P _r	= release probability
PT	= physiological temperature
PTP	= post-tetanic potentiation
q	= quantal size
RRP	= readily releasable pool
RT	= room temperature
SEM	= standard error of the mean
STD	= short term depression
STP	= short term plasticity
TPP ⁺	= tetraphenylphosphonium
γDGG	= gamma-D-glutamylglycine
ΔF	= fluorescence change
ΔF _{AP}	= fluorescent responses evoked by an action potential
ΔF _{APW}	= fluorescent responses evoked by an action potential waveform
ΔQ	= calcium influx

References

- Adler, EM, Augustine, GJ, Duffy, SN & Charlton, MP. (1991). Alien intracellular calcium chelators attenuate neurotransmitter release at the squid giant synapse. *J Neurosci* **11**, 1496-1507.
- Ahmari, SE, Buchanan, J & Smith, SJ. (2000). Assembly of presynaptic active zones from cytoplasmic transport packets. *Nat Neurosci* **3**, 445-451.
- Alle, H, Jonas, P & Geiger, JRP. (2001). PTP and LTP at a hippocampal mossy fiber-interneuron synapse. *Proc Natl Acad Sci U S A* **98**, 14708-14713.
- Alsina, B, Vu, T & Cohen-Cory, S. (2001). Visualizing synapse formation in arborizing optic axons in vivo: dynamics and modulation by BDNF. *Nat Neurosci* **4**, 1093-1101.
- Angleton, JK & Betz, WJ. (2001). Intraterminal Ca²⁺ and spontaneous transmitter release at the frog neuromuscular junction. *J Neurophysiol* **85**, 287-294.
- Augustine, GJ. (1990). Regulation of transmitter release at the squid giant synapse by presynaptic delayed rectifier potassium current. *J Physiol* **431**, 343-364.
- Augustine, GJ. (2001). How does calcium trigger neurotransmitter release? *Curr Opin Neurobiol* **11**, 320-326.
- Augustine, GJ, Adler, EM & Charlton, MP. (1991). The calcium signal for transmitter secretion from presynaptic nerve terminals. *Ann N Y Acad Sci* **635**, 365-381.
- Augustine, GJ, Betz, H, Bommert, K, Charlton, MP, DeBello, WM, Hans, M & Swandulla, D. (1994). Molecular pathways for presynaptic calcium signaling. *Adv Second Messenger Phosphoprotein Res* **29**, 139-154.
- Awatramani, GB, Price, GD & Trussell, LO. (2005). Modulation of transmitter release by presynaptic resting potential and background calcium levels. *Neuron* **48**, 109-121.
- Banks, MI & Smith, PH. (1992). Intracellular recordings from neurobiotin-labeled cells in brain slices of the rat medial nucleus of the trapezoid body. *J Neurosci* **12**, 2819-2837.

- Bao, JX, Kandel, ER & Hawkins, RD. (1997). Involvement of pre- and postsynaptic mechanisms in posttetanic potentiation at *Aplysia* synapses. *Science* **275**, 969-973.
- Barclay, JW, Morgan, A & Burgoyne, RD. (2005). Calcium-dependent regulation of exocytosis. *Cell Calcium* **38**, 343-353.
- Barnes-Davies, M & Forsythe, ID. (1995). Pre- and postsynaptic glutamate receptors at a giant excitatory synapse in rat auditory brainstem slices. *J Physiol* **488 (Pt 2)**, 387-406.
- Bergsman, JB, De Camilli, P & McCormick, DA. (2004). Multiple large inputs to principal cells in the mouse medial nucleus of the trapezoid body. *J Neurophysiol* **92**, 545-552.
- Billups, B & Forsythe, ID. (2002). Presynaptic mitochondrial calcium sequestration influences transmission at mammalian central synapses. *J Neurosci* **22**, 5840-5847.
- Billups, B, Graham, BP, Wong, AY & Forsythe, ID. (2005). Unmasking group III metabotropic glutamate autoreceptor function at excitatory synapses in the rat CNS. *J Physiol* **565**, 885-896.
- Blatow, M, Caputi, A, Burnashev, N, Monyer, H & Rozov, A. (2003). Ca²⁺ buffer saturation underlies paired pulse facilitation in calbindin-D28k-containing terminals. *Neuron* **38**, 79-88.
- Bollmann, JH & Sakmann, B. (2005). Control of synaptic strength and timing by the release-site Ca²⁺ signal. *Nat Neurosci* **8**, 426-434.
- Bollmann, JH, Sakmann, B & Borst, JGG. (2000). Calcium sensitivity of glutamate release in a calyx-type terminal. *Science* **289**, 953-957.
- Borst, JG & Helmchen, F. (1998). Calcium influx during an action potential. *Methods Enzymol* **293**, 352-371.
- Borst, JGG, Helmchen, F & Sakmann, B. (1995). Pre- and postsynaptic whole-cell recordings in the medial nucleus of the trapezoid body of the rat. *J Physiol* **489 (Pt 3)**, 825-840.

- Borst, JGG & Sakmann, B. (1996). Calcium influx and transmitter release in a fast CNS synapse. *Nature* **383**, 431-434.
- Borst, JGG & Sakmann, B. (1998a). Calcium current during a single action potential in a large presynaptic terminal of the rat brainstem. *J Physiol* **506 (Pt 1)**, 143-157.
- Borst, JGG & Sakmann, B. (1998b). Facilitation of presynaptic calcium currents in the rat brainstem. *J Physiol* **513 (Pt 1)**, 149-155.
- Borst, JGG & Sakmann, B. (1999a). Depletion of calcium in the synaptic cleft of a calyx-type synapse in the rat brainstem. *J Physiol* **521 Pt 1**, 123-133.
- Borst, JGG & Sakmann, B. (1999b). Effect of changes in action potential shape on calcium currents and transmitter release in a calyx-type synapse of the rat auditory brainstem. *Philos Trans R Soc Lond B Biol Sci* **354**, 347-355.
- Brager, DH, Cai, X & Thompson, SM. (2003). Activity-dependent activation of presynaptic protein kinase C mediates post-tetanic potentiation. *Nat Neurosci* **6**, 551-552.
- Brain, KL & Bennett, MR. (1995). Calcium in the nerve terminals of chick ciliary ganglia during facilitation, augmentation and potentiation. *Journal of Physiology* **489**, 637-648.
- Burgoyne, RD, O'Callaghan, DW, Hasdemir, B, Haynes, LP & Tepikin, AV. (2004). Neuronal Ca²⁺-sensor proteins: multitalented regulators of neuronal function. *Trends Neurosci* **27**, 203-209.
- Burnashev, N & Rozov, A. (2005). Presynaptic Ca²⁺ dynamics, Ca²⁺ buffers and synaptic efficacy. *Cell Calcium* **37**, 489-495.
- Byrne, JH & Kandel, ER. (1996). Presynaptic facilitation revisited: state and time dependence. *J Neurosci* **16**, 425-435.
- Calakos, N, Schoch, S, Südhof, TC & Malenka, RC. (2004). Multiple roles for the active zone protein RIM1 α in late stages of neurotransmitter release. *Neuron* **42**, 889-896.

- Ceccarelli, B, Grohovaz, F & Hurlbut, WP. (1979). Freeze-fracture studies of frog neuromuscular junctions during intense release of neurotransmitter. II. Effects of electrical stimulation and high potassium. *J Cell Biol* **81**, 178-192.
- Chapman, PF, Frenguelli, BG, Smith, A, Chen, CM & Silva, AJ. (1995). The alpha-Ca₂₊/calmodulin kinase II: a bidirectional modulator of presynaptic plasticity. *Neuron* **14**, 591-597.
- Cheng, Q & Augustine, GJ. (2008). Calcium channel modulation as an all-purpose mechanism for short-term synaptic plasticity. *Neuron* **57**, 171-172.
- Chuhma, N & Ohmori, H. (1998). Postnatal development of phase-locked high-fidelity synaptic transmission in the medial nucleus of the trapezoid body of the rat. *J Neurosci* **18**, 512-520.
- Chuhma, N & Ohmori, H. (2001). Differential development of Ca²⁺ dynamics in presynaptic terminal and postsynaptic neuron of the rat auditory synapse. *Brain Res* **904**, 341-344.
- Chuhma, N & Ohmori, H. (2002). Role of Ca(2+) in the synchronization of transmitter release at calyceal synapses in the auditory system of rat. *J Neurophysiol* **87**, 222-228.
- Cohen-Cory, S & Lom, B. (2004). Neurotrophic regulation of retinal ganglion cell synaptic connectivity: from axons and dendrites to synapses. *Int J Dev Biol* **48**, 947-956.
- Collin, T, Chat, M, Lucas, MG, Moreno, H, Racay, P, Schwaller, B, Marty, A & Llano, I. (2005). Developmental changes in parvalbumin regulate presynaptic Ca₂₊ signaling. *J Neurosci* **25**, 96-107.
- Cummings, DD, Wilcox, KS & Dichter, MA. (1996). Calcium-dependent paired-pulse facilitation of miniature EPSC frequency accompanies depression of EPSCs at hippocampal synapses in culture. *J Neurosci* **16**, 5312-5323.
- Cuttle, MF, Tsujimoto, T, Forsythe, ID & Takahashi, T. (1998). Facilitation of the presynaptic calcium current at an auditory synapse in rat brainstem. *J Physiol* **512 (Pt 3)**, 723-729.

- David, G, Barrett, JN & Barrett, EF. (1997). Stimulation-induced changes in [Ca₂₊] in lizard motor nerve terminals. *J Physiol* **504** (Pt 1), 83-96.
- De Camilli, P, Benfenati, F, Valtorta, F & Greengard, P. (1990). The synapsins. *Annu Rev Cell Biol* **6**, 433-460.
- de Lange, RP, de Roos, AD & Borst, JGG. (2003). Two modes of vesicle recycling in the rat calyx of Held. *J Neurosci* **23**, 10164-10173.
- Deitcher, DL, Ueda, A, Stewart, BA, Burgess, RW, Kidokoro, Y & Schwarz, TL. (1998). Distinct requirements for evoked and spontaneous release of neurotransmitter are revealed by mutations in the *Drosophila* gene neuronal-synaptobrevin. *J Neurosci* **18**, 2028-2039.
- Delaney, KR & Tank, DW. (1994). A quantitative measurement of the dependence of short-term synaptic enhancement on presynaptic residual calcium. *J Neurosci* **14**, 5885-5902.
- Delaney, KR & Zucker, RS. (1990). Calcium released by photolysis of DM-nitrophen stimulates transmitter release at squid giant synapse. *J Physiol* **426**, 473-498.
- Delaney, KR, Zucker, RS & Tank, DW. (1989). Calcium in motor nerve terminals associated with posttetanic potentiation. *Journal of Neuroscience* **9**, 3558-3567.
- Diamond, JS & Jahr, CE. (1997). Transporters buffer synaptically released glutamate on a submillisecond time scale. *J Neurosci* **17**, 4672-4687.
- Dickinson, M. (2005). Multiphoton and Multispectral Laser-scanning Microscopy. In *Live Cell Imaging: A Laboratory Manual*. ed. GOLDMAN, RD & SPECTOR, DL. Cold spring harbor laboratory press.
- DiGregorio, DA, Peskoff, A & Vergara, JL. (1999). Measurement of action potential-induced presynaptic calcium domains at a cultured neuromuscular junction. *J Neurosci* **19**, 7846-7859.
- Dinkelacker, V, Voets, T, Neher, E & Moser, T. (2000). The readily releasable pool of vesicles in chromaffin cells is replenished in a temperature-dependent manner and transiently overfills at 37 °C. *J Neurosci* **20**, 8377-8383.

- Dodge, FA, Jr. & Rahamimoff, R. (1967). Co-operative action a calcium ions in transmitter release at the neuromuscular junction. *J Physiol* **193**, 419-432.
- Dulubova, I, Lou, X, Lu, J, Huryeva, I, Alam, A, Schneggenburger, R, Südhof, TC & Rizo, J. (2005). A Munc13/RIM/Rab3 tripartite complex: from priming to plasticity? *Embo J* **24**, 2839-2850.
- Eliot, LS, Kandel, ER & Hawkins, RD. (1994). Modulation of spontaneous transmitter release during depression and posttetanic potentiation of *Aplysia* sensory-motor neuron synapses isolated in culture. *J Neurosci* **14**, 3280-3292.
- Eliot, LS, Kandel, ER, Siegelbaum, SA & Blumenfeld, H. (1993). Imaging terminals of *Aplysia* sensory neurons demonstrates role of enhanced Ca²⁺ influx in presynaptic facilitation. *Nature* **361**, 634-637.
- Elmqvist, D & Quastel, DMJ. (1965). A quantitative study of end-plate potentials in isolated human muscle. *J Physiol* **178**, 505-529.
- Erazo-Fischer, E, Striessnig, J & Taschenberger, H. (2007). The role of physiological afferent nerve activity during in vivo maturation of the calyx of Held synapse. *J Neurosci* **27**, 1725-1737.
- Faas, GC, Karacs, K, Vergara, JL & Mody, I. (2005). Kinetic properties of DM-nitrophen binding to calcium and magnesium. *Biophys J* **88**, 4421-4433.
- Fedchyshyn, MJ & Wang, LY. (2005). Developmental transformation of the release modality at the calyx of Held synapse. *J Neurosci* **25**, 4131-4140.
- Felmy, F, Neher, E & Schneggenburger, R. (2003). Probing the intracellular calcium sensitivity of transmitter release during synaptic facilitation. *Neuron* **37**, 801-811.
- Felmy, F & Schneggenburger, R. (2004). Developmental expression of the Ca²⁺-binding proteins calretinin and parvalbumin at the calyx of held of rats and mice. *Eur J Neurosci* **20**, 1473-1482.
- Feng, TP. (1941). Neuromuscular junction. XXVI. Changes of end-plate potential during and after prolonged stimulation. *Zhongguo Shenglixue Zazhi (1941)*, *16*, 341-72 CODEN: CHKSA7; ISSN: 0366-6204.

- Few, AP, Lautermilch, NJ, Westenbroek, RE, Scheuer, T & Catterall, WA. (2005). Differential regulation of CaV2.1 channels by calcium-binding protein 1 and visinin-like protein-2 requires N-terminal myristoylation. *J Neurosci* **25**, 7071-7080.
- Fisher, SA, Fischer, TM & Carew, TJ. (1997). Multiple overlapping processes underlying short-term synaptic enhancement. *Trends Neurosci* **20**, 170-177.
- Forsythe, ID. (1994). Direct patch recording from identified presynaptic terminals mediating glutamatergic EPSCs in the rat CNS, in vitro. *J Physiol* **479 (Pt 3)**, 381-387.
- Forsythe, ID & Barnes-Davies, M. (1993). The binaural auditory pathway: excitatory amino acid receptors mediate dual timecourse excitatory postsynaptic currents in the rat medial nucleus of the trapezoid body. *Proc Biol Sci* **251**, 151-157.
- Forsythe, ID, Tsujimoto, T, Barnes-Davies, M, Cuttle, MF & Takahashi, T. (1998). Inactivation of presynaptic calcium current contributes to synaptic depression at a fast central synapse. *Neuron* **20**, 797-807.
- Foster, KA & Regehr, WG. (2004). Variance-mean analysis in the presence of a rapid antagonist indicates vesicle depletion underlies depression at the climbing fiber synapse. *Neuron* **43**, 119-131.
- Futai, K, Okada, M, Matsuyama, K & Takahashi, T. (2001). High-fidelity transmission acquired via a developmental decrease in NMDA receptor expression at an auditory synapse. *J Neurosci* **21**, 3342-3349.
- Geiger, JRP & Jonas, P. (2000). Dynamic control of presynaptic Ca²⁺ inflow by fast-inactivating K⁺ channels in hippocampal mossy fiber boutons. *Neuron* **28**, 927-939.
- Geppert, M, Goda, Y, Hammer, RE, Li, C, Rosahl, TW, Stevens, CF & Sudhof, TC. (1994). Synaptotagmin I: a major Ca²⁺ sensor for transmitter release at a central synapse. *Cell* **79**, 717-727.

- Gomez, M, De Castro, E, Guarin, E, Sasakura, H, Kuhara, A, Mori, I, Bartfai, T, Bargmann, CI & Nef, P. (2001). Ca²⁺ signaling via the neuronal calcium sensor-1 regulates associative learning and memory in *C. elegans*. *Neuron* **30**, 241-248.
- Grothe, B. (2003). New roles for synaptic inhibition in sound localization. *Nat Rev Neurosci* **4**, 540-550.
- Grynkiewicz, G, Poenie, M & Tsien, RY. (1985). A new generation of Ca²⁺ indicators with greatly improved fluorescence properties. *J Biol Chem* **260**, 3440-3450.
- Habets, RLP, Elgersma, Y & Borst, JGG. (2003). Post-tetanic potentiation at the calyx of Held synapse. *Society for Neuroscience Abstracts* **902.6**.
- Hamann, M, Billups, B & Forsythe, ID. (2003). Non-calyceal excitatory inputs mediate low fidelity synaptic transmission in rat auditory brainstem slices. *Eur J Neurosci* **18**, 2899-2902.
- Heidelberger, R, Heinemann, C, Neher, E & Matthews, G. (1994). Calcium dependence of the rate of exocytosis in a synaptic terminal. *Nature* **371**, 513-515.
- Helmchen, F, Borst, JGG & Sakmann, B. (1997). Calcium dynamics associated with a single action potential in a CNS presynaptic terminal. *Biophys J* **72**, 1458-1471.
- Heuser, JE & Reese, TS. (1973). Evidence for recycling of synaptic vesicle membrane during transmitter release at the frog neuromuscular junction. *J Cell Biol* **57**, 315-344.
- Hochner, B, Klein, M, Schacher, S & Kandel, ER. (1986). Action-potential duration and the modulation of transmitter release from the sensory neurons of *Aplysia* in presynaptic facilitation and behavioral sensitization. *Proc Natl Acad Sci U S A* **83**, 8410-8414.
- Hoffpauir, BK, Grimes, JL, Mathers, PH & Spirou, GA. (2006). Synaptogenesis of the calyx of Held: rapid onset of function and one-to-one morphological innervation. *J Neurosci* **26**, 5511-5523.
- Hori, T, Takai, Y & Takahashi, T. (1999). Presynaptic mechanism for phorbol ester-induced synaptic potentiation. *J Neurosci* **19**, 7262-7267.

- Hosoi, N, Sakaba, T & Neher, E. (2007). Quantitative analysis of calcium-dependent vesicle recruitment and its functional role at the calyx of Held synapse. *J Neurosci* **27**, 14286-14298.
- Hu, B, Nikolakopoulou, AM & Cohen-Cory, S. (2005). BDNF stabilizes synapses and maintains the structural complexity of optic axons in vivo. *Development* **132**, 4285-4298.
- Hughes, JR. (1958). Post-tetanic potentiation. *Physiol Rev* **38**, 91-113.
- Inchauspe, CG, Forsythe, ID & Uchitel, OD. (2007). Changes in synaptic transmission properties due to the expression of N-type calcium channels at the calyx of Held synapse of mice lacking P/Q-type calcium channels. *J Physiol* **584**, 835-851.
- Inchauspe, CG, Martini, FJ, Forsythe, ID & Uchitel, OD. (2004). Functional compensation of P/Q by N-type channels blocks short-term plasticity at the calyx of held presynaptic terminal. *J Neurosci* **24**, 10379-10383.
- Ishikawa, T, Kaneko, M, Shin, HS & Takahashi, T. (2005). Presynaptic N-type and P/Q-type Ca²⁺ channels mediating synaptic transmission at the calyx of Held of mice. *J Physiol* **568**, 199-209.
- Ishikawa, T, Sahara, Y & Takahashi, T. (2002). A single packet of transmitter does not saturate postsynaptic glutamate receptors. *Neuron* **34**, 613-621.
- Iwasaki, S & Takahashi, T. (1998). Developmental changes in calcium channel types mediating synaptic transmission in rat auditory brainstem. *J Physiol* **509 (Pt 2)**, 419-423.
- Jackson, MB, Konnerth, A & Augustine, GJ. (1991). Action potential broadening and frequency-dependent facilitation of calcium signals in pituitary nerve terminals. *Proc Natl Acad Sci U S A* **88**, 380-384.
- Jackson, MB & Redman, SJ. (2003). Calcium dynamics, buffering, and buffer saturation in the boutons of dentate granule-cell axons in the hilus. *J Neurosci* **23**, 1612-1621.

- Javaherian, A & Cline, HT. (2005). Coordinated motor neuron axon growth and neuromuscular synaptogenesis are promoted by CPG15 in vivo. *Neuron* **45**, 505-512.
- Jones, HC & Keep, RF. (1988). Brain fluid calcium concentration and response to acute hypercalcaemia during development in the rat. *J Physiol* **402**, 579-593.
- Joris, PX, Michelet, P, Franken, TP & McLaughlin, M. (2008). Variations on a Dexterous theme: peripheral time-intensity trading. *Hear Res* **238**, 49-57.
- Joshi, I, Shokralla, S, Titis, P & Wang, LY. (2004). The role of AMPA receptor gating in the development of high-fidelity neurotransmission at the calyx of Held synapse. *J Neurosci* **24**, 183-196.
- Junge, HJ, Rhee, JS, Jahn, O, Varoqueaux, F, Spiess, J, Waxham, MN, Rosenmund, C & Brose, N. (2004). Calmodulin and Munc13 form a Ca²⁺ sensor/effector complex that controls short-term synaptic plasticity. *Cell* **118**, 389-401.
- Kalkstein, JM & Magleby, KL. (2004). Augmentation increases vesicular release probability in the presence of masking depression at the frog neuromuscular junction. *J Neurosci* **24**, 11391-11403.
- Kamiya, H & Zucker, RS. (1994). Residual Ca²⁺ and short-term synaptic plasticity. *Nature* **371**, 603-606.
- Kandel, ER & Schwartz, JH. (1982). Molecular biology of learning: modulation of transmitter release. *Science* **218**, 433-443.
- Kandler, K & Friauf, E. (1993). Pre- and postnatal development of efferent connections of the cochlear nucleus in the rat. *J Comp Neurol* **328**, 161-184.
- Kaneko, M & Takahashi, T. (2004). Presynaptic mechanism underlying cAMP-dependent synaptic potentiation. *J Neurosci* **24**, 5202-5208.
- Katz, B & Miledi, R. (1968). The role of calcium in neuromuscular facilitation. *J Physiol* **195**, 481-492.

- Kil, J, Kageyama, GH, Semple, MN & Kitzes, LM. (1995). Development of ventral cochlear nucleus projections to the superior olivary complex in gerbil. *J Comp Neurol* **353**, 317-340.
- Kim, JH, Sizov, I, Dobretsov, M & von Gersdorff, H. (2007). Presynaptic Ca²⁺ buffers control the strength of a fast post-tetanic hyperpolarization mediated by the β_3 Na⁺/K⁺-ATPase. *Nat Neurosci* **10**, 196-205.
- Kim, MH, Korogod, N, Schneggenburger, R, Ho, WK & Lee, SH. (2005). Interplay between Na⁺/Ca²⁺ exchangers and mitochondria in Ca²⁺ clearance at the calyx of Held. *J Neurosci* **25**, 6057-6065.
- Kimura, M, Saitoh, N & Takahashi, T. (2003). Adenosine A(1) receptor-mediated presynaptic inhibition at the calyx of Held of immature rats. *J Physiol* **553**, 415-426.
- Klingauf, J & Neher, E. (1997). Modeling buffered Ca²⁺ diffusion near the membrane: implications for secretion in neuroendocrine cells. *Biophys J* **72**, 674-690.
- Klyachko, VA & Stevens, CF. (2006). Temperature-dependent shift of balance among the components of short-term plasticity in hippocampal synapses. *J Neurosci* **26**, 6945-6957.
- Ko, CP. (1981). Electrophysiological and freeze-fracture studies of changes following denervation at frog neuromuscular junctions. *J Physiol* **321**, 627-639.
- Koester, HJ & Johnston, D. (2005). Target cell-dependent normalization of transmitter release at neocortical synapses. *Science* **308**, 863-866.
- Kopp-Scheinflug, C, Fuchs, K, Lippe, WR, Tempel, BL & Rübsamen, R. (2003a). Decreased temporal precision of auditory signaling in Kcna1-null mice: an electrophysiological study *in vivo*. *J Neurosci* **23**, 9199-9207.
- Kopp-Scheinflug, C, Lippe, WR, Dorrscheidt, GJ & Rübsamen, R. (2003b). The medial nucleus of the trapezoid body in the gerbil is more than a relay: comparison of pre- and postsynaptic activity. *J Assoc Res Otolaryngol* **4**, 1-23.
- Korogod, N. (2006). *Mechanisms of posttetanic potentiation and its possible role in maturation of the calyx of Held synapse*.

- Korogod, N, Lou, X & Schneggenburger, R. (2005). Presynaptic Ca²⁺ requirements and developmental regulation of posttetanic potentiation at the calyx of Held. *J Neurosci* **25**, 5127-5137.
- Korogod, N, Lou, X & Schneggenburger, R. (2007). Posttetanic potentiation critically depends on an enhanced Ca²⁺ sensitivity of vesicle fusion mediated by presynaptic PKC. *Proc Natl Acad Sci U S A* **104**, 15923-15928.
- Kreitzer, AC & Regehr, WG. (2000). Modulation of transmission during trains at a cerebellar synapse. *J Neurosci* **20**, 1348-1357.
- Kretz, R, Shapiro, E & Kandel, ER. (1982). Post-tetanic potentiation at an identified synapse in Aplysia is correlated with a Ca²⁺-activated K⁺ current in the presynaptic neuron: evidence for Ca²⁺ accumulation. *Proceedings of the National Academy of Sciences of the USA* **79**, 5430-5434.
- Kuromi, H & Kidokoro, Y. (2003). Two synaptic vesicle pools, vesicle recruitment and replenishment of pools at the *Drosophila* neuromuscular junction. *J Neurocytol* **32**, 551-565.
- Kushmerick, C, Price, GD, Taschenberger, H, Puente, N, Renden, R, Wadiche, JI, Duvoisin, RM, Grandes, P & von Gersdorff, H. (2004). Retroinhibition of presynaptic Ca²⁺ currents by endocannabinoids released via postsynaptic mGluR activation at a calyx synapse. *J Neurosci* **24**, 5955-5965.
- Kushmerick, C, Renden, R & von Gersdorff, H. (2006). Physiological temperatures reduce the rate of vesicle pool depletion and short-term depression via an acceleration of vesicle recruitment. *J Neurosci* **26**, 1366-1377.
- Leão, RM, Kushmerick, C, Pinaud, R, Renden, R, Li, GL, Taschenberger, H, Spirou, G, Levinson, SR & von Gersdorff, H. (2005). Presynaptic Na⁺ channels: locus, development, and recovery from inactivation at a high-fidelity synapse. *J Neurosci* **25**, 3724-3738.
- Leão, RM & Von Gersdorff, H. (2002). Noradrenaline increases high-frequency firing at the calyx of held synapse during development by inhibiting glutamate release. *J Neurophysiol* **87**, 2297-2306.

- Lee, JS, Kim, MH, Ho, WK & Lee, SH. (2008). Presynaptic release probability and readily releasable pool size are regulated by two independent mechanisms during posttetanic potentiation at the calyx of Held synapse. *J Neurosci* **28**, 7945-7953.
- Lev-Tov, A & Rahamimoff, R. (1980). A study of tetanic and post-tetanic potentiation of miniature end-plate potentials at the frog neuromuscular junction. *J Physiol* **309**, 247-273.
- Lichtman, JW & Colman, H. (2000). Synapse elimination and indelible memory. *Neuron* **25**, 269-278.
- Liley, AW & North, KAK. (1953). An electrical investigation of effects of repetitive stimulation on mammalian neuromuscular junction. *J Neurophysiol* **16**, 509-527.
- Lin, JW, Fu, Q & Allana, T. (2005). Probing the endogenous Ca²⁺ buffers at the presynaptic terminals of the crayfish neuromuscular junction. *J Neurophysiol* **94**, 377-386.
- Llinas, R, Sugimori, M & Silver, RB. (1992). Microdomains of high calcium concentration in a presynaptic terminal. *Science* **256**, 677-679.
- Lloyd, DPC. (1959). Early and late post-tetanic potentiation, and post-tetanic block in a monosynaptic reflex pathway. *J Gen Physiol* **42**, 475-488.
- Lohmann, C & Friauf, E. (1996). Distribution of the calcium-binding proteins parvalbumin and calretinin in the auditory brainstem of adult and developing rats. *J Comp Neurol* **367**, 90-109.
- Lou, X, Korogod, N, Brose, N & Schneggenburger, R. (2008). Phorbol esters modulate spontaneous and Ca²⁺-evoked transmitter release via acting on both Munc13 and protein kinase C. *J Neurosci* **28**, 8257-8267.
- Lou, X, Scheuss, V & Schneggenburger, R. (2005). Allosteric modulation of the presynaptic Ca²⁺ sensor for vesicle fusion. *Nature* **435**, 497-501.
- Macleod, GT, Marin, L, Charlton, MP & Atwood, HL. (2004). Synaptic vesicles: test for a role in presynaptic calcium regulation. *J Neurosci* **24**, 2496-2505.

- Magleby, KL. (1973). The effect of tetanic and post-tetanic potentiation on facilitation of transmitter release at the frog neuromuscular junction. *J Physiol* **234**, 353-371.
- Magleby, KL & Zengel, JE. (1976). Augmentation: A process that acts to increase transmitter release at the frog neuromuscular junction. *J Physiol* **257**, 449-470.
- Marek, KW & Davis, GW. (2002). Transgenically encoded protein photoinactivation (FLAsH-FALI): acute inactivation of synaptotagmin I. *Neuron* **36**, 805-813.
- Martin, AR & Pilar, G. (1964). Presynaptic and Post-Synaptic Events During Post-Tetanic Potentiation and Facilitation in the Avian Ciliary Ganglion. *J Physiol* **175**, 17-30.
- Matveev, V, Zucker, RS & Sherman, A. (2004). Facilitation through buffer saturation: constraints on endogenous buffering properties. *Biophys J* **86**, 2691-2709.
- McAllister, AK. (2007). Dynamic aspects of CNS synapse formation. *Annu Rev Neurosci* **30**, 425-450.
- Meinrenken, CJ, Borst, JGG & Sakmann, B. (2003). Local routes revisited: the space and time dependence of the Ca₂₊ signal for phasic transmitter release at the rat calyx of Held. *J Physiol* **547**, 665-689.
- Meyer, MP & Smith, SJ. (2006). Evidence from in vivo imaging that synaptogenesis guides the growth and branching of axonal arbors by two distinct mechanisms. *J Neurosci* **26**, 3604-3614.
- Morest, DK. (1968a). The collateral system of the medial nucleus of the trapezoid body of the cat, its neuronal architecture and relation to the olivo-cochlear bundle. *Brain Res* **9**, 288-311.
- Morest, DK. (1968b). The growth of synaptic endings in the mammalian brain: a study of the calyces of the trapezoid body. *Z Anat Entwicklungsgesch* **127**, 201-220.
- Muller, A, Kukley, M, Stausberg, P, Beck, H, Muller, W & Dietrich, D. (2005). Endogenous Ca₂₊ buffer concentration and Ca₂₊ microdomains in hippocampal neurons. *J Neurosci* **25**, 558-565.

- Muller, M, Felmy, F & Schneggenburger, R. (2008). A limited contribution of Ca²⁺-current facilitation to paired-pulse facilitation of transmitter release at the rat calyx of Held. *J Physiol*.
- Muller, M, Felmy, F, Schwaller, B & Schneggenburger, R. (2007). Parvalbumin is a mobile presynaptic Ca²⁺ buffer in the calyx of held that accelerates the decay of Ca²⁺ and short-term facilitation. *J Neurosci* **27**, 2261-2271.
- Nagerl, UV, Novo, D, Mody, I & Vergara, JL. (2000). Binding kinetics of calbindin-D(28k) determined by flash photolysis of caged Ca(2+). *Biophys J* **79**, 3009-3018.
- Nakamura, T, Yamashita, T, Saitoh, N & Takahashi, T. (2008). Developmental changes in calcium/calmodulin-dependent inactivation of calcium currents at the rat calyx of Held. *J Physiol* **586**, 2253-2261.
- Naraghi, M. (1997). T-jump study of calcium binding kinetics of calcium chelators. *Cell Calcium* **22**, 255-268.
- Neher, E. (1995). The use of fura-2 for estimating Ca buffers and Ca fluxes. *Neuropharmacology* **34**, 1423-1442.
- Neher, E. (1998). Usefulness and limitations of linear approximations to the understanding of Ca⁺⁺ signals. *Cell Calcium* **24**, 345-357.
- Neher, E & Sakaba, T. (2001). Combining deconvolution and noise analysis for the estimation of transmitter release rates at the calyx of held. *J Neurosci* **21**, 444-461.
- Neher, E & Sakaba, T. (2008). Multiple roles of calcium ions in the regulation of neurotransmitter release. *Neuron* **59**, 861-872.
- Oheim, M, Kirchhoff, F & Stuhmer, W. (2006). Calcium microdomains in regulated exocytosis. *Cell Calcium* **40**, 423-439.
- Otis, T, Zhang, S & Trussell, LO. (1996). Direct measurement of AMPA receptor desensitization induced by glutamatergic synaptic transmission. *J Neurosci* **16**, 7496-7504.

- Otsu, Y, Shahrezaei, V, Li, B, Raymond, LA, Delaney, KR & Murphy, TH. (2004). Competition between phasic and asynchronous release for recovered synaptic vesicles at developing hippocampal autaptic synapses. *J Neurosci* **24**, 420-433.
- Owe-Larsson, B, Chaves-Olarte, E, Chauhan, A, Kjaerulff, O, Brask, J, Thelestam, M, Brodin, L & Löw, P. (2005). Inhibition of hippocampal synaptic transmission by impairment of Ral function. *Neuroreport* **16**, 1805-1808.
- Portera-Cailliau, C, Weimer, RM, De Paola, V, Caroni, P & Svoboda, K. (2005). Diverse modes of axon elaboration in the developing neocortex. *PLoS Biol* **3**, e272.
- Postlethwaite, M, Hennig, MH, Steinert, JR, Graham, BP & Forsythe, ID. (2007). Acceleration of AMPA receptor kinetics underlies temperature-dependent changes in synaptic strength at the rat calyx of Held. *J Physiol* **579**, 69-84.
- Propst, JW & Ko, CP. (1987). Correlations between active zone ultrastructure and synaptic function studied with freeze-fracture of physiologically identified neuromuscular junctions. *J Neurosci* **7**, 3654-3664.
- Pyott, SJ & Rosenmund, C. (2002). The effects of temperature on vesicular supply and release in autaptic cultures of rat and mouse hippocampal neurons. *J Physiol* **539**, 523-535.
- Ravin, R, Spira, ME, Parnas, H & Parnas, I. (1997). Simultaneous measurement of intracellular Ca²⁺ and asynchronous transmitter release from the same crayfish bouton. *J Physiol* **501**, 251-262.
- Regehr, WG, Delaney, KR & Tank, DW. (1994). The role of presynaptic calcium in short-term enhancement at the hippocampal mossy fiber synapse. *J Neurosci* **14**, 523-537.
- Reid, CA, Bekkers, JM & Clements, JD. (1998). N- and P/Q-type Ca²⁺ channels mediate transmitter release with a similar cooperativity at rat hippocampal autapses. *J Neurosci* **18**, 2849-2855.
- Rivosecchi, R, Pongs, O, Theil, T & Mallart, A. (1994). Implication of frequenin in the facilitation of transmitter release in *Drosophila*. *J Physiol* **474**, 223-232.
- Rizzoli, SO & Betz, WJ. (2005). Synaptic vesicle pools. *Nat Rev Neurosci* **6**, 57-69.

- Rodríguez, BM, Sigg, D & Bezanilla, F. (1998). Voltage gating of *Shaker* K⁺ channels. The effect of temperature on ionic and gating currents. *J Gen Physiol* **112**, 223-242.
- Rodriguez-Contreras, A, de Lange, RP, Lucassen, PJ & Borst, JGG. (2006). Branching of calyceal afferents during postnatal development in the rat auditory brainstem. *J Comp Neurol* **496**, 214-228.
- Rosahl, TW, Geppert, M, Spillane, D, Herz, J, Hammer, RE, Malenka, RC & Sudhof, TC. (1993). Short-term synaptic plasticity is altered in mice lacking synapsin I. *Cell* **75**, 661-670.
- Rosahl, TW, Spillane, D, Missler, M, Herz, J, Selig, DK, Wolff, JR, Hammer, RE, Malenka, RC & Sudhof, TC. (1995). Essential functions of synapsins I and II in synaptic vesicle regulation. *Nature* **375**, 488-493.
- Rosenmund, C, Sigler, A, Augustin, I, Reim, K, Brose, N & Rhee, JS. (2002). Differential control of vesicle priming and short-term plasticity by Munc13 isoforms. *Neuron* **33**, 411-424.
- Rosenthal, J. (1969). Post-tetanic potentiation at the neuromuscular junction of the frog. *J Physiol* **203**, 121-133.
- Rozov, A, Burnashev, N, Sakmann, B & Neher, E. (2001). Transmitter release modulation by intracellular Ca²⁺ buffers in facilitating and depressing nerve terminals of pyramidal cells in layer 2/3 of the rat neocortex indicates a target cell-specific difference in presynaptic calcium dynamics. *J Physiol* **531**, 807-826.
- Ruthazer, ES, Li, J & Cline, HT. (2006). Stabilization of axon branch dynamics by synaptic maturation. *J Neurosci* **26**, 3594-3603.
- Sabatini, BL & Regehr, WG. (1998). Optical measurement of presynaptic calcium currents. *Biophys J* **74**, 1549-1563.
- Sakaba, T. (2006). Roles of the fast-releasing and the slowly releasing vesicles in synaptic transmission at the calyx of Held. *J Neurosci* **26**, 5863-5871.

- Sakaba, T & Neher, E. (2001a). Calmodulin mediates rapid recruitment of fast-releasing synaptic vesicles at a calyx-type synapse. *Neuron* **32**, 1119-1131.
- Sakaba, T & Neher, E. (2001b). Preferential potentiation of fast-releasing synaptic vesicles by cAMP at the calyx of Held. *Proc Natl Acad Sci U S A* **98**, 331-336.
- Sakaba, T & Neher, E. (2001c). Quantitative relationship between transmitter release and calcium current at the calyx of Held synapse. *J Neurosci* **21**, 462-476.
- Sakaba, T & Neher, E. (2003a). Direct modulation of synaptic vesicle priming by GABA_B receptor activation at a glutamatergic synapse. *Nature* **424**, 775-778.
- Sakaba, T & Neher, E. (2003b). Involvement of actin polymerization in vesicle recruitment at the calyx of Held synapse. *J Neurosci* **23**, 837-846.
- Sakaba, T, Stein, A, Jahn, R & Neher, E. (2005). Distinct kinetic changes in neurotransmitter release after SNARE protein cleavage. *Science* **309**, 491-494.
- Sätzler, K, Söhl, LF, Bollmann, JH, Borst, JGG, Frotscher, M, Sakmann, B & Lübke, JHR. (2002). Three-dimensional reconstruction of a calyx of Held and its postsynaptic principal neuron in the medial nucleus of the trapezoid body. *J Neurosci* **22**, 10567-10579.
- Scheuss, V & Neher, E. (2001). Estimating synaptic parameters from mean, variance, and covariance in trains of synaptic responses. *Biophys J* **81**, 1970-1989.
- Schikorski, T & Stevens, CF. (2001). Morphological correlates of functionally defined synaptic vesicle populations. *Nat Neurosci* **4**, 391-395.
- Schlüter, OM, Basu, J, Südhof, TC & Rosenmund, C. (2006). Rab3 superprimed synaptic vesicles for release: implications for short-term synaptic plasticity. *J Neurosci* **26**, 1239-1246.
- Schneggenburger, R & Forsythe, ID. (2006). The calyx of Held. *Cell Tissue Res* **326**, 311-337.
- Schneggenburger, R, Meyer, AC & Neher, E. (1999). Released fraction and total size of a pool of immediately available transmitter quanta at a calyx synapse. *Neuron* **23**, 399-409.

- Schneggenburger, R & Neher, E. (2000). Intracellular calcium dependence of transmitter release rates at a fast central synapse. *Nature* **406**, 889-893.
- Schneggenburger, R & Neher, E. (2005). Presynaptic calcium and control of vesicle fusion. *Curr Opin Neurobiol* **15**, 266-274.
- Schneggenburger, R, Sakaba, T & Neher, E. (2002). Vesicle pools and short-term synaptic depression: lessons from a large synapse. *Trends Neurosci* **25**, 206-212.
- Silva, AJ, Rosahl, TW, Chapman, PF, Marowitz, Z, Friedman, E, Frankland, PW, Cestari, V, Cioffi, D, Südhof, TC & Bourtschuladze, R. (1996). Impaired learning in mice with abnormal short-lived plasticity. *Curr Biol* **6**, 1509-1518.
- Sinha, SR, Wu, LG & Saggau, P. (1997). Presynaptic calcium dynamics and transmitter release evoked by single action potentials at mammalian central synapses. *Biophys J* **72**, 637-651.
- Sippy, T, Cruz-Martin, A, Jeromin, A & Schweizer, FE. (2003). Acute changes in short-term plasticity at synapses with elevated levels of neuronal calcium sensor-1. *Nat Neurosci* **6**, 1031-1038.
- Somlyo, AV, Wang, H, Choudhury, N, Khromov, AS, Majesky, M, Owens, GK & Somlyo, AP. (2004). Myosin light chain kinase knockout. *J Muscle Res Cell Motil* **25**, 241-242.
- Stevens, CF, Tonegawa, S & Wang, Y. (1994). The role of calcium-calmodulin kinase II in three forms of synaptic plasticity. *Curr Biol* **4**, 687-693.
- Stevens, CF & Wesseling, JF. (1999). Augmentation is a potentiation of the exocytotic process. *Neuron* **22**, 139-146.
- Sun, J, Bronk, P, Liu, X, Han, W & Südhof, TC. (2006). Synapsins regulate use-dependent synaptic plasticity in the calyx of Held by a Ca²⁺/calmodulin-dependent pathway. *Proc Natl Acad Sci U S A* **103**, 2880-2885.
- Sun, J, Pang, ZP, Qin, D, Fahim, AT, Adachi, R & Südhof, TC. (2007). A dual-Ca²⁺-sensor model for neurotransmitter release in a central synapse. *Nature* **450**, 676-682.

- Sun, JY & Wu, LG. (2001). Fast kinetics of exocytosis revealed by simultaneous measurements of presynaptic capacitance and postsynaptic currents at a central synapse. *Neuron* **30**, 171-182.
- Swandulla, D, Hans, M, Zipser, K & Augustine, GJ. (1991). Role of residual calcium in synaptic depression and posttetanic potentiation: fast and slow calcium signaling in nerve terminals. *Neuron* **7**, 915-926.
- Takahashi, T, Forsythe, ID, Tsujimoto, T, Barnes-Davies, M & Onodera, K. (1996). Presynaptic calcium current modulation by a metabotropic glutamate receptor. *Science* **274**, 594-597.
- Takahashi, T, Kajikawa, Y & Tsujimoto, T. (1998). G-Protein-coupled modulation of presynaptic calcium currents and transmitter release by a GABAB receptor. *J Neurosci* **18**, 3138-3146.
- Tang, Y & Zucker, RS. (1997). Mitochondrial involvement in post-tetanic potentiation of synaptic transmission. *Neuron* **18**, 483-491.
- Tank, DW, Regehr, WG & Delaney, KR. (1995). A quantitative analysis of presynaptic calcium dynamics that contribute to short-term enhancement. *J Neurosci* **15**, 7940-7952.
- Taschenberger, H, Leão, RM, Rowland, KC, Spirou, GA & von Gersdorff, H. (2002). Optimizing synaptic architecture and efficiency for high-frequency transmission. *Neuron* **36**, 1127-1143.
- Taschenberger, H & von Gersdorff, H. (2000). Fine-tuning an auditory synapse for speed and fidelity: developmental changes in presynaptic waveform, EPSC kinetics, and synaptic plasticity. *J Neurosci* **20**, 9162-9173.
- Toonen, RFG, Wierda, K, Sons, MS, de Wit, H, Cornelisse, LN, Brussaard, A, Plomp, JJ & Verhage, M. (2006). Munc18-1 expression levels control synapse recovery by regulating readily releasable pool size. *Proc Natl Acad Sci U S A* **103**, 18332-18337.
- Tsujimoto, T, Jeromin, A, Saitoh, N, Roder, JC & Takahashi, T. (2002). Neuronal calcium sensor 1 and activity-dependent facilitation of P/Q-type calcium currents at presynaptic nerve terminals. *Science* **295**, 2276-2279.

- Uziel, A, Romand, R & Marot, M. (1981). Development of cochlear potentials in rats. *Audiology* **20**, 89-100.
- Van der Kloot, W & Molgó, J. (1994). Quantal acetylcholine release at the vertebrate neuromuscular junction. *Physiological Reviews* **74**, 899-991.
- Verstreken, P, Ly, CV, Venken, KJ, Koh, TW, Zhou, Y & Bellen, HJ. (2005). Synaptic mitochondria are critical for mobilization of reserve pool vesicles at *Drosophila* neuromuscular junctions. *Neuron* **47**, 365-378.
- von Gersdorff, H & Borst, JGG. (2002). Short-term plasticity at the calyx of Held. *Nat Rev Neurosci* **3**, 53-64.
- von Gersdorff, H, Schneggenburger, R, Weis, S & Neher, E. (1997). Presynaptic depression at a calyx synapse: the small contribution of metabotropic glutamate receptors. *J Neurosci* **17**, 8137-8146.
- Wadel, K, Neher, E & Sakaba, T. (2007). The Coupling between Synaptic Vesicles and Ca^{2+} Channels Determines Fast Neurotransmitter Release. *Neuron* **53**, 563-575.
- Wang, LY & Kaczmarek, LK. (1998). High-frequency firing helps replenish the readily releasable pool of synaptic vesicles. *Nature* **394**, 384-388.
- Wierda, KD, Toonen, RF, de Wit, H, Brussaard, AB & Verhage, M. (2007). Interdependence of PKC-dependent and PKC-independent pathways for presynaptic plasticity. *Neuron* **54**, 275-290.
- Wimmer, VC, Horstmann, H, Groh, A & Kuner, T. (2006). Donut-like topology of synaptic vesicles with a central cluster of mitochondria wrapped into membrane protrusions: a novel structure-function module of the adult calyx of Held. *J Neurosci* **26**, 109-116.
- Witte, S, Stier, H & Cline, HT. (1996). In vivo observations of timecourse and distribution of morphological dynamics in *Xenopus* retinotectal axon arbors. *J Neurobiol* **31**, 219-234.
- Wojtowicz, JM & Atwood, HL. (1985). Correlation of presynaptic and postsynaptic events during establishment of long-term facilitation at crayfish neuromuscular junction. *J Neurophysiol* **54**, 220-230.

- Wölfel, M & Schneggenburger, R. (2003). Presynaptic capacitance measurements and Ca^{2+} uncaging reveal submillisecond exocytosis kinetics and characterize the Ca^{2+} sensitivity of vesicle pool depletion at a fast CNS synapse. *J Neurosci* **23**, 7059-7068.
- Wong, AYC, Graham, BP, Billups, B & Forsythe, ID. (2003). Distinguishing between presynaptic and postsynaptic mechanisms of short-term depression during action potential trains. *J Neurosci* **23**, 4868-4877.
- Wu, LG & Borst, JGG. (1999). The reduced release probability of releasable vesicles during recovery from short-term synaptic depression. *Neuron* **23**, 821-832.
- Wu, LG, Westenbroek, RE, Borst, JGG, Catterall, WA & Sakmann, B. (1999). Calcium channel types with distinct presynaptic localization couple differentially to transmitter release in single calyx-type synapses. *J Neurosci* **19**, 726-736.
- Wu, XS, Sun, JY, Evers, AS, Crowder, M & Wu, LG. (2004). Isoflurane inhibits transmitter release and the presynaptic action potential. *Anesthesiology* **100**, 663-670.
- Wu, XS & Wu, LG. (2001). Protein kinase C increases the apparent affinity of the release machinery to Ca^{2+} by enhancing the release machinery downstream of the Ca^{2+} sensor. *J Neurosci* **21**, 7928-7936.
- Xu, J & Wu, LG. (2005). The decrease in the presynaptic calcium current is a major cause of short-term depression at a calyx-type synapse. *Neuron* **46**, 633-645.
- Xu, T, Naraghi, M, Kang, H & Neher, E. (1997). Kinetic studies of Ca^{2+} binding and Ca^{2+} clearance in the cytosol of adrenal chromaffin cells. *Biophys J* **73**, 532-545.
- Yang, F, He, XP, Russell, J & Lu, B. (2003). Ca^{2+} influx-independent synaptic potentiation mediated by mitochondrial Na^{+} - Ca^{2+} exchanger and protein kinase C. *J Cell Biol* **163**, 511-523.
- Yang, YM & Wang, LY. (2006). Amplitude and kinetics of action potential-evoked Ca^{2+} current and its efficacy in triggering transmitter release at the developing calyx of held synapse. *J Neurosci* **26**, 5698-5708.

- Youssoufian, M, Couchman, K, Shivdasani, MN, Paolini, AG & Walmsley, B. (2008). Maturation of auditory brainstem projections and calyces in the congenitally deaf (dn/dn) mouse. *J Comp Neurol* **506**, 442-451.
- Zengel, JE & Magleby, KL. (1981). Changes in miniature endplate potential frequency during repetitive nerve stimulation in the presence of Ca^{2+} , Ba^{2+} , and Sr^{2+} at the frog neuromuscular junction. *J Gen Physiol* **77**, 503-529.
- Zengel, JE, Magleby, KL, Horn, JP, McAfee, DA & Yarowsky, PJ. (1980). Facilitation, augmentation, and potentiation of synaptic transmission at the superior cervical ganglion of the rabbit. *J Gen Physiol* **76**, 213-231.
- Zenisek, D, Davila, V, Wan, L & Almers, W. (2003). Imaging calcium entry sites and ribbon structures in two presynaptic cells. *J Neurosci* **23**, 2538-2548.
- Zhao, Y & Klein, M. (2004). Changes in the readily releasable pool of transmitter and in efficacy of release induced by high-frequency firing at *Aplysia* sensorimotor synapses in culture. *J Neurophysiol* **91**, 1500-1509.
- Zhong, N, Beaumont, V & Zucker, RS. (2001). Roles for mitochondrial and reverse mode $\text{Na}^+/\text{Ca}^{2+}$ exchange and the plasmalemma Ca^{2+} ATPase in post-tetanic potentiation at crayfish neuromuscular junctions. *J Neurosci* **21**, 9598-9607.
- Zhong, Y & Wu, CF. (1991). Altered synaptic plasticity in *Drosophila* memory mutants with a defective cyclic AMP cascade. *Science* **251**, 198-201.
- Zucker, RS, Delaney, KR, Mulkey, R & Tank, DW. (1991). Presynaptic calcium in transmitter release and posttetanic potentiation. *Ann N Y Acad Sci* **635**, 191-207.
- Zucker, RS & Lara Estrella, LO. (1983). Post-tetanic decay of evoked and spontaneous transmitter release and a residual-calcium model of synaptic facilitation at crayfish neuromuscular junctions. *J Gen Physiol* **81**, 355-372.
- Zucker, RS & Lara-Estrella, LO. (1979). Is synaptic facilitation caused by presynaptic spike broadening? *Nature* **278**, 57-59.
- Zucker, RS & Regehr, WG. (2002). Short-term synaptic plasticity. *Annu Rev Physiol* **64**, 355-405.